



University of Tennessee, Knoxville  
**TRACE: Tennessee Research and Creative  
Exchange**

---

Doctoral Dissertations

Graduate School

---

12-2022

## **Microwave Frequency Control Algorithms for Use in a Solid-State System to Achieve Improved Heating Performance**

Ran Yang

*University of Tennessee, Knoxville, ryang17@vols.utk.edu*

Follow this and additional works at: [https://trace.tennessee.edu/utk\\_graddiss](https://trace.tennessee.edu/utk_graddiss)



Part of the [Food Processing Commons](#)

---

### **Recommended Citation**

Yang, Ran, "Microwave Frequency Control Algorithms for Use in a Solid-State System to Achieve Improved Heating Performance. " PhD diss., University of Tennessee, 2022.  
[https://trace.tennessee.edu/utk\\_graddiss/7635](https://trace.tennessee.edu/utk_graddiss/7635)

This Dissertation is brought to you for free and open access by the Graduate School at TRACE: Tennessee Research and Creative Exchange. It has been accepted for inclusion in Doctoral Dissertations by an authorized administrator of TRACE: Tennessee Research and Creative Exchange. For more information, please contact [trace@utk.edu](mailto:trace@utk.edu).

To the Graduate Council:

I am submitting herewith a dissertation written by Ran Yang entitled "Microwave Frequency Control Algorithms for Use in a Solid-State System to Achieve Improved Heating Performance." I have examined the final electronic copy of this dissertation for form and content and recommend that it be accepted in partial fulfillment of the requirements for the degree of Doctor of Philosophy, with a major in Food Science.

Jiajia Chen, Major Professor

We have read this dissertation and recommend its acceptance:

Aly E. Fathy, Zhenbo Wang, Mark T. Morgan, Curtis R. Lockett

Accepted for the Council:

Dixie L. Thompson

Vice Provost and Dean of the Graduate School

(Original signatures are on file with official student records.)

**Microwave Frequency Control Algorithms for Use in a Solid-State  
System to Achieve Improved Heating Performance**

**A Dissertation Presented for the  
Doctor of Philosophy  
Degree  
The University of Tennessee, Knoxville**

**Ran Yang  
December 2022**

Copyright © 2022 by Ran Yang.

All rights reserved.

## DEDICATION

To Mom.

For showing me the way to being brave.

To Dad.

For endless support and silent love.

And to the special girls.

My confidante, Miss *Miao An*, for always standing by my side.

And my bestie, Miss *Xiaoyi Guo*, for coming into my life.

## ACKNOWLEDGEMENTS

I would first thank my advisor, Dr. Jiajia Chen for offering this Ph.D. position, which completely rewrote my life. None of these works could have been done without his patience, support, and always timely feedback on my work. His impressive hardworking constantly stimulated me through my journey of science. I will forever appreciate this fantastic opportunity which let me see the other side of food science. I would also like to offer my sincere appreciation to my committee members, Dr. Aly Fathy, Dr. Zhenbo Wang, Dr. Mark Morgan and Dr. Curtis Lockett, for their advice, guidance, and always encouraging me to think more and pursue more. I am also grateful to all lab mates, friends, and staff in the department and in UTK, for being always helpful and supportive.

I also want to express my sincere appreciation to all friends for always being supportive and caring. Specific thanks to the girls over around US, and to old friends back in China, for always being there when I am in need. And special appreciation goes to Dr. Jingyi Zhou, for all the cookies, cakes, scones. Life is never lonely or boring with all you guys.

My final acknowledgments go out to those mean the most to me in life, my parents, for always supporting my decision and for allowing me to be who I really am.

## ABSTRACT

Microwave is a popular food heating technique. Its unique volumetric heating principle enables fast heating while also leads to poor heating uniformity. The main reason for the nonuniform heating is the presence of standing wave patterns inside the oven cavity, which is due to the use of single frequency by magnetron as the microwave source. Solid-state microwave generator is a promising solution to the nonuniform heating, as it allows flexible microwaves, with varied frequencies rather than one fixed frequency, and thereby, the thermal patterns by different frequencies could overcome the standing wave pattern issue. Previous studies on the frequency control strategy mainly focused on orderly shifting frequencies in range, while not fully utilized the information provided by frequency-related pattern variation, where the complementary patterns could contribute to better heating uniformity. Besides, such in order frequency-shifting did not consider sample variation and only applied a common shifting strategy to all products. Hence, the objective of this project is to develop a dynamic microwave frequency shifting algorithm that makes use of complementary-frequency and can accommodatively shifts frequencies according to real-time collected information.

Preliminary experiments were first conducted to validate the complementary-frequency concept, where the pre-collected thermal patterns under different frequencies were used as initial dataset to design the frequency shifting path. Compared with orderly shifting, the complementary-frequency shifting algorithm was demonstrated to have improved microwave heating performance. Based on the validated concept, and to eliminate the pre-collection of data for path design, the complementary-frequency shifting algorithm was improved to be a dynamic version with a thermal camera mounted to the oven that could monitor the heating performance in real time. The dynamic complementary-frequency shifting algorithm was proven to compete the orderly shifting strategies. Furthermore, the dynamic heating was compared with the rotatory magnetron heating, i.e., the domestic oven heating, where the performance evaluation was conducted on various types of commercial or prepared foods. The comparison results showed that

the proposed dynamic complementary-frequency shifting algorithm, realized in a solid-state microwave system, successfully competed with the rotatory magnetron heating in a domestic oven.

Conclusions from the current dissertation shall provide useful information for the future design and commercialization of the solid-state microwave ovens.

**Keywords** microwave heating, solid-state, frequency control, thermal pattern, performance improvement



# TABLE OF CONTENTS

CHAPTER I Introduction and literature review .....	1
1.1 Background.....	2
1.2 Microwave as a thermal processing technique .....	5
1.2.1 Heating principle.....	5
1.2.2 Inherent problems of magnetron-based microwave oven .....	7
1.3 Strategies to improve microwave heating performance.....	7
1.3.1 Currently applied methods .....	7
1.3.1.1 Turntable and Mode stirrer .....	7
1.3.1.2 Modulated Power .....	9
1.3.2 Proposed smart microwave oven .....	10
1.4 Solid-state technique as a replacement of magnetron.....	12
1.5 Specific objectives .....	14
List of References .....	15
CHAPTER II Development of a Complementary-Frequency Strategy to Improve Microwave Heating of Gellan Gel in a Solid-state System .....	21
2.1 Abstract.....	22
2.2 Introduction.....	23
2.3 Material and Methods .....	26
2.3.1 Microwave system .....	26
2.3.2 Model food preparation.....	27
2.3.3 Microwave heating performance evaluation .....	28
2.3.4 Microwave frequency-shifting strategies.....	29
2.3.5 Data analysis .....	31
2.4 Results and Discussion .....	31
2.4.1 Temperature profiles for Fixed-Frequency heating .....	31

2.4.2 Complementary-Frequency strategies.....	33
2.4.3 Microwave heating performance using different heating strategies .....	34
2.4.3.1 Comparison between Fixed-Frequency and Sweeping-Frequency strategies .....	34
2.4.3.2 Comparison between Sweeping-Frequency and Complementary-Frequency strategies.....	36
2.4.3.3 Effect of frequency-shifting time steps on microwave heating performance .....	37
2.4.4 Usefulness, limitations, and future work .....	38
2.5 Conclusions.....	39
2.6 Acknowledgments .....	40
List of References .....	42
Appendix.....	46
<b>CHAPTER III Development of Online Closed-Loop Frequency Shifting Strategies to Improve Heating Performance of Foods in a Solid-State microwave System.....</b>	<b>60</b>
3.1 Abstract.....	61
3.2 Introduction.....	62
3.3 Material and Methods .....	65
3.3.1 Microwave system .....	65
3.3.2 Model foods preparation and dielectric properties .....	65
3.3.3 Online microwave frequency shifting strategies with closed-loop feedback ..	67
3.3.3.1 Orderly frequency shifting strategy .....	67
3.3.3.2 Pre-determined complementary-frequency shifting strategy .....	68
3.3.3.3 Dynamic complementary-frequency algorithm .....	71
3.3.4 Microwave heating performance evaluation.....	71
3.3.5 Data analysis .....	73
3.4 Results and Discussion .....	73
3.4.1 Comparison of the three online closed-loop frequency shifting algorithms....	73

3.4.1.1 Selected frequencies based on high power efficiency (low power reflection) .....	73
3.4.1.2 Characterization of the spatial thermal contributions from each selected frequency .....	74
3.4.1.3 Frequency shifting sequences .....	75
3.4.2 Comparison of microwave heating performance .....	78
3.4.2.1 Performance comparison during heating .....	78
3.4.2.2 Performance comparison after heating .....	79
3.4.3 Usefulness and future work.....	80
3.5 Conclusions.....	83
3.6 Acknowledgements.....	84
List of References .....	85
Appendix.....	89
CHAPTER IV Comprehensive evaluation of microwave heating performance using dynamic complementary-frequency shifting strategy in a solid-state system .....	109
4.1 Abstract.....	110
4.2 Introduction.....	111
4.3 Materials and Methods.....	113
4.3.1 Microwave systems.....	113
4.3.2 Food product preparation .....	114
4.3.3 Heating strategies.....	116
4.3.4 Heating performance evaluation .....	117
4.3.5 Data analysis .....	119
4.4 Results and Discussion .....	120
4.4.1 Microwave heating performance .....	120
4.4.2.1 Single-component commercial Pulled Chicken in original package .....	120
4.4.2.2 Multicomponent commercial Beef in Gravy in original package.....	121

4.4.2.3 Multilayer commercial Lasagna .....	122
4.4.2.4 Multicompartment meal of Pulled Chicken & Lasagna .....	123
4.4.2.5 Multicompartment meal of Mashed Potato & Beef in Gravy .....	124
4.4.2 Overall comparison of the microwave heating performance .....	125
4.4.2.1 Cold spot temperature .....	125
4.4.2.2 Overall improvement .....	125
4.4.2.3 Correlation between food product factors and the improvement.....	126
4.4.3 Usefulness and future work.....	128
4.5 Conclusions.....	130
4.6 Acknowledgements.....	130
List of References .....	131
Appendix.....	135
CHAPTER V Conclusions and Future work .....	149
5.1 Conclusions.....	150
5.2 Future work.....	152
VITA.....	154

## LIST OF TABLES

Table II-1 Microwave heating performances of combined top and middle layers with fixed-frequency from 2.40 to 2.47 GHz after six minutes of heating .....	47
Table II-2 Microwave heating performance of the combined top and middle layers for different frequency shifting strategies after six minutes of heating .....	48
Table III-1. The calculated superimposed thermal results of microwave heating of gellan gum for the first dynamic frequency selection after frequency sweeping ( $t \approx 90$ s). .....	90
Table III-2. The thermal results collected by the top camera for gellan gum samples during 6 min microwave heating with different frequency shifting strategies. ....	91
Table III-3 The thermal results collected by the top camera for mashed potato samples during 6 min microwave heating with different frequency shifting strategies. ....	92
Table III-4 Microwave heating performances of combined top and middle layers with three different frequency shifting strategies on gellan gel samples. ....	93
Table III-5 Microwave heating performances of combined top and middle layers with three different frequency shifting strategies on mashed potato samples. ....	94
Table IV-1 Sample information .....	136
Table IV-2 Overall improvement in Temperature and Uniformity by using solid-state microwave with dynamic frequency .....	137

## LIST OF FIGURES

Figure II-1 Diagram for the solid-state system assembly (unit: mm). .....	49
Figure II-2 Dielectric properties of the prepared gellan gel sample in the range of 2.40 to 2.50 GHz, (A) dielectric constant and loss factor; (B) penetration depth.....	50
Figure II-3 Statistical t-test results on analysis of the difference caused by image resizing. ....	51
Figure II-4 Sweeping-Frequency strategies for a six-minute microwave heating process. (A) incremental shifting-45s step; (B) decremental shifting-45s step; (C) incremental shifting-15s step; (D) mixed shifting-15s step.....	52
Figure II-5 Algorithm I to determine the complementary-frequency shifting order based on heating uniformity index only.....	53
Figure II-6 Algorithm II to determine the complementary-frequency shifting order based on both heating rate and standard deviations.....	54
Figure II-7 Temperature profiles at the top and middle layers after six minutes of heating with fixed frequency from 2.40 to 2.47 GHz.....	55
Figure II-8 Microwave heating performance at top and middle layers after six microwave heating with fixed-frequency from 2.40 to 2.47 GHz. (The results and error bars were calculated as the average and standard deviation from experiments done in triplicate separately).....	56
Figure II-9 Complementary-frequency shifting strategies developed based on heating uniformity index only (A & B), both heating rate and standard deviation (C&D) with shifting steps of 45 (A&C) and 15 (B&D) s. ....	57

Figure II-10 Temperature profiles of top and middle layers after six-minute microwave heating with various frequency-shifting strategies (only one replicate out of three shown here to illustrate the results). ..... 58

Figure II-11 Microwave heating performance at top and middle layers after six microwave heating with various frequency-shifting strategies. (A) Average temperature for four 45s-step shifting strategies; (B) Heating Uniformity Index (*HUI*) profiles for four 45s-step shifting strategies; (C) Average temperature for four 15s-step shifting strategies; (D) *HUI* profiles for four 15s-step shifting strategies. All results are shown in mean  $\pm$  standard deviation. Different letters in each figure (top layer with lower-case letters, middle layer with capital letters) indicate a significant difference ( $p < 0.05$ ). The results and error bars were calculated as the average and standard deviation from experiments done in triplicate separately). ..... 59

Figure III-1 A schematic diagram for the solid-state microwave system setup. .... 95

Figure III-2 Frequency-dependent dielectric properties of gellan gel and mashed potatoes measured in triplicate at room temperature. (A) Dielectric constant (B) dielectric loss factor and (C) loss tangent (ratio of loss factor to dielectric constant). ..... 96

Figure III-3 Orderly frequency shifting algorithm. .... 97

Figure III-4 Pre-determined complementary-frequency shifting algorithm. .... 98

Figure III-5 Illustration of the food boundary detection by the thermal imaging camera mounted at the top of the oven cavity. (A) thermal image captured by the top camera, (B) food boundary (white line) detected, (C) created mask used to determine the food domain for data analysis. .... 99

Figure III-6 Illustration of the superposition assumption to determine the spatial thermal contribution from each frequency. .... 100

Figure III-7 Dynamic complementary-frequency shifting algorithm. .... 101

Figure III-8 Selected frequencies by the frequency sweeping process for three replications of three algorithms (Orderly, Pre-determined, and Dynamic) for gellan gel (A) and mashed potato (B) samples. .... 102

Figure III-9 Determined spatial thermal contribution from the selected frequencies by pre-determined strategy, with only food domain shown in color. .... 103

Figure III-10 Developed orderly frequency shifting sequences for gellan gel (A) and mashed potato (B) samples. .... 104

Figure III-11 Developed pre-determined complementary-frequency shifting sequences for gellan gel (A) and mashed potato (B) samples. .... 105

Figure III-12 Developed frequency shifting sequences following the dynamic complementary algorithm (red lines) and pre-determined complementary algorithm (blue dash lines) for gellan gel (A) and mashed potato (B) samples. .... 106

Figure III-13 Layered heating performance (A: Average temperature, B: **HUI** profiles) at top and middle layers for gellan gel samples after 6 min heating following the three different algorithms. The results and error bars were calculated as the average and standard deviation from triplicated experiments. Different letters (top layer with lower-case letters, middle layer with capital letters) indicate a significant difference ( $p < 0.05$ )..... 107

Figure III-14 Layered heating performance (A: Average temperature, B: **HUI** profiles) at top and middle layers for mashed potato samples after 6 min heating following the three different algorithms. The results and error bars were calculated as the average and standard deviation from triplicated experiments. Different letters (top layer with lower-case letters, middle layer with capital letters) indicate a significant difference ( $p < 0.05$ )..... 108

Figure IV-1 Illustration for the solid-state microwave system and the dynamic complementary-frequency shifting. .... 138



Figure IV-2 Magnetron-based microwave power output records under power level 1 for calibration. .... 139

Figure IV-3 Image processing (A) raw thermal image, (B) manually drawn food boundary (red line), (C) mask created based on the boundary in (B). .... 140

Figure IV-4 Top and middle layers of Lasagna samples for heating performance evaluation. .... 141

Figure IV-5 Heating performance of Pulled Chicken and Beef in Gravy samples heated in original packages (A) solid-state frequency records; (B) final thermal images; (C) after-heating temperature, (D) after-heating **HUI**. The results and error bars were calculated as the average and standard deviation from triplicated experiments. (\*  $p < 0.05$ , \*\*  $p < 0.01$ , \*\*\*  $p < 0.001$ , \*\*\*\*  $p < 0.0001$ ). .... 142

Figure IV-6 Heating performance of sliced Lasagna heated in rectangular container (A) solid-state frequency records; (B) final thermal images for both top and middle layers; (C) after-heating temperature, and (D) after-heating **HUI** for top, middle and combined layers. The results and error bars were calculated as the average and standard deviation from triplicated experiments (\*  $p < 0.05$ , \*\*  $p < 0.01$ , \*\*\*  $p < 0.001$ , \*\*\*\*  $p < 0.0001$ ). .... 143

Figure IV-7 Heating performance of Pulled Chicken & Lasagna heated in two-compartment containers. (A) solid-state frequency records; (B) final thermal images; (C) after-heating temperature, and (D) after-heating **HUI** for separate and combined portions. The results and error bars were calculated as the average and standard deviation from triplicated experiments (\*  $p < 0.05$ , \*\*  $p < 0.01$ , \*\*\*  $p < 0.001$ , \*\*\*\*  $p < 0.0001$ ). .... 144

Figure IV-8 Heating performance of Mashed Potato & Beef in Gravy heated in two-compartment container (A) solid-state frequency records; (B) final thermal images; (C) after-heating temperature, and (D) after-heating **HUI**. The results and error bars

were calculated as the average and standard deviation from triplicated experiments (\* p < 0.05, \*\* p < 0.01, \*\*\* p < 0.001, \*\*\*\* p < 0.0001)..... 145

Figure IV-9 Cold spot temperature of different food products after heating obtained from thermal imaging profiles. The results and error bars were calculated as the average and standard deviation from triplicated experiments (\* p < 0.05, \*\* p < 0.01, \*\*\* p < 0.001, \*\*\*\* p < 0.0001)..... 146

Figure IV-10 Comparison of overall performance by different heating methods. The results and error bars were calculated as the average and standard deviation from triplicated experiments (\* p < 0.05, \*\* p < 0.01, \*\*\* p < 0.001, \*\*\*\* p < 0.0001). ..... 147

Figure IV-11 (A) Correlation heatmap with correlation coefficients between every two variables. Labels in black color denote sample properties, and in red color denote performance variables to be studied. (B) **HUI** comparison between dynamic solid-state heating and rotatory magnetron heating with the number of container compartment as an affecting factor. .... 148

**CHAPTER I**  
**INTRODUCTION AND LITERATURE REVIEW**

## 1.1 Background

Microwave is well accepted as an efficient and convenient heating method, and is widely used for cooking, heating, etc., for its fast-heating feature. Because of the unique volumetric heat transfer strategy, which requires no medium between the power source and the target product, the microwave heating process suffers less from heat loss, compared to other heating methods based on heat conduction and/or heat convection. The microwave oven market in the U.S. was valued at over \$ 7000 million in 2020, at a Compound Annual Growth Rate (CAGR) of 4.18%. And the CAGR can be expected to be increased at 4.72 % for 2022-2026 period (Research and Markets, 2022). Moreover, the market for microwaveable food products grows with the popularity of microwave ovens, with an expected value of \$ 142 billion by 2024 (Zion Market Research, 2018). The simultaneous increases in ovens and food products demonstrated the rising reliance on microwave power.

Even characterized as an efficient, environmentally-friendly, and convenient cooking method, the microwave oven, when used to heat foods, raises concerns about food safety and quality (Guzik et al., 2021). The standing wave patterns generated inside the oven cavity lead to hot and cold spots over foods, and the thermal runaway phenomenon caused by the temperature change during the microwave process further enlarge the temperature gaps between these spots (Akkari et al., 2006; Kamol et al., 2010; Vriezinga et al., 2002). Along with the development of microwave ovens, various strategies have been proposed to deal with the nonuniformity problem. The rotatory turntables are applied to almost all ovens to disturb the fixed thermal patterns over the foods and have proven useful. Another successful strategy is the mode stirrer, which is a mobile metallic element that works to disturb the distribution of the electric fields inside the oven cavity. However, these methods are all based on arbitrary increases of the relative movement between the foods and the microwaves, where the turntable can only increase the temperature uniformity along the rotatory direction and the mode stirrer can only make a random improvement (Geedipalli et al., 2007; Liu et al., 2013; Plaza-

González et al., 2005; Sebera et al., 2012; Wiedenmann et al., 2012). While since the microwave process is complicated with a large amount of affecting factors involved, such as oven geometry, food ingredient, package dimension, load location, the turntable, and mode stirrer cannot guarantee the sample level improvement of heating performance in different ovens and with different foods to be cooked. Therefore, a more adaptive microwave strategy is required to address the nonuniformity issue that can be applied to different ovens and foods. A critical reason for this inherent nonuniformity heating of microwave oven is the use of magnetron as its power source, which allows only 2.45 GHz frequency for use in the current microwave ovens. Nowadays, an emerging technique, the solid-state microwave generator, is considered a promising replacement for the magnetron as the microwave power source. The solid-state generator shows its advantage over the magnetron in lifetime, flexible and stable control over frequency, feedback collection from the system, cooperation with multiple equipment, and programmable system.

Given the advantages provided by the solid-state generator, novel methods have been developed to discover the way to better utilize this technique. The reported studies mainly focused on the control over microwave frequency, since in a microwave process, using a different frequency can generate different heating patterns, and the pattern diversity can be utilized to create various patterns in one heating process by shifting the frequencies (Luan et al., 2017). Following this idea, modeling work and experimental study by Danial et al. (2021) and Du et al. (2019) all demonstrated significantly improved heating performance by orderly shifting the frequency in range by solid-state (between 2.40 and 2.50 GHz) at a constant frequency step and a constant shifting rate. In addition, Tang et al. (2018) proposed to conduct simulation first to select several frequencies that could generate good heating efficiencies and then only orderly shift these pre-selected frequencies. The results also showed significantly improved heating performance. Similar results were also reported by Yakovlev (2018) through the modeling method. The improvement by the frequency shifting methods could be attributed to the diverse

locations of the hot and cold spots generated by different frequencies, which made it possible to shift the locations of the spots and thereby, increase the heating uniformity. Although all previously developed frequency selection and shifting strategies showed promising results by flexibly controlling the frequency during heating, these orderly-shifting frequency control algorithms can be further improved. First, all these algorithms did not well consider the specific pattern information from different frequencies, where the complementary locations of spots (Luan et al., 2017) generated by different frequencies may be combined and the combined patterns may yield even better heating performance. The ignored *complementarity* of different frequencies shall be utilized. Second, all the previously proposed frequency control algorithms only worked solely based on the solid-state system, without integrating other devices. The programmability of the solid-state system can be better used through the method of synergy among multiple equipment, with the purpose to generate dynamically adapted microwave frequency shifting path that automatically accommodates foods with different microwave features. This concept also aligns with the ongoing development of smart kitchens, which also includes the novel microwave oven (Ding et al., 2011; Trieu Minh & Khanna, 2018). Recently, more novel techniques are being embedded in the conventional microwave ovens, such as humidity sensors and thermal sensors, aiming to realize real-time data collection and thereby, automatic microwave heating.

With the advanced solid-state technique and the requirement for more novel functions in commercial microwave ovens for the development of smart appliances, it is promising to build a solid-state microwave oven to achieve automatic and adaptive cooking to realize better microwave heating performance. However, problems from previous research are concentrated in frequency control algorithm development, which is the key to the automatic and adaptative microwave ovens equipped with heating condition monitoring devices. The *overall goal* of this project is to develop microwave frequency control algorithms based on the use of a solid-state microwave generator, to realize automatic and adaptive microwave cooking, and improve the overall heating

performance, by properly arranging the real-time data collection, heating processing tracking, and frequency adaption processes and utilizing the thermal pattern variation due to frequency change. This project will enhance the quality of foods cooked in the microwave oven and will enable the future design of smart solid-state based microwave ovens.

## **1.2 Microwave as a thermal processing technique**

Microwaves are electromagnetic waves that are in the frequency range of 300 to 300,000 MHz (Clark et al., 2000; Guzik et al., 2021; Ramaswamy and Tang, 2008). The unique heat delivery strategy, which asks for no transfer medium, makes microwave a highly efficient thermal technique. The microwave oven is now a commonly seen household appliance and is taking advantage of the fast-heating property of microwaves, while at the same time, it is also suffering the inherent nonuniformity heat distribution problem by the magnetron, a typical source currently used for microwave power.

### **1.2.1 Heating principle**

Microwave heating is an efficient and environmentally-friendly food treatment method. Owing to the unique volumetric heat transfer strategy, the energy is supplied by the emitted electric field directly to the target food products (Thostenson and Chou, 1999). The inherent nonuniformity heating issue by the microwave oven is due to the variation in the dielectric, thermal and physical properties of the food materials (K. Pitchai et al., 2012). The dielectric properties, which describe the ability of one material to convert microwave power to heat, include dielectric constant and dielectric loss factor, shown as follows:

$$\varepsilon^* = \varepsilon' - j\varepsilon'' \quad (\text{I-1})$$

where  $\varepsilon'$  is the dielectric constant, which implies the material's ability to store electric energy;  $\varepsilon''$  is the dielectric loss factor, which denotes the ability to convert the electric energy into heat, and  $j = \sqrt{-1}$ . The dielectric properties are dependent mainly on the temperature and the frequency used.

An important parameter to describe the microwave heating is the penetration depth ( $D_p$ ) (DATTA and DAVIDSON, 2000), following:

$$D_p = \frac{c}{\sqrt{2}\pi f \left[ \kappa' \left\{ \sqrt{1 + \left(\frac{\kappa''}{\kappa'}\right)^2} - 1 \right\} \right]^{\frac{1}{2}}} \quad (\text{I-2})$$

Where  $c$  is the velocity of light,  $f$  is the frequency (Hz),  $\kappa'$  is the relative dielectric constant, given as  $\kappa' = \frac{\varepsilon'}{\varepsilon_0}$ ;  $\kappa''$  is the relative dielectric loss factor, as  $\kappa'' = \frac{\varepsilon''}{\varepsilon_0}$ , and  $\varepsilon_0$  is the permittivity of free space ( $8.854 \times 10^{-12} \text{ F/m}$ ). The value of penetration depth is defined as the distance at which the power density drops to a value of  $\frac{1}{e}$  from its value at the material surface (Metaxas and Meredith, 1983).

And the dissipated thermal energy from microwaves is calculated as:

$$q = \frac{1}{2} \omega \varepsilon_0 \kappa'' |E|^2 \quad (\text{I-3})$$

Where  $q$  is the dissipated power density ( $V/m^3$ ),  $\omega$  is the angular frequency ( $\omega = 2\pi f$ ), and  $E$  is the intensity of the electric field ( $V/m$ ).

Other than electromagnetic heating, heat conduction, heat convection, mass movement, moisture phase changing, and food ingredient reaction are all happening simultaneously, and interacting with each other, making microwave heating a complex Multiphysics problem.



### **1.2.2 Inherent problems of magnetron-based microwave oven**

According to the equations, the heating pattern created by microwave heating can be affected by the temperature- and frequency-dependent properties, e.g., dielectric constant ( $\epsilon'$ ) and dielectric loss factor ( $\epsilon''$ ), the frequency used for heating. And in a multi-mode oven cavity, where the waves bounce around within, for example, a microwave oven, the nonuniformity problem is referred to as standing wave pattern. The microwaves reflected from the cavity wall generate hot spots over the food load at the beginning of the heating process. And the temperatures of hot spots, where the patterns stand, increase rapidly, leading accordingly increasing dielectric loss factor, and consequently, more microwave energy is to be absorbed by the hot areas. As a result, during the whole microwave heating process, the hot spots tend to have increasingly higher temperatures, compared to the cold areas. Even the cold areas can also be heated by heat conduction from the surrounding hot spots, the heating rate is much slower than the microwave heating.

During a microwave heating process, the initial nonuniform distribution of the dielectric properties within the food domain, the varied temperature change along the heating process, the moisture movement due to heat gradient, and the boundary condition between the food and surrounding domains are all affecting factors, making the interactions between the waves and the foods complicated. The resulting hot and cold spots in the foods after microwave heating would lower the food quality and cause food safety problems. Hence, to better utilize the convenience provided by microwave heating, it is necessary to develop strategies to improve the heating performance, making the microwave a more reliable power source for cooking.

## **1.3 Strategies to improve microwave heating performance**

### **1.3.1 Currently applied methods**

#### **1.3.1.1 Turntable and Mode stirrer**

To address the non-uniform heating problem by the use of microwaves, various methods have been proposed and validated based on the use of magnetron. The most accepted strategy is the use of a turntable, which keeps rotating the food during the microwave heating in a domestic microwave oven. The model by Geedipalli et al. (2007) demonstrated an increase of the heating uniformity by about 40% with the use of a turntable. A similar improvement in the microwave heating uniformity was also observed through modeling by Liu et al. (2013). While the rotatory movement of the food could only raise the uniformity along the direction tangent to the rotation (Geedipalli et al., 2007; Liu et al., 2013). Experimental results by Pitchai et al. (2012) showed that the heating results in a domestic microwave oven were also affected by the location of the foods on the turntable and placing the food near the turntable edge could yield the best heating uniformity. In addition, the heating performance, including the heating rate and uniformity, could be influenced by the sample size, oven cavity size, microwave power level, etc., making the microwave process difficult to predict.

Other than the turntable that is used to move the foods, the mode stirrer is also applied to some commercial microwave ovens to disturb the microwaves (Plaza-González et al., 2005, 2004). The heating uniformity could be improved by 2% to 20% by the use of a fan-like mode stirrer in an oven cavity without a turntable, located in front of the waveguide (Sebera et al., 2012). Such raised heating performance was also proven through experiments by Nasswetrová et al. (2013). The mode stirrer mounted to the top wall inside the oven could achieve a similar improvement in heating uniformity (Kurniawan et al., 2015; Wiedenmann et al., 2012). The mode stirrer could also work if placed over the bottom wall of the oven cavity (Liu et al., 2014). Another design of the mode stirrer was realized by building multi-material turntables. The experimental result showed that a turntable consisting of polyethylene and aluminum could yield the best heating uniformity (Ye et al., 2017).

### 1.3.1.2 Modulated Power

In addition to modification of the cavity design, another strategy to improve the microwave performance is using a controlled power level to realize microwave power modulation. Two types of scenarios are commonly applied, including intermittent heating and continuous heating, to defrost frozen foods or to cook instant foods. Intermittent heating is performed by switching the power on-and-off regularly while continuous heating is done by reducing the power level, following a pre-designed power adaption path, without being interrupted.

In a magnetron-microwave oven equipped with only a traditional power transformer which is used to raise the household line voltage to be high enough to support the operation of the magnetron, the power output cannot be modified since the transformer can merely work at 60 Hz (North America) or 50 Hz. Hence, the only way to realize power modulation is by continuously switching on and off the power; and during the power-on time period, the system would work at full power level. While in an inverter-equipped microwave oven, the input AC power at 60 or 50 Hz is freely converted to be many kHz when used in a microwave oven, and therefore, the power of the magnetron can be precisely controlled to be desired level by adjusting the frequency. With no need for the on-off control of the power, the inverter-based magnetron has longer service life and relatively higher power efficiency considering the potential energy loss during the switching operation.

Under these two modes, less energy is exported from the energy source in a unit time period compared to the normal operation mode at full power level. The lower microwave power rate allows more time for the conductive and convective heat transfer between the hot spots and their surrounding parts inside the food load (Cha-ching and Datta, 1999; Yang and Gunasekaran, 2001). If neglecting the slight difference in wear and tear of the device mentioned above, when under the condition where the energy delivery rates are the same, there is no obvious difference between these two modes, in terms of temperature uniformity and average temperature (Chen et al., 2016; Yang et al.,

2021). For the intermittent mode, with the same level of energy exported in unit time, a longer power-off time provides a higher uniformity level of the temperature (Yang and Gunasekaran, 2001), for continuous heating, lower operation power improves the uniformity of heat distribution (Cha-ching and Datta, 1999). However, the processing time is prolonged under both these two modes compared with the full-power continuous heating. The less time-efficient result weakens the rapid-process advantage of microwave energy. The food processed by a microwave oven under modulated power is more susceptible to undergo oxidation or degradation because of longer exposure to air and light. Whereas the improved uniformity by the power modulation strategies, compared to the constant microwave heating at full power (the maximum power output by the microwave oven) with only fixed parameters, demonstrated the necessity of a well-designed microwave parameter shifting path. But the presently applied power modulation strategies are only arbitrarily using a pre-designed power shifting path, which cannot adjust the parameters according to the real-time heating conditions. Since the interactions between the microwaves and the oven cavity are highly dependent on many factors, such as sample materials, sample sizes, sample locations, and oven geometries, even one pre-design shifting path could work well in one specific oven with one specific food product, it may not work as well if either the oven cavity or the food is modified. Thus, such strategies, even achieved significant improvement, can be further optimized to be less dependent.

### **1.3.2 Proposed smart microwave oven**

Recently, various novel smart microwave ovens have been proposed and some of which were even implemented based on the currently used domestic microwave ovens. To develop a smart oven, different ideas were applied, such as food recognition, heating condition tracking, and automatic motion. The key idea for such smart ovens is still based

on the use of turntable and/or modulated power, but in an automatic sense, rather than simply following pre-defined scenarios.

A conceptual oven by Jinx et al. (2019) utilized real-time collected data by a thermal camera to adjust the actuation plan for the turntable accordingly. Besides, the self-customized microwave oven by Khan (2020) had two cameras attached over the top wall of the oven cavity, one for food image capture and one for thermal condition tracking. The captured food image was used to determine the type of the product, based on which a final target temperature was suggested from a previously trained deep-learning model. And the temperature data from the thermal camera were used to decide whether the desired target temperature was met or not, and when the temperature was reached, the oven would be shut down.

An automated microwave oven by Huang and Sites (2010), by coupling with an infrared sensor for real-time surface temperature collection, processed the food in two separate stages. During the first stage, the food was heated to a defined target temperature and when the temperature reached, which was determined by the data collected by the infrared sensor, the heating went to the second stage, where the food was still continuously heated but with a much lower microwave power sent (5% of the one used for the first stage). This automated power modulation method, with a follow-up continuous heating stage, could significantly eliminate the target foodborne bacteria.

All the mentioned methods proposed and/or have applied to improve the microwave performance are all based on the magnetron-equipped microwave oven, which does not overcome the inherent standing wave patterns generated in the oven cavity, leaving space for further improvement. Meanwhile, all the proposed strategies revealed that the real-time heating performance tracking device, e.g., the thermal camera used in previous experiments, had a promising role to play in assisting in enhancing the performance of a microwave heating system, where the real-time collected data could provide feedback for adapting the microwave parameters to obtain better heating results.

#### **1.4 Solid-state technique as a replacement of magnetron**

Compared to the constant microwaves emitted from a magnetron, the microwaves by a solid-state generator are more flexible and controllable in terms of the frequency, power level, and relative phase (if multiple power sources are applied) (Atuonwu and Tassou, 2019, 2018; Gerling, 2016). With a wider range of frequencies for selection, even the standing wave pattern cannot be throughout overcome, the more diverse patterns generated under different frequencies raise the possibility of alleviating hot and cold spots by combining multiple frequencies in one heating process.

Following the idea of utilizing the pattern variation, recent research on the shifting frequency during microwave heating generally employed an in-order frequency shifting algorithm, where the selected frequencies were shifted in incremental or decremental order. Du et al. (2019) conducted experiments on the microwave heating performance using constant frequency (2.45 GHz, which is the frequency used by commercial domestic microwave ovens) and shifting frequency in the range of 2.40 and 2.50 GHz, at the step of different frequency steps and ramping rates. By heating the sample chicken nuggets under different frequency shifting strategies, starting from a refrigerated temperature (5 °C), for 60 s, the experimental results showed that the frequency-shifting heating improved both thermal uniformity and efficiency. In addition, Multiphysics models were implemented based on the oven used for experiments and helped further quantify the improved heating results by using the frequency-shifting method. Similar heating experiments by Dinani et al. (2021), which also investigated the influence by using shifting frequency to heat gellan gum food model from 10 °C for about 240 s, provided the same results compared to the constant frequency (2.45 GHz), the shifting frequency method could yield better heating result. What is more, by applying different ramping rates and shifting time steps, results further implied that the selection of frequencies was more critical to the heating performance than the shifting step and the looping number (calculated as the total heating time divided by the shifting time step). Hereby, the frequency selection should be a more vital research objective for

further study, which can be related to the pattern variation due to frequency diversity, and the way how the patterns were combined and/or interacted. The frequency selection by preliminary modeling investigation by Tang et al. (2018), with the aim to determine frequencies that had high power efficiency for latter shifting, demonstrated that shifting pre-selected frequencies in a microwave process could improve both heating uniformity and efficiency, compared to strategies used only constant frequency and shifted all possible frequencies.

All mentioned research results demonstrated the effectiveness of using multiple frequencies during one microwave heating process, and the frequency selection could further enhance the performance, leaving room for later study on methods to select proper frequencies and design the frequency shifting path. However, the frequency shifting strategies from previous research were all arbitrarily following the order from high to low or from low to high frequency. The shifting paths were not specifically designed. Besides, the solid-state system can also access feedback from the forward and reflected power signals (Atuonwu and Tassou, 2018), making it possible to develop more accommodative scenarios based on the real-time retrieved signals, which was not utilized in previous studies. In addition, this programmable technique can also be coupled with other devices, making accommodative adjustments to the microwave parameters based on the retrieved feedback from multiple sources, e.g., thermal camera or the solid-state generator itself. However, not yet a comprehensive strategy has been proposed to well organize all the useable information and properly design the microwave parameters. Furthermore, all previous strategies were only validated on simple model foods, e.g., gellan gel. Considering the complexity of the realistic foods, it is necessary to evaluate the developed frequency shifting strategies on various food products, and compare the performance between a solid-state oven using the proposed strategies and the current commercial microwave oven.

## **1.5 Specific objectives**

To achieve the proposed project, the goal to develop an automatically adaptive microwave frequency control algorithm was split to be three specific objectives:

1) Demonstrate the complementarity concept of the thermal patterns by different frequencies in a self-assembled solid-state microwave oven.

2) Develop and test dynamic frequency control algorithms with model food, and evaluate the performance of this real-time algorithm.

3) Evaluate the performance of the dynamic frequency algorithm by comprehensively testing various types of foods.



## List of References

Akkari, E., Chevallier, S., Boillereaux, L., 2006. Observer-based monitoring of thermal runaway in microwaves food defrosting. *Journal of Process Control* 16, 993–1001. <https://doi.org/10.1016/j.jprocont.2006.05.005>

Atuonwu, J.C., Tassou, S.A., 2019. Energy issues in microwave food processing: A review of developments and the enabling potentials of solid-state power delivery. *Critical Reviews in Food Science and Nutrition* 59, 1392–1407. <https://doi.org/10.1080/10408398.2017.1408564>

Atuonwu, J.C., Tassou, S.A., 2018. Quality assurance in microwave food processing and the enabling potentials of solid-state power generators: A review. *Journal of Food Engineering* 234, 1–15. <https://doi.org/10.1016/j.jfoodeng.2018.04.009>

Chamchong, M., Datta, A.K., 1999. Thawing of foods in a microwave oven: I. Effect of power levels and power cycling. *Journal of Microwave Power and Electromagnetic Energy* 34, 9–21. <https://doi.org/10.1080/08327823.1999.11688384>

Chen, F., Warning, A.D., Datta, A.K., Chen, X., 2016. Thawing in a microwave cavity: Comprehensive understanding of inverter and cycled heating. *Journal of Food Engineering* 180, 87–100. <https://doi.org/10.1016/j.jfoodeng.2016.02.007>

Clark, D.E., Folz, D.C., West, J.K., 2000. Processing materials with microwave energy. *Materials Science and Engineering A* 287, 153–158. [https://doi.org/10.1016/s0921-5093\(00\)00768-1](https://doi.org/10.1016/s0921-5093(00)00768-1)

DATTA, A.K., DAVIDSON, P.M., 2000. Microwave and Radio Frequency Processing. *Journal of Food Science* 65, 32–41. <https://doi.org/10.1111/j.1750-3841.2000.tb00616.x>

Dinani, T.S., Feldmann, E., Kulozik, U., 2021. Effect of heating by solid-state microwave technology at fixed frequencies or by frequency sweep loops on heating

profiles in model food samples. *Food and Bioproducts Processing* 127, 328–337.  
<https://doi.org/10.1016/j.fbp.2021.03.018>

Ding, D., Cooper, R.A., Pasquina, P.F., Fici-Pasquina, L., 2011. Sensor technology for smart homes. *Maturitas* 69, 131–136.  
<https://doi.org/10.1016/j.maturitas.2011.03.016>

Du, Z., Wu, Z., Gan, W., Liu, G., Zhang, X., Liu, J., Zeng, B., 2019. Multi-physics modeling and process simulation for a frequency-shifted solid-state source microwave oven. *IEEE Access* 7, 184726–184733.  
<https://doi.org/10.1109/ACCESS.2019.2960317>

Geedipalli, S.S.R., Rakesh, V., Datta, A.K., 2007. Modeling the heating uniformity contributed by a rotating turntable in microwave ovens. *Journal of Food Engineering* 82, 359–368.

Gerling, J.F., 2016. Recent developments in solid-state microwave heating. *AMPERE Newsletter Issue* 8–10.

Guzik, P., Kulawik, P., Zając, M., Migdał, W., 2021. Microwave applications in the food industry: an overview of recent developments. *Critical Reviews in Food Science and Nutrition* 0, 1–20. <https://doi.org/10.1080/10408398.2021.1922871>

Huang, L., Sites, J., 2010. New Automated Microwave Heating Process for Cooking and Pasteurization of Microwaveable Foods Containing Raw Meats. *Journal of Food Science* 75, E110–E115. <https://doi.org/10.1111/j.1750-3841.2009.01482.x>

Jin, H., Wang, J., Kumar, S., Hong, J., 2019. Software-Defined Cooking using a Microwave Oven, in: *The 25th Annual International Conference on Mobile Computing and Networking*. ACM, Los Cabos, pp. 1–16. <https://doi.org/10.1145/3300061.3345441>

Kamol, S., Limsuwan, P., Onreabroy, W., 2010. Three-dimensional standing waves in a microwave oven. *American Journal of Physics* 78, 492–495.  
<https://doi.org/10.1119/1.3329286>

Khan, T., 2020. An Intelligent Microwave Oven with Thermal Imaging and Temperature Recommendation Using Deep Learning. *Applied System Innovation* 3, 13. <https://doi.org/10.3390/asi3010013>

Kurniawan, H., Alapati, S., Che, W.S., 2015. Effect of mode stirrers in a multimode microwave-heating applicator with the conveyor belt. *International Journal of Precision Engineering and Manufacturing - Green Technology* 2, 31–36. <https://doi.org/10.1007/s40684-015-0004-0>

Liu, S., Fukuoka, M., Sakai, N., 2013. A finite element model for simulating temperature distributions in rotating food during microwave heating. *Journal of Food Engineering* 115, 49–62. <https://doi.org/10.1016/j.jfoodeng.2012.09.019>

Liu, S., Ogiwara, Y., Fukuoka, M., Sakai, N., 2014. Investigation and modeling of temperature changes in food heated in a flatbed microwave oven. *Journal of Food Engineering* 131, 142–153. <https://doi.org/10.1016/j.jfoodeng.2014.01.028>

Luan, D., Wang, Y., Tang, J., Jain, D., 2017. Frequency Distribution in Domestic Microwave Ovens and Its Influence on Heating Pattern. *Journal of Food Science* 82, 429–436. <https://doi.org/10.1111/1750-3841.13587>

Metaxas, A.C., Meredith, R.J., 1983. *Industrial Microwave Heating*. P. Peregrinus, London.

Nasswetrová, A., Nikl, K., Zejda, J., Sebera, V., Klepárník, J., 2013. The analysis and optimization of high-frequency electromagnetic field homogeneity by mechanical homogenizers within the space of wood microwave heating device. *Wood Research* 58, 11–24.

Pitchai, Krishnamoorthy, Birla, S.L., Jones, D., Subbiah, J., 2012. Assessment of Heating Rate and Non-uniform Heating in Domestic Microwave Ovens. *Journal of Microwave Power and Electromagnetic Energy* 46, 229–240. <https://doi.org/10.1080/08327823.2012.11689839>

Pitchai, K., Birla, S.L., Subbiah, J., Jones, D., Thippareddi, H., 2012. Coupled electromagnetic and heat transfer model for microwave heating in domestic ovens. *Journal of Food Engineering* 112, 100–111. <https://doi.org/10.1016/j.jfoodeng.2012.03.013>

Plaza-González, P., Monzó-Cabrera, J., Catalá-Civera, J.M., Sánchez-Hernández, D., 2005. Effect of mode-stirrer configurations on dielectric heating performance in multimode microwave applicators. *IEEE Transactions on Microwave Theory and Techniques* 53, 1699–1705. <https://doi.org/10.1109/TMTT.2005.847066>

Plaza-González, P., Monzó-Cabrera, J., Catalá-Civera, J.M., Sánchez-Hernández, D., 2004. New approach for the prediction of the electric field distribution in multimode microwave-heating applicators with mode stirrers. *IEEE Transactions on Magnetics* 40, 1672–1678. <https://doi.org/10.1109/TMAG.2003.821560>

Ramaswamy, H., Tang, J., 2008. Microwave and radio frequency heating. *Food Science and Technology International* 14, 423–427. <https://doi.org/10.1177/1082013208100534>

Research and Markets, 2022. *Global Microwave Oven Market, By Product (Convection, Grill and Solo), By Application (Household and Commercial), By Structure (Free-Standing and Built-in), By Region, Competition, Forecast & Opportunities, 2026F.*

Sebera, V., Nasswetrová, A., Nikl, K., 2012. Finite Element Analysis of Mode Stirrer Impact on Electric Field Uniformity in a Microwave Applicator. *Drying Technology* 30, 1388–1396. <https://doi.org/10.1080/07373937.2012.664800>

Tang, Z., Hong, T., Liao, Y., Chen, F., Ye, J., Zhu, H., Huang, K., 2018. Frequency-selected method to improve microwave heating performance. *Applied Thermal Engineering* 131, 642–648. <https://doi.org/10.1016/j.applthermaleng.2017.12.008>

Thostenson, E.T., Chou, T.-W., 1999. Microwave processing: fundamentals and applications, in: *Composites Part A: Applied Science and Manufacturing*. pp. 1055–1071. [https://doi.org/10.1016/S1359-835X\(99\)00020-2](https://doi.org/10.1016/S1359-835X(99)00020-2)

Trieu Minh, V., Khanna, R., 2018. Application of Artificial Intelligence in Smart Kitchen. *International Journal of Innovative Technology and Interdisciplinary Sciences* www. IJITIS.org 1, 1–8. <https://doi.org/10.15157/IJITIS.2018.1.1.1-8>

Vriezinga, C.A., Sánchez-Pedreno, S., Grasman, J., 2002. Thermal runaway in microwave heating: A mathematical analysis. *Applied Mathematical Modelling* 26, 1029–1038. [https://doi.org/10.1016/S0307-904X\(02\)00058-6](https://doi.org/10.1016/S0307-904X(02)00058-6)

Wiedenmann, O., Ramakrishnan, R., Kiliç, E., Saal, P., Siart, U., Eibert, T.F., 2012. A multi-physics model for microwave heating in metal casting applications embedding a mode stirrer. 2012 the 7th German Microwave Conference, GeMiC 2012.

Yakovlev, V. v., 2018. Effect of frequency alteration regimes on the heating patterns in a solid-state-fed microwave cavity. *Journal of Microwave Power and Electromagnetic Energy* 52, 31–44. <https://doi.org/10.1080/08327823.2017.1417105>

Yang, H.W., Gunasekaran, S., 2001. Temperature Profiles in a Cylindrical Model Food During Pulsed Microwave Heating. *Journal of Food Science* 66, 998–1004. <https://doi.org/10.1111/j.1365-2621.2001.tb08225.x>

Yang, R., Chen, Q., Chen, J., 2021. Comparison of heating performance between inverter and cycled microwave heating of foods using a coupled multiphysics-kinetic model. *Journal of Microwave Power and Electromagnetic Energy* 55, 45–65. <https://doi.org/10.1080/08327823.2021.1877244>

Ye, J., Hong, T., Wu, Y., Wu, L., Liao, Y., Zhu, H., Yang, Y., Huang, K., 2017. Model Stirrer Based on a Multi-Material Turntable for Microwave Processing Materials. *Materials* 10, 95. <https://doi.org/10.3390/ma10020095>

Zion Market Research, 2018. Microwavable Foods Market By Type (Chilled Microwavable Foods, Shelf Stable Microwavable Foods, and Frozen Microwavable Foods): Global Industry Perspective, Comprehensive Analysis, and Forecast, 2017 – 2024.

**CHAPTER II**  
**DEVELOPMENT OF A COMPLEMENTARY-FREQUENCY**  
**STRATEGY TO IMPROVE MICROWAVE HEATING OF GELLAN**  
**GEL IN A SOLID-STATE SYSTEM**

A version of this chapter was originally published by Yang, R., Fathy, A. E., Morgan, M. T., & Chen, J:

Yang, R., Fathy, A. E., Morgan, M. T., & Chen, J. (2022). Development of a complementary-frequency strategy to improve microwave heating of gellan gel in a solid-state system. *Journal of Food Engineering*, 314 (April 2021), 110763. <https://doi.org/10.1016/j.jfoodeng.2021.110763>.

As the first author of this research article, I was the main contributor to Conceptualization, Methodology, Data curation, Investigation, Software, Visualization, Writing of the manuscript. Dr. Jiajia Chen, as the major professor and corresponding author, contributed to Conceptualization, Investigation, Supervision, Project administration, Funding acquisition, Writing - Reviewing and Editing of the manuscript. The co-authors, as the committed members of the Ph.D. program, offered suggestion in the experiment design, provided help in manuscript revising.

## **2.1 Abstract**

As a helpful step towards the future development of a solid-state microwave system that can dynamically control microwave source parameters to deliver better heating performance, a complementary-frequency heating strategy has been developed and will be discussed here. The proposed complementary-frequency heating strategy is based on potential microwave heating uniformity enhancement through microwave frequency shifting during heating has shown promise to improve the microwave heating performance. The average temperature and heating uniformity results of this strategy were compared to conventional heating strategies like Fixed-Frequency and Sweeping-Frequency strategies. Typically, the Complementary-Frequency strategy could selectively use specific frequencies in the microwave heating process. These frequencies could be identified based on their associated complementary temperature profile of the top surface



of the food product collected by a thermal imaging camera and sequenced in a specific order dictated by a predefined algorithm. The results indicated that both the Sweeping-Frequency and the Complementary-Frequency strategies could uniformly heat food products more than the Fixed-Frequency strategy. Meanwhile, the Complementary-Frequency strategy can trade-off microwave power absorption efficiency and heating uniformity to deliver a higher heating rate than the Sweeping-Frequency strategy does.

**Keywords:** microwave heating, temperature uniformity, solid-state, frequency shifting, complementary

## 2.2 Introduction

Food processing using domestic microwave ovens could produce non-uniform volumetric temperature distribution, which has been a big concern. Nonuniformity could lead to various problems on the final product, including unexpected sensory quality change and nutrient degradation at random hot spots, and potential microbial survival at cold spots (Alsuhaimeh et al., 2014; Atuonwu and Tassou, 2018; Bornhorst et al., 2017a; F. Chen et al., 2016; Huang et al., 2015; Rougier et al., 2014). This nonuniformity concern comes as a result of the inherent standing waves within the microwave cavity excited by magnetrons that are currently used as microwave generators, where the electric field is not uniformly distributed within the oven cavity and generates hot and cold spots in the food products. Additionally, thermal runaways could occur because of the sharp change of the temperature-dependent material properties (Zhu et al., 2012), causing severe nonuniformity. The hot spots of the food products usually have high electric loss factors and convert more electromagnetic energy to heat at these locations.

In order to improve the microwave heating uniformity, different approaches to addressing the problem due to standing wave patterns have been proposed, including modifying the microwave oven cavity configuration. For example, a glass turntable and

mode stirrer have been used in domestic microwave ovens to disturb the electromagnetic wave distribution within the cavity and cause multi-modes (hot and cold spots) during the heating process. Based on the success of these two rotatory devices, several other studies are currently undergoing to improve the food-microwave interactions even further, including a multi-material turntable (Ye et al., 2017), rotating metal patch (Meng et al., 2018), rotary radiation structure (Zhu et al., 2018), and different types of mode stirrers (Kurniawan et al., 2015; Plaza-González et al., 2005; Sebera et al., 2012; Wiedenmann et al., 2012). In other words, upon increasing the relative position between the food and the microwave source, hot and cold spot locations may vary with time and lead to relatively lower heating nonuniformity. However, such improvement is limited and uncontrollable. For example, the rotated foods on the turntable often have over-heated edges and under-heated centers (Chen et al., 2015; J. Chen et al., 2016; Pitchai et al., 2015). However, the mode stirrers repeatedly have unpredictable heating results because of the complicated interactions between the foods and the randomly disturbed waves during the heating process (Kurniawan et al., 2015; Meng et al., 2018; Ye et al., 2017).

In addition to modifying microwave oven configurations, the adaption of optimized microwave source parameters (i.e., frequencies and relative phases in case of more than one source) has shown great promise in improving microwave heating performance (Yang et al., 2020). This success is related to the recent development of solid-state microwave source technology that has enabled accurate control of various microwave operating parameters. The semiconductor-based Gallium nitride (GaN) transistors can operate at high temperature and voltages, and are excellent candidates for high power amplification at microwave frequencies. Technically, compared to the traditional magnetron generator, the solid-state technology has shown its advantages in longer lifetime, lower operational voltage, frequency accuracy and stability, independent control over multiple sources and accessibility to scenario feedback (Atuonwu and Tassou, 2018). The flexible and reliable control over the operational parameters of the

solid-state generator provides more targeted heat delivery to overcome the nonuniformity issue by heating under fixed frequency (Dinani et al., 2021).

Previous research showed that operating microwave frequency selection has significantly influenced the microwave heating patterns (Luan et al., 2017). This observation led to microwave heating experiments with shifting frequencies, which was demonstrated to improve food temperature uniformity. Du et al. (2019) compared the microwave heating uniformity of chicken block samples using two heating strategies: fixed frequency (2.45 GHz) and shifting frequencies (from 2.40 to 2.50 GHz with different frequency steps and ramping rates) using both computer simulation and experimental validation. The results showed that orderly shifting the operating frequency could improve heating uniformity. Dinani et al. (2021) conducted microwave heating experiments with the gellan gum food model using a solid-state microwave system to compare the heating performance between the fixed frequencies strategy (in the range of 2.40 to 2.50 GHz) and sweeping frequencies strategy with different numbers of frequencies and/or time steps. Their results demonstrated that the application of frequency sweep loops, regardless of the time steps or the number of the loops, could improve both the temperature uniformity and power absorption.

Alternatively, instead of shifting frequencies in the whole frequency range, Tang et al. (2018) only shifted frequencies among pre-selected frequencies that had higher heating efficiencies (smaller electromagnetic scattering S11 parameters, bigger average temperature, and average electric field). These frequencies were selected using experimentally-validated computer simulation models for microwave heating, and the results showed that shifting between the pre-selected frequencies not only improves the heating uniformity but also increases the average temperature. Yakovlev (2018) made similar observations but based on modeling only (i.e., no experimental validation) of a multiple-source solid-state microwave system. The successes of the frequency selection and shifting algorithms illustrate the feasibility and importance of using a shifting algorithm for frequency selection in improving heating uniformity.

Although previous frequency selection and shifting algorithms showed promises in improving microwave heating performance, these algorithms can still be further improved. It is worth noting that while microwave heating of foods showed different hot and cold spot locations at different frequencies, it is still promising to not only use all potential frequencies or select frequencies with high efficiency but also choose frequencies that have complementary heating patterns and shift the operating frequencies to them in a proper order to further improve the heating performance. Thus, there is a need to develop better frequency selection (map) and efficient shifting algorithms that utilize the complementary characteristics of microwave frequencies.

The objectives of this study are to:

- 1) evaluate the effect of using fixed frequencies on heating performance (temperature and heating uniformity);
- 2) develop complementary-frequency shifting strategies using temperature profiles collected at fixed frequencies;
- 3) compare the microwave heating performance among different frequency-shifting strategies with fixed, sweeping, and complementary frequencies.

## **2.3 Material and Methods**

### **2.3.1 Microwave system**

For this study, a domestic microwave oven cavity (Panasonic Model NN-SN936W) was modified, whose magnetron source was replaced with a solid-state microwave generator (PA-2400-2500MHz-200W-4, Junze Technology). The generator has four power sources connected to the oven through four separate waveguides (CWR340 CentricRF) launcher ports (Figure II-1), and the phase, power level, and frequency of each source can be independently controlled in real-time. In this study, only one port was used to initially study the effect of single-port frequency control. The port

was fed by the maximum available power output of 200 W through one of these launching ports in this study.

### **2.3.2 Model food preparation**

The gellan gel sample was used as a model food in this study for its preparation ease, its homogeneity for reducing experimental error, and adaptability for representing a variety of food products, such as vegetables, meat, and pasta (Zhang et al., 2015a). The gellan gel sample consisted of 1% gellan gum powder (CP Kelco U.S., Inc., Atlanta, GA), 0.17% calcium chloride (Honeywell Research Chemicals, Muskegon, MI, USA), and deionized water. The calcium chloride was added to generate a firm and stable gel sample that is suitable for cutting (Bornhorst et al., 2017b). In order to prepare the gel sample, the gellan gum powder was stirred with deionized water at 90°C for 15 min; CaCl<sub>2</sub> was then added to the hot solution (Birla et al., 2009). The mixture was stirred for another 10 min, and then 300 g of this prepared sample was quickly poured into food containers. The hot samples in the food containers were kept at room temperature for 30 minutes to ensure gel setting and stored at 0 °C overnight in a refrigerator for later use. The dielectric properties of the gellan gel from 2.40 to 2.50 GHz at room temperature (23 °C) were measured by a vector network analyzer (Agilent E8363B, Agilent Technologies, Inc., Santa Clara, USA), and 85070B Open-End Coaxial Dielectric Probe (Agilent Technologies, Santa Clara, USA). The samples were placed in a plastic tray, same as in Figure II-1. The measurements were carried out using a procedure reported before (Zhang et al., 2015a). The dielectric properties were shown in Figure II-2. Both the dielectric constant and loss factor increased slightly with frequency, and the penetration depth decreased slightly with frequency from 3.03 to 2.97 cm.

### 2.3.3 Microwave heating performance evaluation

The refrigerated model foods were placed on the top of the glass turntable at center (the motor coupler was removed to disable the rotation of the turntable). The foods were heated from 0 °C for six minutes with the right-side port activated (200 W) using different frequency-shifting strategies (as described in section 2.4). After heating, the samples were quickly removed from the containers and bisected right in the middle with a slicer. The temperature profiles of both the top and middle layers of each sample were captured by a thermal image camera (FLIR C3, Boston, MA) and exported as value files in 320 ×240 pixels by software FLIR Tools (2020 © FLIR® Systems, Inc.) for further analysis.

In these temperature profiles, different scene regions were identified, and only the temperature values within the food regions were selected and used for evaluation. Owing to the slight mismatch of food regions among different thermal imaging processes, an open-source Image module from Pillow library (Pillow, 2021) in Python was used to resize the food temperature profiles to be 320 ×240 pixels. The effect of resizing on the temperature accuracy was evaluated by comparing the raw pixel temperature profiles and the resized ones at different frequencies and replications using t-test. The p-values for each experiment were all greater than 0.99, as shown in Figure II-3, indicating few errors caused by the resizing process. The average temperature value was determined from the average temperature of 320×240 pixels data file for each thermal image. The spatial variation values were determined from the standard deviation value of each thermal imaging temperature profile. The heating uniformity was assessed by the heating uniformity index (*HUI*) following Eq. (II-1) (Alfaifi et al., 2014):

$$HUI = \frac{\frac{1}{S_{layer}} \int_{S_{layer}} \sqrt{(T - T_{ave})^2} dS_{layer}}{\Delta T_{ave}} \quad \text{(II-1)}$$

where  $S_{layer}$  is the area of each layer, and  $\Delta T_{ave}$  (°C) is the mean temperature rise over the layer after heating. A smaller *HUI* value indicates a more uniform heating result.

### 2.3.4 Microwave frequency-shifting strategies

Three types of microwave frequency-shifting strategies were used in this study to compare their microwave heating uniformity. In the first strategy, a fixed frequency throughout the whole microwave heating process (6 minutes) without changing was used as a reference. Eleven microwave frequencies from 2.40 to 2.50 GHz with a 0.01 GHz step were evaluated individually. Preliminary experiments showed a high microwave reflection (> 25%) at the following frequencies (2.48, 2.49, and 2.50 GHz), and the microwave generator shut off automatically for system protection; thus, these frequencies were excluded in our experiment. Therefore, microwave frequencies within the 2.40 to 2.47 GHz frequency range with a step of 0.01 GHz were used in this Fixed-Frequency strategy.

In the second strategy, orderly-sweeping shifting frequencies that swept microwave frequencies between 2.40 and 2.47 GHz with a step of 0.01 GHz in an incremental, decremental, and mixed order were used. This strategy is referred to as the Sweeping-Frequency strategy. Two different shifting rates (45 s and 15 s) were applied, as shown in Figure II-4 A-D. The total heating time was also six minutes.

The third strategy was developed based on the complementary top layer heating profiles of different fixed frequencies, following the two specifically designed algorithms shown in Figure II-5 and Figure II-6. The key concept of the Complementary-Frequency strategy is to find a complementary-frequency set that could superimpose hot and cold spot heating patterns to deliver a better heating performance. The input data to the Complementary-Frequency algorithms were the temperature profiles obtained from the Fixed-Frequency strategy. In Algorithm I (Figure II-5), within all the profiles, the frequency that had the lowest *HUI* was chosen as an initial frequency. To determine the next complementary-frequency, all available profiles at different frequencies were superimposed with the initial frequency separately, and the updated *HUI* values based on each superimposed profile were calculated. The superimposed effect from two consecutive heating steps was calculated as the sum of the two corresponding

temperature profiles. The second frequency that complements the initial frequency was determined to be the one that resulted in the smallest updated *HUI*. The superimposed steps were repeated until enough frequencies were selected for a six-minute heating process.

In Algorithm II (shown in Figure II-6 and noted by Complementary-Frequency II), we further consider the microwave power absorption efficiency aside from the heating uniformity factor that is investigated by the Complementary-Frequency I. The key point of this strategy is to balance between microwave power absorption and heating uniformity, where some frequencies with higher microwave power absorption (temperature increase) may be selected while sacrificing little uniformity. Similar to Algorithm I, Algorithm II start from the initial frequency that has the lowest *HUI* value. Then, the frequency with the smallest superimposed *HUI* (similar to Algorithm I) was utilized as a baseline frequency, which may not be determined as the second frequency. Furthermore, two additional parameters (specifically the increased average temperature ( $\Delta T$ ) of the surface and the increased standard deviation of the top surface average temperature ( $\Delta STD$ )) for all the possible superimposed frequencies were calculated and compared to the baseline frequency. A qualified frequency must yield a change ratio of the average temperature larger than 5%, and also a change ratio of the standard deviation smaller than 5%. Otherwise, the second frequency would still be the baseline frequency (i.e., the one with the smallest superimposed *HUI* value). If multiple frequencies meet the change ratio criteria, the one with the smallest *HUI* change ratio is selected. To be clear that, the baseline frequency is determined for each superimposed step. The superimposed steps are repeated until enough frequencies are determined for the six-minute heating process. Two shifting rates (45 s and 15 s) are used in this study for the Complementary-Frequency I & II strategies.



### **2.3.5 Data analysis**

In our study, all microwave heating experiments with various frequency strategies were conducted in triplicate. Data are presented as the mean  $\pm$  standard deviation of three replicates. Statistical analysis was performed by using the one-way analysis of variance (ANOVA) followed by HSD Tukey's post-test with a 95% confidence interval using GraphPad Prism Version 8.3 (GraphPad Software, La Jolla California USA). *p* values smaller than 0.05 were considered statistically significant.

## **2.4 Results and Discussion**

### **2.4.1 Temperature profiles for Fixed-Frequency heating**

The thermal images of the top and middle layers taken after six minutes of microwave heating with various fixed frequencies are shown in Figure II-7. The results showed that microwave frequency influenced the heating patterns considerably. Generally, all the hot areas (light color in these images) were located at or close to the edges or the corners of the samples. However, the locations of the cold areas (dark color in images) varied considerably depending on the heating frequency. For microwave heating with frequency values 2.40, 2.44, 2.47 GHz, the cold spots were located at the edge of the samples; while for other frequencies, they tend to be in the central areas at different layers. The effect of frequency on microwave heating pattern is contributed by both the microwave propagation characteristics within the cavity including the excited modes, and the frequency and temperature-dependent dielectric properties of the food, as well as their interactions within the oven cavity. The microwave signal wavelength in air varies from 12.49 to 11.99 cm between 2.40 to 2.50 GHz, which influences the electric field distribution within the oven cavity and excited modes. Meanwhile, any slight change of dielectric properties also influences the interactions between microwave and food products at different frequencies and temperature, which would change the heating pattern as well. Similar patterns of data diversity caused by using different heating

frequencies were also reported in previous studies. For example, Luan et al. (2017) reported simulated stationary microwave heating results under different operational frequencies, where both the heating patterns and power absorption levels changed a lot because of the frequency change. In the same investigation, similar patterns between the top and middle layers were also reported. This is consistent with our experimental results shown in Figure II-7, where the hot and cold spots generally matched well in the slices of top and middle layers. This might be related to the utilized sample thickness (~2.2 cm) is relatively smaller than the penetration depth (~3.0 cm), which allowed microwaves to penetrate more into the product. The difference in how the patterns were horizontally distributed among the various fixed-frequency heating scenarios exhibited a potential scenario that could take advantage of grouped complementary frequencies to improve microwave heating uniformity.

In addition to the heating patterns of hot and cold spots, microwave frequencies also influenced the heating performance (average temperature and heating uniformity for both top and middle layers). Figure II-8 summarizes the average temperature and *HUI* values of top and middle layers that were determined from the thermal imaging profiles for samples heated using fixed frequencies. The average temperatures for the top surface ranged from  $28.64 \pm 0.21$  (at 2.46 GHz) to  $34.87 \pm 0.11$  °C (at 2.44 GHz) for eight frequencies between 2.40 and 2.47 GHz. At the middle layer, the average temperatures were between  $28.60 \pm 0.35$  (at 2.46 GHz) and  $36.91 \pm 0.65$  °C (at 2.43 GHz) for different frequencies. The *HUI* values for the top surface were between  $0.212 \pm 0.008$  (at 2.43 GHz) and  $0.315 \pm 0.017$  (at 2.46 GHz). While for the middle layer, the *HUI* values were between  $0.237 \pm 0.012$  (at 2.43 GHz) and  $0.362 \pm 0.034$  (at 2.46 GHz).

Table II-1 summarizes the heating performance of the combined top and middle layers. At 2.46 GHz, the sample had the lowest average temperature and highest *HUI* compared to other frequencies, with about 50% microwave power absorbed, which was considerably lower than that at other frequencies. This implied that constant frequency at 2.46 GHz led to a low heating efficiency and had worse heating uniformity, and was

unlikely to contribute to the improvement of the overall temperature uniformity. On the contrary, constant frequencies of 2.41, 2.43, and 2.47 GHz resulted in a better heating uniformity, and the frequencies of 2.44 and 2.45 GHz led to higher heating average temperatures of the combined top and middle layers compared to other frequencies. These frequencies are highly possible to help improve the heating performance if their heating patterns are complementary to each other.

#### **2.4.2 Complementary-Frequency strategies**

Two types of complementary shifting strategies were developed following the procedures described in the two algorithms ( Figure II-5 and Figure II-6) using the preliminarily determined temperature profiles at various constant frequencies (2.40 to 2.47 GHz), as shown in Figure II-9. Two frequency-shifting rates (45 s and 15 s) were also used in the two Complementary-Frequency shifting strategies.

The Complementary-Frequencies I based on *HUI* only (Algorithm I) with shifting rates of 45 s and 15 s are shown in Figure II-9 A&B, respectively. It can be observed that the frequencies used in the shifting rates of 45 s (Figure II-9A) were the first eight frequencies from those used in the rates of 15 s (Figure II-9B). This is reasonable because the same Algorithm I was used, and the shifting rate of 45 s only needed eight frequencies for a six-minute heating process, while the shifting rate of 15 s needed 16 more frequencies after the first eight. For both shifting rates, frequencies of 2.41, 2.43, and 2.47 GHz were extensively used because of their significantly smaller *HUI* values (Table II-1). Their complementary spatial temperature distributions are shown in Figure II-7, which enabled this Complementary-Frequency strategy to achieve potential minimized *HUI* value after heating. However, it is worth noting that the top-layer average temperatures were also relatively low for these three frequencies. Thus, the microwave absorption efficiency might be sacrificed for more uniform heating.

To deal with the potential low microwave power absorption in the Complementary-Frequency strategy based on Algorithm I, Algorithm II (Figure II-6) that balanced the microwave power absorption (average temperature increase) and heating uniformity (spatial variations) was used to develop the Complementary-Frequency II strategy, as shown in Figure II-9 C&D for two shifting rates of 45 s and 15 s, respectively. Compared with the Complementary-Frequency I strategy, the Complementary-Frequency II strategy had several same frequencies (2.41, 2.43, and 2.47 GHz) at the beginning of the heating process because of their relatively more uniform heating. While, at the later period of the heating process, the Complementary-Frequency II strategy selected more frequencies from 2.43, 2.44, and 2.45 GHz because of the incorporation of the average temperature increase in the top layers in Algorithm II. As seen from Figure II-8 and Table II-1, the frequencies of 2.43, 2.44, and 2.45 GHz had significantly higher temperature profiles than other frequencies.

### **2.4.3 Microwave heating performance using different heating strategies**

The model foods were heated using three types of Fixed-Frequency, Sweeping-Frequency, and Complementary-Frequency with two shifting rates of 15 s and 45 s for six minutes. The microwave heating performances (average temperature and heating uniformity at the top and middle layers) were compared among these heating strategies.

#### **2.4.3.1 Comparison between Fixed-Frequency and Sweeping-Frequency strategies**

The temperature profiles at the top and middle layers are summarized in Figure II-7 for the Fixed-Frequency strategy and in Figure II-10 for the Sweeping-Frequency strategy. As discussed previously in Figure II-7, hot spots were typically observed at some corners or edges, and cold spots were observed at the center region of the model foods for the Fixed-Frequency strategy. Although the Sweeping-Frequency strategy also heated the corners and edges more than the central regions, as shown in Figure II-10, the

spatial temperature distributions were more uniform than that of the Fixed-Frequency strategy. Relative lower hot spot temperatures and higher cold spot temperatures were observed in the Sweeping-Frequency Strategies. Du et al. (2019) orderly swept microwave frequency from 2.40 to 2.50 GHz with various shifting rates and evaluated the effect of the frequency-shifting on the microwave heating performance of chicken blocks after 60 s heating. The results showed that sweeping-frequency could improve the microwave heating uniformity and efficiency when compared to the Fixed-Frequency strategy. However, the improvement was dependent on the frequency-sweeping directions (from 2.40 to 2.50 GHz versus from 2.50 to 2.40 GHz) and the frequency-shifting rates.

In this study, various sweeping-frequency sub-strategies (incremental, decremental, and mixed) with two shifting rates of 45 s and 15 s were evaluated, and all of them showed better heating uniformity than the Fixed-Frequency strategy. Among these sub-strategies, although the spatial temperature patterns showed a slight difference, as shown in Figure II-9, the average temperature showed no significant difference in top and middle layers, respectively. For example, as summarized in Figure II-11 for the Sweeping-Frequency strategy (Incremental-45, Decremental-45, Incremental-15, and Mixed-15), all scenarios have realized an improvement of the heating uniformity compared to the Fixed-Frequency heating (Figure II-8) at both top and middle layers. The average temperatures were between 31.98 and 32.61 °C for the top layers and between 33.29 and 35.22 °C for the middle layers. Compared to Fixed-Frequency heating scenarios (Figure II-8), there was a similar top-layer temperature but a relatively lower middle-layer temperature, which indicated a smaller difference between the top and middle layers when applying the Sweeping-Frequency heating strategy, and therefore a decreased overall nonuniformity, as shown in Table II-2.

#### 2.4.3.2 Comparison between Sweeping-Frequency and Complementary-Frequency strategies

In addition to the Sweeping-Frequency strategy, this study further developed and evaluated the Complementary-Frequency strategy. Note that there were two Complementary-Frequency sub-strategies: the Complementary-Frequency (I) only included frequencies whose superimposed temperature profiles had minimal *HUI* values; the Complementary-Frequency (II) selected frequencies that could balance both the microwave power absorption (temperature increase) and the heating uniformity.

As shown in Figure II-11, generally, the Complementary-Frequency (I) heating strategy did not show significantly different average temperatures in both top and middle layers (Figure II-11 A&C) and *HUI* (Figure II-11 B&D) than the Sweeping-Frequency strategy for both shifting rates of 45 s and 15 s. Although the *HUI* values of the Complementary-Frequency (I) heating scenario at both top and middle layers were lower than those of the Sweeping-Frequency strategy, respectively, the difference was not significant. As summarized in Table II-2, the overall microwave heating performance (average temperature, *HUI* and power absorption rate based on combined top and middle layers data) of the Complementary-Frequency (I) heating scenario also did not show a significant difference from that of the Sweeping-Frequency strategy, although it was better than the Fixed-Frequency strategy. The fact that the Complementary-Frequency (I) strategy did not improve the heating uniformity when compared to the Sweeping-Frequency might be due to slightly lower microwave power absorptions in the Complementary-Frequency (I) strategy. As seen from the Complementary-Frequency (I) profile in Figure II-9 A&B, 2.47 GHz contributed about 37.5% of the processing time. However, the microwave power absorption was slightly lower than most of the other frequencies, as observed from the average temperature increase in Table II-1. The lower average temperature increase at 2.47 GHz may lead to a slightly higher *HUI* values for the Complementary-Frequency (I) strategy than the Sweeping-Frequency strategy.

Considering the limitation of the Complementary-Frequency (I) strategy, the Complementary-Frequency (II) strategy was developed to balance between the microwave power absorption and heating uniformity. As shown in Figure II-11, the Complementary-Frequency (II) strategy had a significantly higher average temperature than the Sweeping-Frequency strategy for both top and middle layers. The higher average temperatures of the Complementary-Frequency (II) heating scenarios were observed because of the incorporation of frequencies that has relatively higher microwave power absorption (e.g., 2.44 and 2.45 GHz), which also sacrificed the heating uniformity slightly. Based on the combined top- and middle-layer results, the Complementary-Frequency (II) heating scenarios had a significantly higher average temperature increase than the Sweeping-Frequency heating scenarios, while with similar or slightly higher *HUI* values. Thus, the proposed Complementary-Frequency (II) strategy that considered both power absorption efficiency and temperature uniformity could properly determine a better shifting sequence of frequencies to improve the heating performance where the power efficiency was significantly increased while the *HUI* was maintained at a low level.

#### 2.4.3.3 Effect of frequency-shifting time steps on microwave heating performance

Both the Sweeping-Frequency and Complementary-Frequency strategies used two frequency-shifting time steps of 45 s and 15 s. For the frequency-shifting time steps of 45 s scenarios, the average temperatures (Figure II-11A) were between 30.41 and 35.08 °C for top layers and between 34.16 and 38.27 °C for the middle layers. Compared to the frequency-shifting time steps of 45 s scenarios, both the top and middle temperatures of the 15 s scenarios increased slightly. The *HUI* values of the frequency-shifting time step of 15 s scenarios were also higher than those of the 45 s scenarios. When combining the top and middle layers of temperature for comparison, both the average temperature and *HUI* values increased slightly but not significantly for the smaller shifting time step

scenario, as shown in Table II-2. Previous studies from Du et al. (2019) and Dinani et al. (2021) also had similar conclusions.

#### **2.4.4 Usefulness, limitations, and future work**

This study showed that different microwave frequencies could lead to different heating patterns with different hot and cold spot locations. The microwave frequencies can be selected and developed as a Complementary-Frequency strategy using the top surface heating profiles. The Complementary-Frequency strategy could deliver better heating performance than using fixed frequency and orderly sweeping frequencies. The results are helpful for food scientists to better understand the solid-state microwave heating process and are useful for future development of the domestic microwave oven next generation using a solid-state microwave system that could dynamically change microwave frequencies to achieve better heating performances. For example, if the heating patterns at different frequencies can be collected by a thermal imaging camera that is mounted on the top of the oven cavity at the beginning of the heating process, these heating patterns can be processed simultaneously and used to develop the dynamic control heating algorithms.

There are several limitations in this study that can be further improved to develop futuristic solid-state microwave technology. First of all, the microwave power of the single port was only 200 W, which is much lower than current commercial high power domestic microwave ovens (~1200 W). The lower microwave power caused a low heating rate and longer heating time. In this study, the average temperature increased about 33 °C during a six-minute microwave heating process. A high-power microwave source may need to be used for future research but should not influence the conclusions made from this study.

Secondly, the temperature profiles used for algorithm development were collected from heating the food products with a uniform initial temperature. However, during a real



heating process, the spatial temperature increases non-uniformly, which may change the dielectric properties and thus the real heating performance. Thus, the spatial temperature increase contributed by a frequency in a real heating process might be different from the pre-collected temperature profiles from fixed frequencies. This difference might be a problem for developing algorithms for frozen food products, whose dielectric properties change significantly from frozen to thawed states. In this study, the gellan gel was heated from refrigerated temperature, where the material characteristics did not significantly change, hence it did not substantially influence the algorithm development.

Thirdly, the Complementary-Frequency strategy developed in this study used the temperature profiles at the end of heating processes with various fixed frequencies. To achieve dynamic control frequencies during a microwave heating process, the temperature profiles need to be dynamically collected during the heating. A low-cost thermal imaging system mounted to the solid-state microwave system may be necessary. Khan (2020) modified a commercial microwave oven cavity into an intelligent microwave oven by mounting a thermal image camera that could detect the heating performance of food products in the oven. A similar modification to the solid-state microwave system can be conducted for future work.

Moreover, a more robust control algorithm that could collect and process the dynamic thermal images and simultaneously control multiple parameters (e.g., frequency, relative phase, and power) of multiple microwave sources is necessary. This strategy can be incorporated into an intelligent solid-state microwave system to deliver desired heating performance.

## **2.5 Conclusions**

This study compared the heating performances of a model food (gellan gel) after six-minute microwave heating among three types of frequency-shifting strategies. The Fixed-Frequency used various fixed frequencies (2.40 to 2.47 GHz with a step of 0.01

GHz) throughout the whole heating process. The Sweeping-Frequency orderly swept the microwave frequencies increasingly from 2.40 to 2.47 GHz, decreasingly from 2.47 to 2.40 GHz, and back and forth between 2.40 to 2.47 GHz. The Complementary-Frequency specifically selected several frequencies based on their complementary heating profiles collected by thermal imaging profiles of fixed frequencies. The key conclusions of this study are:

- Different microwave frequencies influenced the heating patterns significantly with different hot and cold spot locations.
- The Complementary-Frequency I strategy that considered only *HUI* delivered a similar heating performance to the Sweeping-Frequency strategy, while the Complementary-Frequency II strategy that also included power absorption efficiency resulted in a higher temperature increase than and similar heating uniformity to the Sweeping-Frequency strategy.
- Two frequency-shifting time steps of 15 s and 45 s were compared for different Sweeping-Frequency and Complementary-Frequency strategies and showed little difference.
- The Complementary-Frequency strategy is useful for the future development of intelligent solid-state microwave systems to achieve dynamic control of microwave parameters and deliver desired heating results.

## **2.6 Acknowledgments**

This project (or patent) is based on research that was supported by the Tennessee Agricultural Experiment Station with funding from the USDA National Institute of Food and Agriculture Hatch Multistate Research capacity funding program (Accession Number 1023982) and the USDA National Institute of Food and Agriculture, AFRI project (proposal number 2020-04022). The authors also thank CP Kelco U.S., Inc. for providing

the gellan gum powder and Mr. Peter Alley for assisting the solid-state microwave system fabrication.

## List of References

- Alfaifi, B., Tang, J., Jiao, Y., Wang, S., Rasco, B., Jiao, S., Sablani, S., 2014. Radio frequency disinfestation treatments for dried fruit: Model development and validation. *Journal of Food Engineering* 120, 268–276. <https://doi.org/10.1016/j.jfoodeng.2013.07.015>
- Alsuhaime, H.S., Vojisavljevic, V., Pirogova, E., 2014. Effects of low power microwaves at 1.8, 2.1, and 2.3 GHz on l-Lactic dehydrogenase and Glutathione peroxidase enzymes. *Journal of Electromagnetic Waves and Applications* 28, 1726–1735. <https://doi.org/10.1080/09205071.2014.934924>
- Atuonwu, J.C., Tassou, S.A., 2018. Quality assurance in microwave food processing and the enabling potentials of solid-state power generators: A review. *Journal of Food Engineering* 234, 1–15. <https://doi.org/10.1016/j.jfoodeng.2018.04.009>
- Birla, S., Pitchai, K., Subbiah, J., Jones, D.D., 2009. Development of Novel Microwave Cooking Model for Not-Ready-to Eat Foods International Microwave 43rd Annual Symposium, in: International Microwave Power Institute's 43rd Annual Symposium.
- Bornhorst, E.R., Liu, F., Tang, J., Sablani, S.S., Barbosa-Cánovas, G. v., 2017a. Food Quality Evaluation using Model Foods: a Comparison Study between Microwave-Assisted and Conventional Thermal Pasteurization Processes. *Food and Bioprocess Technology* 10, 1248–1256. <https://doi.org/10.1007/s11947-017-1900-9>
- Bornhorst, E.R., Tang, J., Sablani, S.S., Barbosa-Cánovas, G. v., 2017b. Thermal pasteurization process evaluation using mashed potato model food with Maillard reaction products. *LWT - Food Science and Technology* 82, 454–463. <https://doi.org/10.1016/j.lwt.2017.04.019>
- Chen, F., Warning, A.D., Datta, A.K., Chen, X., 2016. Thawing in a microwave cavity: Comprehensive understanding of inverter and cycled heating. *Journal of Food Engineering* 180, 87–100. <https://doi.org/10.1016/j.jfoodeng.2016.02.007>

Chen, J., Pitchai, K., Birla, S., Jones, D., Negahban, M., Subbiah, J., 2016. Modeling heat and mass transport during microwave heating of frozen food rotating on a turntable. *Food and Bioproducts Processing* 99, 116–127.  
<https://doi.org/10.1016/j.fbp.2016.04.009>

Chen, J., Pitchai, K., Jones, D., Subbiah, J., 2015. Effect of decoupling electromagnetics from heat transfer analysis on prediction accuracy and computation time in modeling microwave heating of frozen and fresh mashed potato. *Journal of Food Engineering* 144, 45–57. <https://doi.org/10.1016/j.jfoodeng.2014.07.013>

Dinani, S.T., Feldmann, E., Kulozik, U., 2021. Effect of Heating by Solid-State Microwave Technology at Fixed Frequencies or by Frequency Sweep Loops on Heating Profiles in Model Food Samples. *Food and Bioproducts Processing* 105084.  
<https://doi.org/10.1016/j.fbp.2021.03.018>

Du, Z., Wu, Z., Gan, W., Liu, G., Zhang, X., Liu, J., Zeng, B., 2019. Multi-physics modeling and process simulation for a frequency-shifted solid-state source microwave oven. *IEEE Access* 7, 184726–184733.  
<https://doi.org/10.1109/ACCESS.2019.2960317>

Huang, Z., Zhu, H., Yan, R., Wang, S., 2015. Simulation and prediction of radio frequency heating in dry soybeans. *Biosystems Engineering* 129, 34–47.  
<https://doi.org/10.1016/j.biosystemseng.2014.09.014>

Khan, T., 2020. An Intelligent Microwave Oven with Thermal Imaging and Temperature Recommendation Using Deep Learning. *Applied System Innovation* 3, 13.  
<https://doi.org/10.3390/asi3010013>

Kurniawan, H., Alapati, S., Che, W.S., 2015. Effect of mode stirrers in a multimode microwave-heating applicator with the conveyor belt. *International Journal of Precision Engineering and Manufacturing - Green Technology* 2, 31–36.  
<https://doi.org/10.1007/s40684-015-0004-0>

Luan, D., Wang, Y., Tang, J., Jain, D., 2017. Frequency Distribution in Domestic Microwave Ovens and Its Influence on Heating Pattern. *Journal of Food Science* 82, 429–436. <https://doi.org/10.1111/1750-3841.13587>

Meng, Q., Lan, J., Hong, T., Zhu, H., 2018. Effect of the rotating metal patch on microwave heating uniformity. *Journal of Microwave Power and Electromagnetic Energy* 52, 94–108. <https://doi.org/10.1080/08327823.2018.1440341>

Pillow, 2021. Image Module — Pillow (PIL Fork) 8.1.2 documentation [WWW Document]. URL <https://pillow.readthedocs.io/en/stable/reference/Image.html> (accessed 3.8.21).

Pitchai, K., Chen, J., Birla, S., Jones, D., Gonzalez, R., Subbiah, J., 2015. Multiphysics Modeling of Microwave Heating of a Frozen Heterogeneous Meal Rotating on a Turntable. *Journal of food science* 80, E2803–E2814. <https://doi.org/10.1111/1750-3841.13136>

Plaza-González, P., Monzó-Cabrera, J., Catalá-Civera, J.M., Sánchez-Hernández, D., 2005. Effect of Mode-Stirrer Configurations on Dielectric Heating Performance in Multimode Microwave Applicators. *IEEE Transactions on Microwave Theory and Techniques* 53, 1699–1705. <https://doi.org/10.1109/TMTT.2005.847066>

Rougier, C., Prorot, A., Chazal, P., Leveque, P., Leprat, P., 2014. Thermal and nonthermal effects of discontinuous microwave exposure (2.45 Gigahertz) on the cell membrane of *Escherichia coli*. *Applied and Environmental Microbiology* 80, 4832–4841. <https://doi.org/10.1128/AEM.00789-14>

Sebera, V., Nasswetrová, A., Nikl, K., 2012. Finite Element Analysis of Mode Stirrer Impact on Electric Field Uniformity in a Microwave Applicator. *Drying Technology* 30, 1388–1396. <https://doi.org/10.1080/07373937.2012.664800>

Tang, Z., Hong, T., Liao, Y., Chen, F., Ye, J., Zhu, H., Huang, K., 2018. Frequency-selected method to improve microwave heating performance. *Applied*

Thermal Engineering 131, 642–648.

<https://doi.org/10.1016/j.applthermaleng.2017.12.008>

Wiedenmann, O., Ramakrishnan, R., Kiliç, E., Saal, P., Siart, U., Eibert, T.F., 2012. A multi-physics model for microwave heating in metal casting applications embedding a mode stirrer. 2012 the 7th German Microwave Conference, GeMiC 2012.

Yakovlev, V. v., 2018. Effect of frequency alteration regimes on the heating patterns in a solid-state-fed microwave cavity. *Journal of Microwave Power and Electromagnetic Energy* 52, 31–44. <https://doi.org/10.1080/08327823.2017.1417105>

Yang, Y., Fan, Z., Hong, T., Chen, M., Tang, X., He, J., Chen, X., Liu, C., Zhu, H., Huang, K., 2020. Design of microwave directional heating system based on phased-array antenna. *IEEE Transactions on Microwave Theory and Techniques* 68, 4896–4904. <https://doi.org/10.1109/TMTT.2020.3002831>

Ye, J., Hong, T., Wu, Y., Wu, L., Liao, Y., Zhu, H., Yang, Y., Huang, K., 2017. Model stirrer based on a multi-material turntable for microwave processing materials. *Materials* 10, 1–13. <https://doi.org/10.3390/ma10020095>

Zhang, W., Luan, D., Tang, J., Sablani, S.S., Rasco, B., Lin, H., Liu, F., 2015. Dielectric properties and other physical properties of low-acyl gellan gel as relevant to microwave assisted pasteurization process. *Journal of Food Engineering* 149, 195–203. <https://doi.org/10.1016/j.jfoodeng.2014.10.014>

Zhu, H., He, J., Hong, T., Yang, Q., Wu, Y., Yang, Y., Huang, K., 2018. A rotary radiation structure for microwave heating uniformity improvement. *Applied Thermal Engineering* 141, 648–658. <https://doi.org/10.1016/j.applthermaleng.2018.05.122>

Zhu, X., Guo, W., Wu, X., 2012. Frequency- and temperature-dependent dielectric properties of fruit juices associated with pasteurization by dielectric heating. *Journal of Food Engineering* 109, 258–266. <https://doi.org/10.1016/j.jfoodeng.2011.10.005>

## Appendix



**Table II-1 Microwave heating performances of combined top and middle layers with fixed-frequency from 2.40 to 2.47 GHz after six minutes of heating**

Frequency, GHz	Average Temperature*, °C	HUI*	Power Absorption†, %
2.40	33.13 ± 0.11 <sup>a</sup>	0.300 ± 0.004 <sup>ab</sup>	58.00
2.41	34.42 ± 0.68 <sup>b</sup>	0.250 ± 0.014 <sup>cde</sup>	60.26
2.42	34.13 ± 0.11 <sup>b</sup>	0.292 ± 0.008 <sup>bc</sup>	59.75
2.43	35.40 ± 0.14 <sup>c</sup>	0.231 ± 0.010 <sup>e</sup>	61.97
2.44	35.44 ± 0.14 <sup>c</sup>	0.281 ± 0.001 <sup>bcd</sup>	62.04
2.45	34.80 ± 0.12 <sup>bc</sup>	0.292 ± 0.026 <sup>bc</sup>	60.92
2.46	28.61 ± 0.20 <sup>d</sup>	0.339 ± 0.028 <sup>a</sup>	50.09
2.47	31.37 ± 0.20 <sup>e</sup>	0.246 ± 0.012 <sup>de</sup>	54.92

\* Results shown as mean ± std. Different letters in the same column indicate statistically different results ( $p < 0.05$ ).

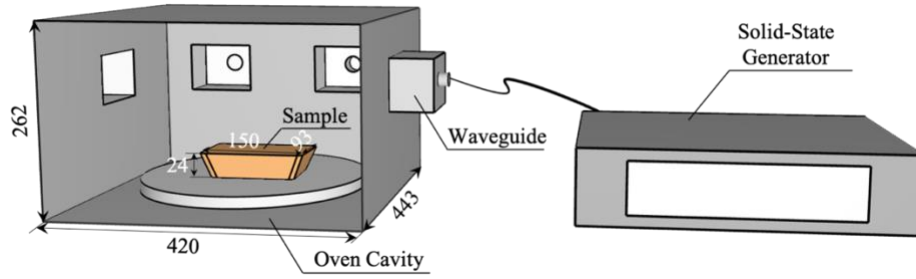
† Based on the average temperature of the combined top and middle layers.

**Table II-2 Microwave heating performance of the combined top and middle layers for different frequency shifting strategies after six minutes of heating**

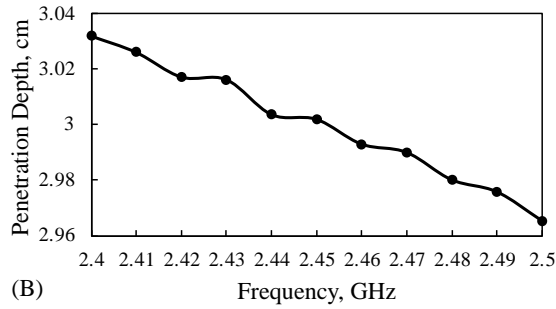
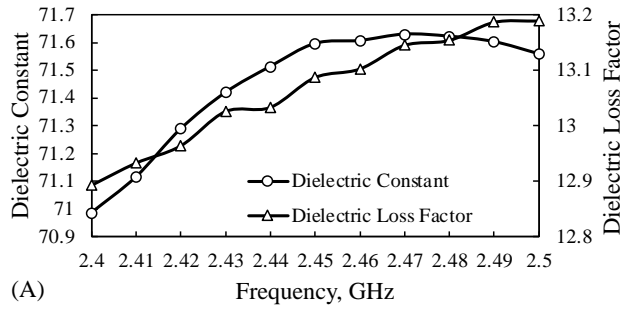
Frequency Shifting Step, s	Frequency Shifting Strategy	Average Temperature*, °C	HUI*	Power Absorption†, %
45	incremental	32.68 ± 0.65 <sup>a</sup>	0.173 ± 0.013 <sup>a</sup>	57.21
	decremental	33.22 ± 0.43 <sup>a</sup>	0.178 ± 0.005 <sup>a</sup>	58.16
	complementary-I	32.48 ± 0.62 <sup>a</sup>	0.177 ± 0.018 <sup>a</sup>	56.86
	complementary-II	35.66 ± 0.33 <sup>b</sup>	0.179 ± 0.011 <sup>a</sup>	64.43
15	incremental	33.79 ± 1.25 <sup>a</sup>	0.173 ± 0.006 <sup>a</sup>	59.16
	mixed	33.66 ± 0.67 <sup>a</sup>	0.190 ± 0.006 <sup>ab</sup>	58.93
	complementary-I	32.42 ± 0.29 <sup>a</sup>	0.183 ± 0.010 <sup>ab</sup>	56.76
	complementary-II	37.01 ± 0.17 <sup>b</sup>	0.208 ± 0.002 <sup>b</sup>	64.79

\* Results shown as mean ± std. Different letters in the same column indicate statistically different results ( $p < 0.05$ ).

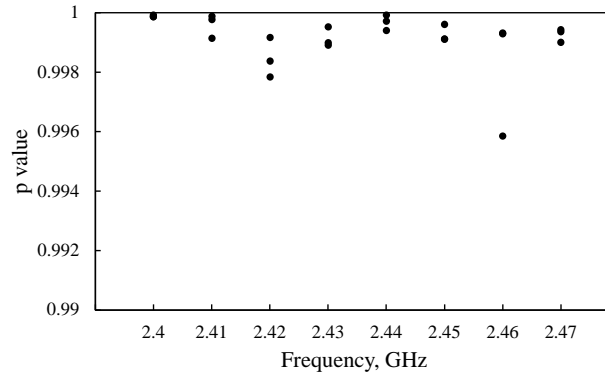
† Based on the average temperature of the combined top and middle layers



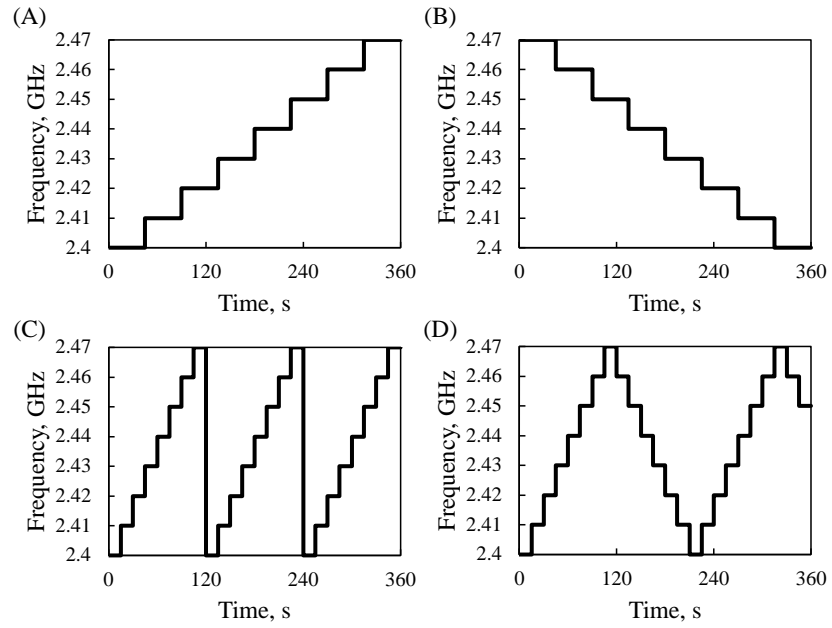
**Figure II-1 Diagram for the solid-state system assembly (unit: mm).**



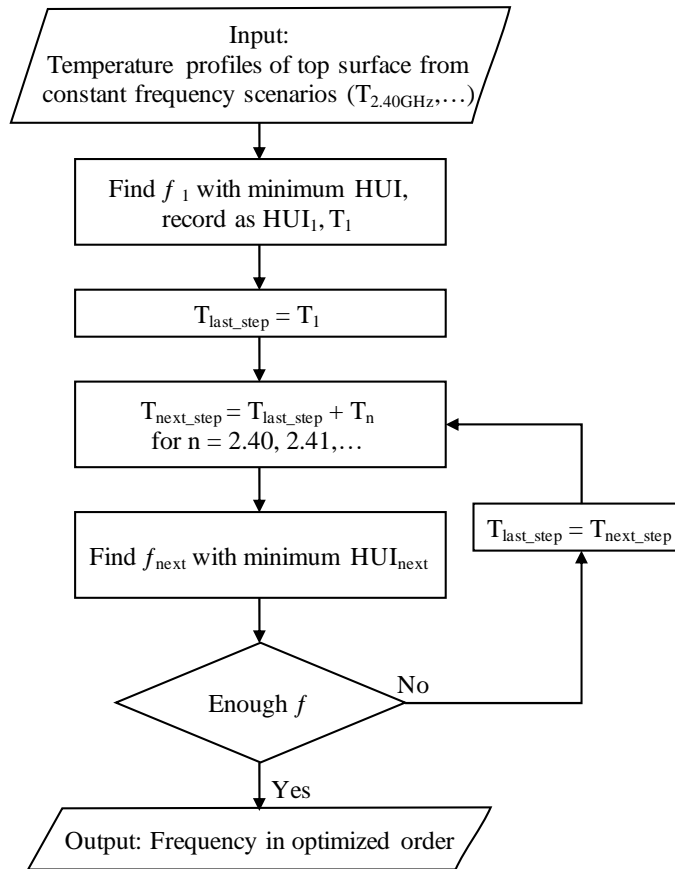
**Figure II-2 Dielectric properties of the prepared gellan gel sample in the range of 2.40 to 2.50 GHz, (A) dielectric constant and loss factor; (B) penetration depth.**



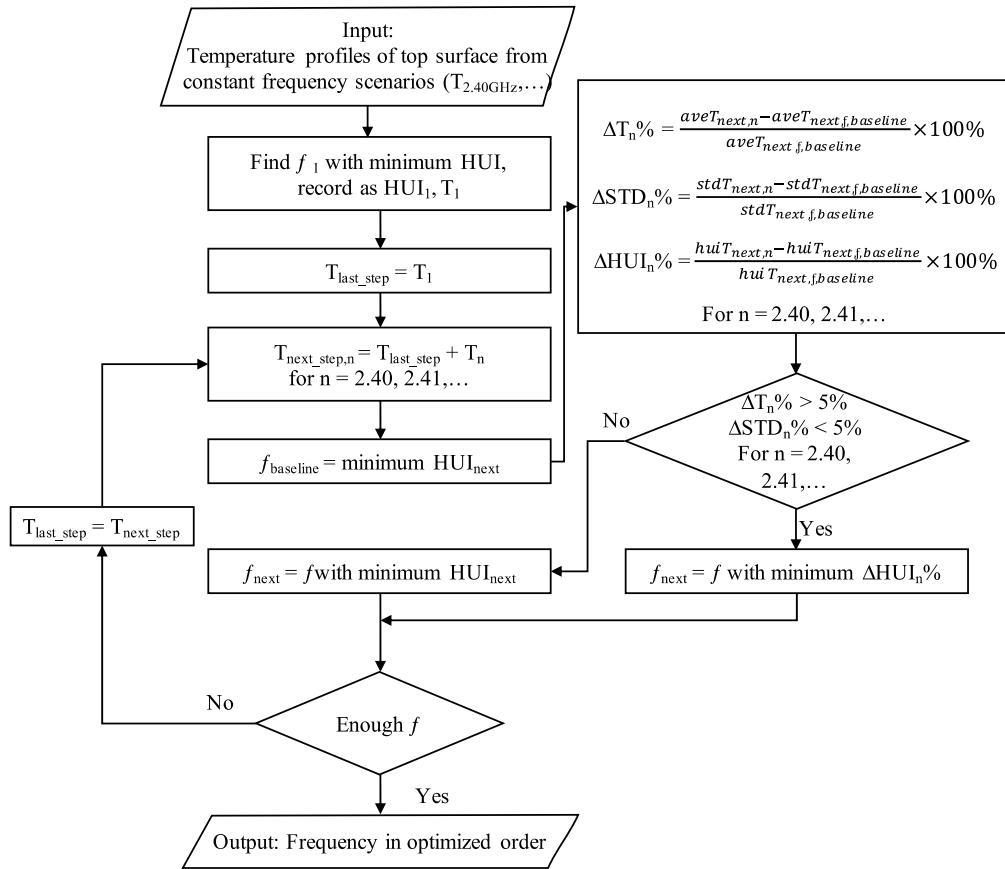
**Figure II-3 Statistical t-test results on analysis of the difference caused by image resizing.**



**Figure II-4 Sweeping-Frequency strategies for a six-minute microwave heating process. (A) incremental shifting-45s step; (B) decremental shifting-45s step; (C) incremental shifting-15s step; (D) mixed shifting-15s step.**



**Figure II-5 Algorithm I to determine the complementary-frequency shifting order based on heating uniformity index only.**



**Figure II-6 Algorithm II to determine the complementary-frequency shifting order based on both heating rate and standard deviations.**



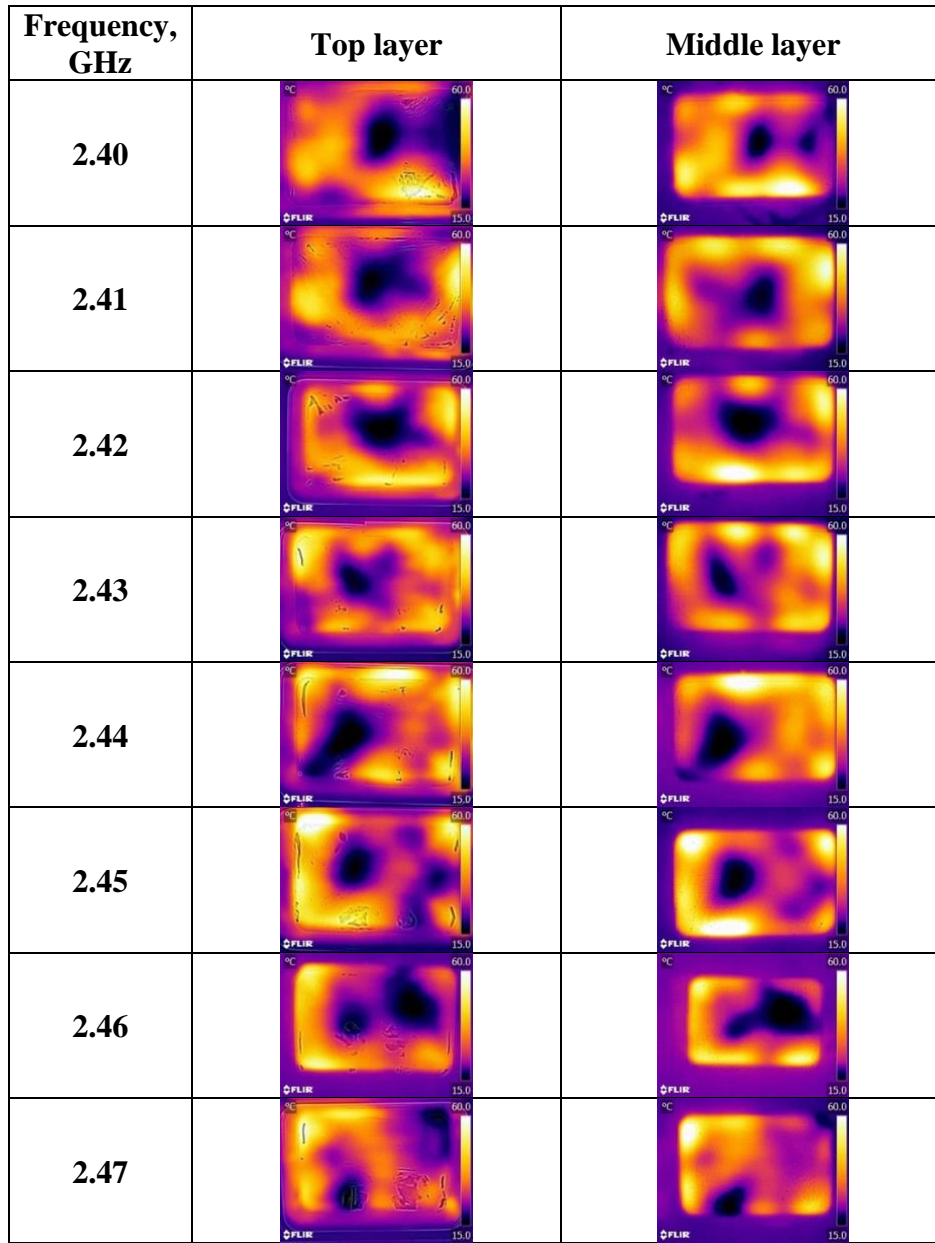
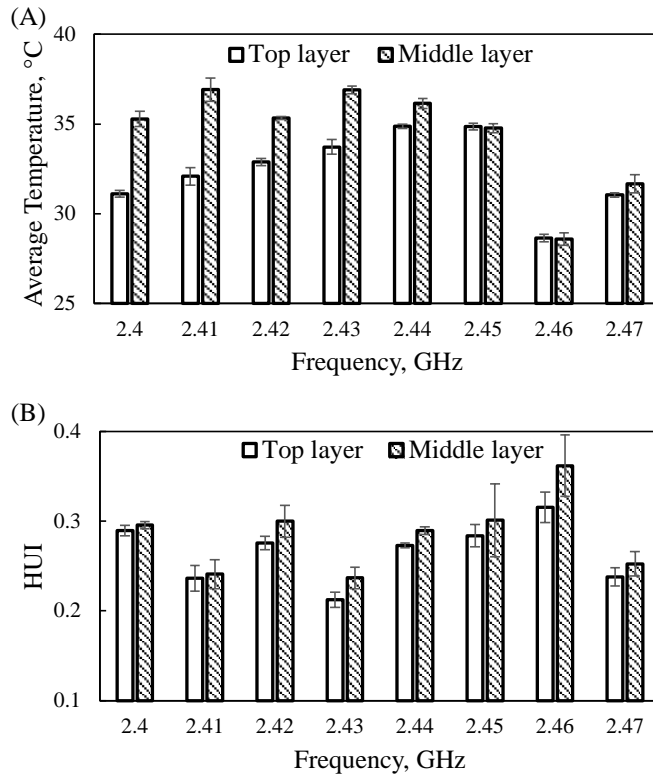
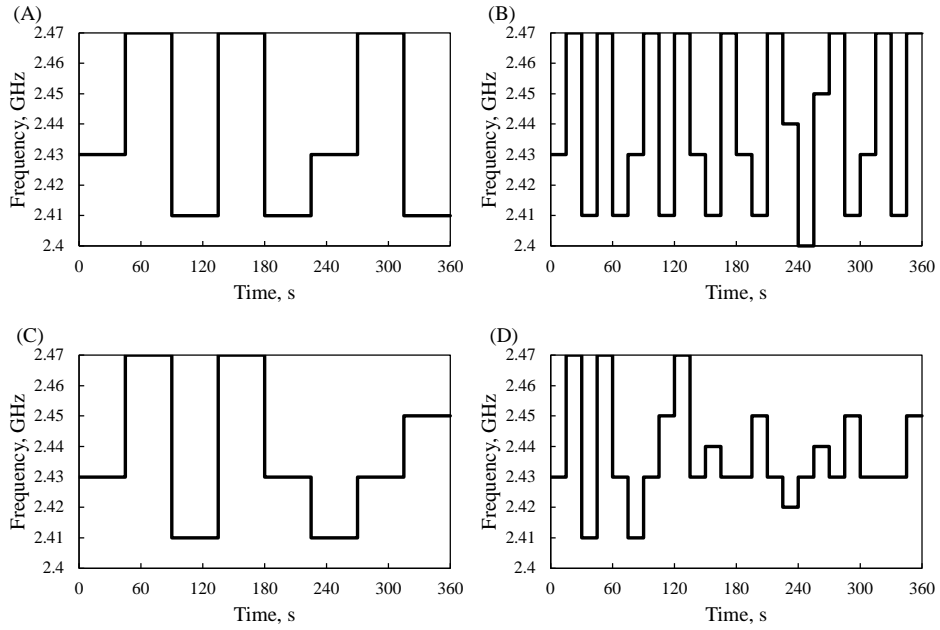


Figure II-7 Temperature profiles at the top and middle layers after six minutes of heating with fixed frequency from 2.40 to 2.47 GHz.



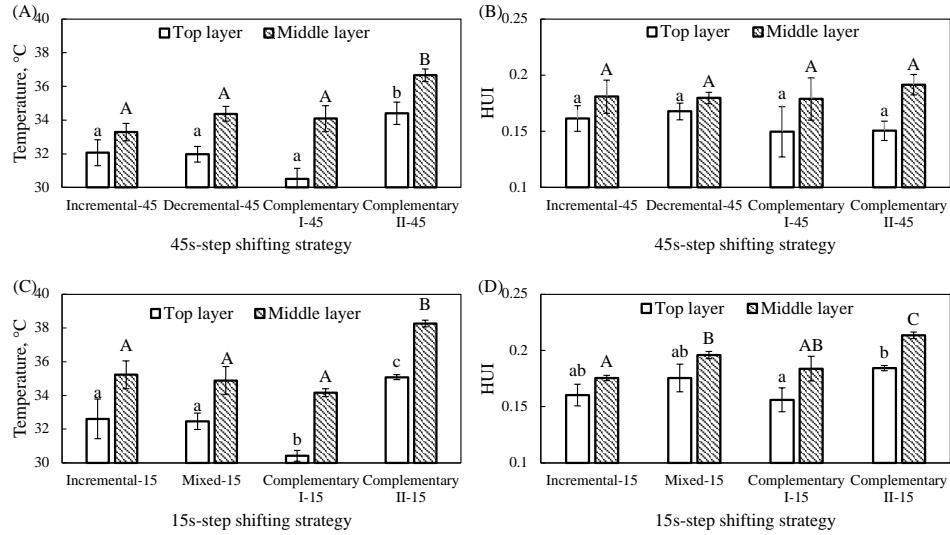
**Figure II-8 Microwave heating performance at top and middle layers after six microwave heating with fixed-frequency from 2.40 to 2.47 GHz. (The results and error bars were calculated as the average and standard deviation from experiments done in triplicate separately).**



**Figure II-9 Complementary-frequency shifting strategies developed based on heating uniformity index only (A & B), both heating rate and standard deviation (C&D) with shifting steps of 45 (A&C) and 15 (B&D) s.**

Shifting strategy	Top layer	Middle layer
45s incremental shifting		
45s decremental shifting		
45s complementary shifting-I		
45s complementary shifting-II		
15s incremental shifting		
15s mixed shifting		
15s complementary shifting-I		
15s complementary shifting-II		

Figure II-10 Temperature profiles of top and middle layers after six-minute microwave heating with various frequency-shifting strategies (only one replicate out of three shown here to illustrate the results).



**Figure II-11 Microwave heating performance at top and middle layers after six microwave heating with various frequency-shifting strategies. (A) Average temperature for four 45s-step shifting strategies; (B) Heating Uniformity Index (HUI) profiles for four 45s-step shifting strategies; (C) Average temperature for four 15s-step shifting strategies; (D) HUI profiles for four 15s-step shifting strategies. All results are shown in mean  $\pm$  standard deviation. Different letters in each figure (top layer with lower-case letters, middle layer with capital letters) indicate a significant difference ( $p < 0.05$ ). The results and error bars were calculated as the average and standard deviation from experiments done in triplicate separately).**

**CHAPTER III**  
**DEVELOPMENT OF ONLINE CLOSED-LOOP FREQUENCY**  
**SHIFTING STRATEGIES TO IMPROVE HEATING**  
**PERFORMANCE OF FOODS IN A SOLID-STATE MICROWAVE**  
**SYSTEM**

A version of this chapter was originally published by Yang, R., Fathy, A. E., Morgan, M. T., & Chen, J:

Yang, R., Fathy, A.E., Morgan, M.T., Chen, J., Development of Online Closed-Loop Frequency Shifting Strategies to Improve Heating Performance of Foods in a Solid-State Microwave System, Food Research International (2022), doi: <https://doi.org/10.1016/j.foodres.2022.110985>

As the first author of this research article, I was the main contributor to Conceptualization, Methodology, Data curation, Investigation, Software, Visualization, Writing of the manuscript. Dr. Jiajia Chen, as the major professor and corresponding author, contributed to Conceptualization, Investigation, Supervision, Project administration, Funding acquisition, Writing - Reviewing and Editing of the manuscript. The co-authors, as the committed members of the Ph.D. program, offered suggestion in the experiment design, provided help in manuscript revising.

### **3.1 Abstract**

The solid-state microwave generator is promising to replace magnetron as a power source in domestic ovens for its precise and flexible control over a wide range of operational parameters and its potential to improve heating performance. Shifting frequency during microwave heating, either orderly or using complementary heating patterns, has yielded better heating performance than traditional single-frequency heating. This study developed three online frequency shifting strategies (orderly, pre-determined complementary, and dynamic complementary) that simultaneously collected heating performances and provided closed-loop feedback through customized algorithms to control the frequency shifting during the microwave heating processes. Each algorithm was implemented and tested on two model foods with different dielectric properties (gellan gel and mashed potato). The three frequency shifting algorithms had similar

frequency sweeping processes but considerably different frequency shifting procedures for different replications and food products. The dynamic complementary-frequency shifting strategy simultaneously evaluated the heating performance and determined the next-step complementary-frequency. The method had shown better heating uniformity than the orderly and pre-determined complementary-frequency shifting strategies. The dynamic complementary-frequency shifting strategy could accommodate different food products and can be incorporated into future smart microwave ovens.

**Keywords:** Solid-state microwave, online, closed-loop, complementary-frequency, shifting, heating uniformity

### 3.2 Introduction

Non-uniform heating in the conventional domestic microwave oven has been a great concern since it lowers the quality and safety of the foods. This inherent non-uniform problem is mainly caused by the standing wave patterns generated inside the oven cavity by a magnetron-based microwave source (Datta and Anantheswaran, 2001; Luan et al., 2017; Zhang and Datta, 2000). In addition, due to the temperature-dependent dielectric properties of food materials, the hot areas of the foods tend to absorb more microwave power as the temperature increases, which is known as the “thermal runaway” phenomenon and worsens the non-uniform heating problem (Zhu et al., 2012).

A solid-state microwave generator is a promising replacement for the magnetron as the power source in microwave ovens to solve the standing wave pattern issue. The solid-state microwave system allows precise and flexible control over the operational parameters of frequency, power, and relative phase (if multiple sources are used) during the heating process, which makes it promising to dynamically change the heating patterns and thus achieve better heating performance (Yang et al., 2020). Meanwhile, it has been demonstrated that the heating patterns of foods differ significantly under various



frequencies (Luan et al., 2017; Taghian Dinani et al., 2021; Yang et al., 2022). This has led to extensive research on developing frequency-shifting strategies to improve microwave heating performance. The commonly used frequency-shifting method was based on an in-order sweeping strategy (Du et al., 2019; Taghian Dinani et al., 2021) where frequencies were swept orderly between 2.40 GHz and 2.50 GHz. The orderly shifting strategy was proven to have better heating uniformity than the conventional fixed-frequency (i.e., 2.45 GHz) in microwave heating of chicken nuggets (Du et al., 2019) and gellan gel model food (Dinani 2021).

Since the microwave power efficiency varies with frequency (Taghian Dinani et al., 2021; Yakovlev, 2018; Yang et al., 2022), another frequency-shifting strategy was developed by Tang et al. (2018), which included a pre-selection process in determining the frequencies that have high power efficiency first and then used only the shift frequencies among those with high-power-efficiency in a microwave heating process. This frequency-shifting strategy showed higher power absorption and better heating uniformity than the conventional orderly shifting strategy. However, the frequency pre-selection process was performed by using multiphysics modeling only, and not during a real microwave heating process.

Furthermore, in addition to utilizing the varying microwave power efficiency at different frequencies, complementary heating patterns at various frequencies were used to improve the microwave heating performance (Yang et al., 2022). Following this complementary-frequency strategy, the thermal images of the model food (gellan gel) were first collected after the heating processes at various fixed frequencies. After analyzing the heating patterns (hot and cold spots locations) of the thermal images, the complementary frequencies were selected and assigned in designed orders for shifting during a microwave heating process. Compared to the orderly shifting strategy, the temperature uniformity of samples heated with the complementary shifting strategy was maintained at a similar level while the power absorption was significantly raised.

Previous frequency shifting strategies showed promising effects in disturbing the standing wave pattern and improving the microwave heating performance. However, these strategies have limitations to deal with microwave heating processes when implemented for different oven cavities and different food loads with varied locations, sizes, and geometries (Luan et al., 2017). Since the selected frequencies were pre-determined by either modeling or experiments in advance, these algorithms cannot be applied directly in real microwave heating processes that involve various ovens and/or food products. Hence, there is a need to develop online strategies that can monitor the real-time microwave heating performances (e.g., power absorption, heating pattern, etc.) and provide closed-loop feedback to dynamically shift the frequencies to improve the microwave heating performance. To achieve this online and closed-loop control of microwave parameters, our solid-state microwave system design was slightly customized. For example, the power absorption information usually can be monitored by the solid-state microwave generator, while the heating patterns can be monitored by a thermal imaging camera mounted at the top of the oven cavity (Khan, 2020).

The overall goal of this study was to develop online, closed-loop frequency shifting strategies to improve the microwave heating performance of foods. The specific objectives of this study were to:

Develop three online frequency shifting (orderly frequency shifting, pre-determined complementary-frequency shifting, and dynamic complementary-frequency shifting) strategies that collect microwave heating performance and provide closed-loop feedback controls;

Compare the frequency shifting sequences determined by the three frequency-shifting strategies; and

Compare the microwave heating performances yielded by the three online closed-loop frequency shifting strategies.

### **3.3 Material and Methods**

#### **3.3.1 Microwave system**

The utilized solid-state microwave system in our experiments is comprised of a generator (PA-2400-2500MHz-200W-4, Junze Technology, China) and a cavity modified from a domestic microwave oven (Panasonic Model NN-SN936W), with the glass turntable left inside the oven while without rotation during heating. The generator has four power sources and was connected to the oven cavity through four waveguides (CWR340 CentricRF) launcher ports (Figure III-1). The frequency, phase, power level of the four ports can be individually controlled by a customized program. In this study, only the port on the right wall was in use, while the power level was set to a maximum of 200 W. A radiometric-capable thermal camera module (Lepton 3.5, 160×120) was attached outside the top wall of the oven cavity to collect real-time thermal images through a 4 mm size hole during the microwave heating process (Khan, 2020).

#### **3.3.2 Model foods preparation and dielectric properties**

Two model foods (gellan gel and mashed potato) with different dielectric properties were used as samples in this study. The gellan gel represents a low loss material, which consists of a 1% low-acyl gellan gum powder (CP Kelco U.S., Inc., GA, USA), 0.17% calcium chloride (CaCl<sub>2</sub>) (Honeywell Research Chemicals, Muskegon, MI, USA), and deionized water (Birla et al., 2008a, 2008b; Mao et al., 2000; Zhang et al., 2015b). The use of low-acyl gellan gel is to help prepare a firm gel that could remain solid during microwave heating process (Birla et al., 2008a; Lee et al., 2011; Okiror and Jones, 2012; Zhang et al., 2015b). To prepare the sample, the gellan gum powder was first stirred with deionized water at 90 °C for 15 min; and then CaCl<sub>2</sub> was added to the hot solution for preparing a firm and stable gel (Pitchai et al., 2012; Zhang et al., 2015b). The mixture of the solution was stirred at around 90 °C for an extra 10 min to ensure homogeneity, and then 300 g of solution was poured into plastic containers. The hot

samples loaded in the food containers were kept at room temperature for 30 min to ensure gel setting and then were stored at 4 °C overnight in a refrigerator for later use.

The mashed potato represents a high loss food, which was made of 23.8% mashed potato flakes (Real Premium mashed potato, Idahoan Foods, Idaho Falls, ID, USA), 18.6% whole milk (Grade A homogenized whole milk, Kroger CO., Cincinnati, OH, USA), 4.1% unsalted butter (Land O' Lakes® Unsalted Butter Sticks, Land O' Lakes, Inc, Arden Hills, MN, USA) and 53.5% deionized water by weight basis. The water and milk were heated on a hot plate magnetic stirrer to be over 50 °C. The butter was later added to the liquid until fully melted. The solution was poured into a stand mixer with the potato flakes loaded in the bowl. The mixture was then stirred for 5 min to ensure homogeneity of the materials. The prepared mashed potato was loaded into the same plastic containers used for gellan gel samples. Each sample was also 300 g in total, with a piece of mesh cloth horizontally placed at the center to separate the sample into two layers for capturing the middle layer thermal images after the microwave heating experiments. The selected mesh cloth is made of nylon with coarse mesh, which does not interact with the microwaves much but allows the moisture to move freely, and thus not affect the microwave heating process. The samples were then stored at 4 °C overnight for later use.

The dielectric properties of gellan gel were obtained from a previous study by Yang et al. (2022). The dielectric properties of the mashed potato were measured at room temperature (23 °C) between frequencies (2.40 – 2.50 GHz) using a vector network analyzer (Agilent E8363B, Agilent Technologies, Inc., Santa Clara, CA, USA), and 85070B Open-End Coaxial Dielectric Probe (Agilent Technologies, Santa Clara, CA, USA). The dielectric properties and the loss tangent (calculated as the dielectric loss factor divided by the dielectric constant) were summarized in Figure III-2. The mashed potato has a relatively higher loss compared to the gellan gel.

### **3.3.3 Online microwave frequency shifting strategies with closed-loop feedback**

Three online microwave frequency shifting strategies with closed-loop feedback (as indicated previously as: orderly frequency shifting, pre-determined complementary-frequency shifting, and dynamic complementary-frequency shifting) were developed and evaluated in this study. The word “online” refers to the fact that heating of food, evaluation of the microwave heating performance (e.g., power reflection, heating pattern, etc.), and adjustment of the frequency shifting take place simultaneously during a real microwave heating process. Each online strategy had two stages to complete a microwave heating process: frequency sweeping and frequency shifting. During the frequency sweeping stage, microwave power reflection was evaluated to determine the high-power efficiency frequencies, and/or the thermal images of the top surface layer were recorded and evaluated to determine the spatial thermal contributions (spatial temperature change) for each frequency. During the frequency shifting stage, the power reflection and/or spatial thermal contributions were then analyzed to provide closed-loop control of the frequency shifting.

For all frequency shifting strategies, the refrigerated samples were placed at the center of the stationary turntable and heated from 4 °C for 360 s. Based on the previous study using the same microwave system with the same total heating time, the 360 s-heating would increase the temperature by about 33 °C, which could ensure the firm structure of the samples after heating (Yang et al., 2022).

#### **3.3.3.1 Orderly frequency shifting strategy**

The algorithm for the orderly frequency shifting strategy is shown in Figure III-3. After the food product was placed inside the oven cavity, the orderly frequency shifting strategy started the frequency sweeping stage by heating the food using 11 frequencies from 2.40 to 2.50 GHz with a step of 0.1 GHz. The solid-state generator simultaneously detected the reflected power at each frequency. If the reflected power was over 45 W

(slightly lower than the designed safe limit power reflection of 50 W for the generator) at a specific frequency, this frequency was only used for 2 s (systems needs up to 2 s to detect a stable reflection power) and next frequency would be in use instead; otherwise, the frequency with power reflection lower than 45 W would be used for 10 s heating. After a full sweep from 2.40 to 2.50 GHz, a list of frequencies with relatively high-power efficiency (i.e., power reflection lower than 45 W) was completed.

Immediately after the frequency sweeping stage, the frequency shifting stage started by sweeping the determined frequencies with low power reflection “orderly” in a loop at a constant rate of 10 s for the following heating process until a total heating time (360 s) was completed. Note that, since several frequencies showed high power reflection and each of them was only in use for 2 s during the frequency sweeping stage, the last shifting step would be less than the assigned 10 s to match the assigned total heating time (360 s). In this study, only the incremental frequency shifting strategy was used because previous research showed that the sweeping directions did not significantly influence the heating results (Yang et al., 2022).

### 3.3.3.2 Pre-determined complementary-frequency shifting strategy

The algorithm for the pre-determined complementary-frequency shifting strategy is shown in Figure III-4. Similar to the orderly frequency shifting strategy, the pre-determined complementary-frequency shifting strategy started the frequency sweeping stage by evaluating the power reflection and then preparing a frequency list with high-power efficiency. In addition, after a 10 s heating of each frequency (only high-efficiency ones), the thermal images of the top surface of the food were recorded by a thermal imaging camera that was mounted outside the top wall of the oven cavity.

The collected thermal images were used to determine the spatial thermal contribution from each frequency. Before the microwave heating process started (i.e.,  $t = 0$  s), a thermal image of the food product with the oven cavity background was recorded

(Figure III-5A). Because there is a temperature difference between the food product (just removed from the refrigerator) and the oven cavity background, the food boundary could be determined by an OpenCV function, shown as a white line in Figure III-5B. Generally, the OpenCV function first converted the thermal results to be gray-scale images based on temperature values and detected the boundary based on the brightness of the images, which were expressed as numbers between 0 and 255. In this study, a commonly used brightness threshold value of 127 was used to separate the food region from the oven cavity region (OpenCV, 2021). Given that the sample location was fixed during the whole heating process, then the image pixels that represent the food domain were unchanged. A mask was then created following the detected food boundary, and the white color region represented the food region, as shown in Figure III-5C. This food region was used to process all other thermal images recorded at other time steps during the whole heating process. With this thermal image, the food boundary was determined by an OpenCV function, shown as a white line in Figure III-5B. Given that the sample location was fixed during the whole heating process, then the image pixels that represent the food domain were unchanged. A mask was then created following the detected food boundary, and the white color region represented the food region, as shown in Figure III-5C. This food region was used to process all other thermal images recorded at other time steps during the whole heating process. The spatial thermal contribution by 10 s heating at each frequency was determined based on the concept of superimposed effect (Yang et al., 2022). Generally, the spatial thermal contribution of a frequency was calculated as the difference between the thermal images collected after and before the 10 s heating of one frequency, as shown in Figure III-6. After sweeping all frequencies, the high-power efficiency frequencies and the corresponding spatial thermal contributions were obtained.

The spatial thermal contributions were then used to determine the frequency shifting sequences for the remaining heating time to form closed-loop feedback. The frequency sequence determination was performed following the complementary

algorithm (II) developed by Yang et al. (2022), which has been proven to be a better frequency shifting algorithm than the orderly frequency shifting algorithm. The general principle of the complementary-frequency algorithm was that only the frequencies with complementary heating patterns (hot and cold spots) were specifically selected and used in a proper sequence to heat the food for improving the heating performance rather than sweeping all frequencies non-differentially. In this study, the spatial temperature distribution at the top surface at the end of the frequency sweeping stage was used as a baseline heating profile. The spatial thermal contribution of each frequency (only high-efficiency ones) collected during the frequency sweeping stage was superimposed with the baseline heating profile individually. The heating uniformity index ( $HUI$ , will be discussed in Section 2.4 Eq. (III-1) with detail) and the average temperature of the superimposed thermal profiles were calculated. The frequency with a balanced minimum  $HUI$  and the maximum average temperature of the superimposed thermal profile was selected as a complementary-frequency, which followed the approach described by Yang et al., (2022). In brief, the selected complementary-frequency should result in a minimum  $HUI$  for the superimposed thermal profile, if its average temperature is not 5% smaller than the maximum average temperature from all potential superimposed thermal profiles; otherwise, the frequency with maximum average temperature may be selected as the complementary-frequency to ensure high power absorption, if its  $HUI$  value is not 5% higher than the minimum  $HUI$  value. Then, this selected superimposed thermal profile was used as a new baseline heating profile for repeating the superimpose steps for determining the frequency shifting sequences. Each of these selected complementary frequencies was used, following the determined sequence, for 10 s heating until the total heating time of 360 s was achieved. Since the frequency shifting sequence was determined for the whole heating process based on the thermal profile after frequency sweeping and the spatial thermal contributions without monitoring the real-time heating performance, this algorithm is referred as “Pre-determined” complementary-frequency shifting algorithm.



### 3.3.3.3 Dynamic complementary-frequency algorithm

The algorithm for the dynamic complementary-frequency shifting strategy is shown in Figure III-7. The dynamic complementary-frequency algorithm started with the determination of the high-power efficiency frequencies and the corresponding spatial thermal contributions, which was similar to the pre-determined complementary-frequency strategy. While after the sweeping stage, the dynamic complementary-frequency strategy did not finalize all the frequencies for the whole heating process all at once. Instead, this algorithm only determined one frequency for the following heating step (10 s). This frequency was determined based on the superimposed thermal profiles from the real-time heating profile and the collected spatial thermal contributions. The frequency with a balanced minimum *HUI* and maximum average temperature (Yang et al., 2022) of the superimposed thermal profile was selected as a complementary frequency and used for the following 10 s heating immediately. The real-time thermal profile collection and next-one frequency determination were repeated through the whole heating process until the end. Since the frequency shifting sequence was determined based on real-time dynamic heating results, this frequency selection process is referred to as “Dynamic” complementary-frequency shifting algorithm.

### 3.3.4 Microwave heating performance evaluation

After a whole microwave heating process, the food samples were quickly removed from the microwave oven for capturing the thermal images at the top and middle layers using a handheld thermal camera (FLIR C3, Boston, MA). To capture the spatial thermal profiles at the middle layer, the gellan gel samples were sliced from the middle layer with a slicer; the mashed potato samples were separated by the mesh cloth that was placed inside the sample during preparation. Then the spatial temperature profiles of the top and middle layer were exported as data files in  $320 \times 240$  pixels by the FLIR Tools (2020 © FLIR® Systems, Inc.) for further analysis.

To detect the boundary of the food products for heating results evaluation, the exported data files were converted into images with Matplotlib module (Hunter, 2007), and the boundaries were detected by OpenCV module (OpenCV, 2021) with a customized Python program similar to the boundary detection during the heating process. While owing to the nonuniform distribution of the temperature over the samples, the boundary between the food sample and the oven cavity background area was less clear. Hence, different brightness threshold values for these images were arbitrarily tested to ensure good boundary detection, and the optimized threshold values were between 30 and 50. The temperatures of the food regions within the boundary were used to assess the heating performance of foods.

The heating uniformity was assessed by the layered heating uniformity index (*HUI*), which is expressed by Eq. (IV-1) (Alfaifi et al., 2014):

$$HUI = \frac{1}{S_{layer}} \int_{S_{layer}} \sqrt{(T - T_{ave})^2} dS_{layer} \quad (III-1)$$

where  $S_{layer}$  is the area of each layer,  $\Delta T_{ave}$  ( $^{\circ}\text{C}$ ) is the average temperature increase over the layer during heating. A smaller *HUI* value indicates a better heating result with a higher heating uniformity.

The power absorption efficiency was estimated from the combined top and middle layer temperatures by using Eq. (IV-2):

$$Power\ Efficiency = \frac{m \cdot C_p \cdot \Delta T}{P_{input} \cdot \Delta t} \quad (III-2)$$

where  $m$  is the sample weight (300 g in this study),  $C_p$  is the specific heat capacity of the samples ( $\text{J} \cdot \text{g}^{-1} \cdot ^{\circ}\text{C}^{-1}$ ) ( $4.16 \text{ J} \cdot \text{g}^{-1} \cdot ^{\circ}\text{C}^{-1}$  for gellan gel (Birla et al., 2008b) and  $3.78 \text{ J} \cdot \text{g}^{-1} \cdot ^{\circ}\text{C}^{-1}$  for mashed potato samples (Chen et al., 2013)),  $\Delta T$  is the mean temperature increase ( $^{\circ}\text{C}$ ) for the combined top and middle layers,  $P_{input}$  is the input microwave power (200 W in this study), and  $\Delta t$  is the total heating time (360 s).

### **3.3.5 Data analysis**

In this study, all the frequency shifting algorithms were tested with both gellan gel and mashed potato samples in triplicate, separately. Data are presented as mean  $\pm$  standard deviation of the three replicates. Statistical analysis was conducted using the one-way analysis of variance (ANOVA), followed by an HSD Tukey's post-test with a 95% confidence interval. All the analysis was performed using GraphPad Prism Version 8.3 (GraphPad Software, La Jolla California, USA). *p* values smaller than 0.05 were considered statistically significant.

## **3.4 Results and Discussion**

### **3.4.1 Comparison of the three online closed-loop frequency shifting algorithms**

All heating scenarios started with a frequency sweeping stage to select frequencies with high-power efficiency, followed by a frequency shifting stage to heat the food products with changing frequencies determined after the sweeping stage. Owing to the small variations of the prepared model foods and their locations inside the cavity, the online algorithms selected different frequencies and sequences in the microwave heating processes between replications.

#### **3.4.1.1 Selected frequencies based on high power efficiency (low power reflection)**

During the frequency sweeping stage, only frequencies that had good power efficiency (i.e., a good load match:  $\leq 45$  W reflected power with a 200 W input power) would be retained for the following frequency shifting stage. The selected frequencies for the three heating replications using three online algorithms for gellan gel and mashed potato are shown in Figure III-8 A&B, respectively. Generally, the frequencies from 2.40 to 2.47 GHz (2.48 GHz for several scenarios) showed relatively high power efficiency, which was aligned with our previous study (Yang et al., 2022). The high-power reflection

at 2.49 and 2.50 GHz might be due to the relatively large impedance mismatch between the load (food) and microwave system (Yang et al., 2022). The occasional selection of 2.48 GHz for some replications might be attributed to the slight sample variations, such as the surface roughness and the exact placement inside the oven, which led to relatively high reflected power around 45 W or more. The difference of the selected frequencies in these different replications/algorithms reflects the flexibility of the online closed-loop system, which could adjust (tweak) the operating frequency properly according to the specific conditions.

#### 3.4.1.2 Characterization of the spatial thermal contributions from each selected frequency

During the frequency sweeping stage, in addition to monitoring and selecting the high-power efficiency frequencies, the pre-determined and dynamic complementary-frequency shifting algorithms also included evaluation of the spatial thermal contributions from each selected frequency. Theoretically, for a model food product, the spatial thermal contributions from a specific frequency would be similar for the three replications. In reality, owing to the slight variations in sample preparation and/or the sample's exact location inside the oven cavity, the thermal profiles might be slightly different. For example, as shown in Figure III-9, the three replications of the spatial thermal contributions from each frequency (2.40 to 2.48 GHz) mostly matched well on hot and cold spot locations, but there were some minor differences. However, the heating pattern diversity can be clearly observed for different frequencies. For example, at 2.40 GHz, the hot spot over the gellan gel sample was located at the left side, while at 2.46 GHz, the hot spot was at the right side, which makes them be potential complementary frequencies to improve the overall heating performance. The spatial thermal contributions also varied between different model food products. For example, at 2.43 GHz, the temperature change in the gellan gel sample was much lower than that in the mashed potato sample.

The spatial thermal contribution variations among different frequencies for different food products and replications indicated that complementary frequencies could be and need to be selected and shifted in sequences through online and closed-loop control strategies. The spatial thermal contributions from different frequencies were used as input data to determine the frequency shifting sequences for the pre-determined and dynamic complementary-frequency shifting algorithms.

#### 3.4.1.3 Frequency shifting sequences

In all frequency shifting sequences, the frequency shifting started with a frequency sweeping stage (starts from 0 s), where each frequency was used for 10 s (if reflected power  $\leq 45$  W) or 2 s (if reflected power  $> 45$  W); and then moved to the frequency shifting stages where the frequency sequences were determined using three algorithms. Figure III-10, Figure III-11 and Figure III-12 summarize three replications of the frequency shifting sequences for the orderly frequency shifting, pre-determined complementary-frequency shifting, and dynamic complementary-frequency shifting algorithms, respectively.

##### 3.4.1.3.1 Orderly frequency shifting sequences

With the orderly frequency shifting algorithm, all the selected frequencies with high-power efficiency were swept indistinguishably in an incremental sequence, as shown in Figure III-10, where the time from 0 to 76 s (2.48, 2.49, and 2.50 GHz was excluded) or 84 s (2.49 and 2.50 GHz was excluded) was the frequency sweeping stage, and the remaining time was used for frequency shifting heating.

#### 3.4.1.3.2 Pre-determined complementary-frequency shifting sequences

The frequency shifting sequences determined by the pre-determined complementary-frequency shifting algorithm (Figure III-11) had the same frequency sweeping stage as the orderly frequency shifting algorithm but showed greatly different frequency sequences during the frequency shifting stage. Instead of using all selected frequencies, the pre-determined complementary-frequency shifting algorithm only used several frequencies that had complementary heating patterns. For example, for gellan gel samples (Figure III-11A), 2.40, 2.41, 2.45, and 2.46 GHz were mainly used in all three replications. As shown in Figure III-9, 2.40/2.41 GHz and 2.45/2.46 GHz had opposite hot spot locations, making them complementary frequencies. However, the frequency shifting sequences also showed differences among three replications, which was due to the sample variations among replications. Compared to the previous research that determined the frequency shifting sequences based on an average of triplicated pre-experimental results (Yang et al., 2022), the online algorithm developed in this study could accommodate the sample variations and adjust the frequency shifting sequences accordingly for each replication.

Figure III-11 A&B also showed that there were considerable differences in the frequency shifting sequences between gellan gel and mashed potato samples. The frequencies of 2.40 and 2.46 GHz were the dominant frequencies for microwave heating of mashed potato samples because of their complementary thermal profiles.

#### 3.4.1.3.3 Dynamic complementary-frequency shifting sequences

For the dynamic complementary-frequency strategy, the frequency in the shifting stage was selected based on their complementary heating patterns at various frequencies. As an example, Table III-1 shows the real-time thermal image right after the frequency sweeping stage and its potential superimpose thermal images with spatial thermal contributions of various frequencies to demonstrate the first dynamic frequency selection

for one replication of gellan gel sample. After the frequency sweeping stage, the average temperature and *HUI* values were 17.60 °C and 0.238 at the top surface of the gellan gel sample. The dynamic complementary-frequency strategy superimposed this thermal image with all potential spatial thermal contribution individually and analyzed the average temperature and *HUI* values for the superimposed thermal images. As shown in Table III-1, the superimposed thermal image at 2.46 GHz showed the minimum *HUI* with acceptable average temperature (only 1.6% smaller than the maximum average temperature of the superimposed thermal results by 2.45 GHz). Thus, 2.46 GHz was selected as the first dynamic frequency after the sweeping stage for this replication.

As shown in Figure III-12, the dynamic complementary-frequency shifting sequences (solid red lines) started with similar frequency sweeping and then dynamically changed during the frequency shifting stage. For comparison purpose, the frequency shifting sequences using the pre-determined algorithm was also determined based on this group of frequency sweeping result (not the pre-determined frequency sweeping result), shown as the blue dotted lines in Figure III-12. Note that the slight sample variations generated different frequency sequences for different replications, which had been observed from the pre-determined algorithm. For the same reason, the pre-determined frequency shifting sequences in Figure III-12 were also different from those in Figure III-11.

For gellan gel samples, the frequency of 2.46 GHz was mostly used in both the dynamic and pre-determined sequences for all replications, showing its complementary heating patterns to other frequencies. However, compared to the pre-determined frequency shifting sequences, the dynamic ones changed their operational frequencies less frequently. This might be because the real-time spatial thermal contribution, calculated as the difference between two adjacent thermal profiles during the frequency shifting stage, was slightly different from the spatial thermal contribution determined from the frequency sweeping stage. This change of spatial thermal contributions during the microwave heating process might be caused by the dielectric properties change of the

samples. Other than the frequent use of frequency (2.46 GHz), the dynamic and pre-determined sequences were considerably different. A similar trend was also observed in the mashed potato sample in Figure III-12B.

### 3.4.2 Comparison of microwave heating performance

To evaluate the heating performance during and after the heating process, thermal results collected by both the top and the handheld cameras were used for comparison among the three shifting strategies. For the process comparison, the thermal data collected by the top camera were used and for final results assessment, thermal data by the handheld camera were use, respectively.

#### 3.4.2.1 Performance comparison during heating

With the top camera, the thermal images were recorded every 10 s for all strategies no matter the thermal results were used or not. Table III-2 and Table III-3 summarized the thermal image profiles on the top surfaces, and the corresponding average temperature and *HUI* values at 2, 4, and 6 min, for gellan gel and mashed potato, respectively.

For gellan gel samples (Table III-2), during the whole heating process, all three frequency shifting strategies showed declined *HUI* values with time, indicating an improved heating uniformity with time. The dynamic shifting strategy yielded lower average ( $\pm$  standard deviation) *HUI* values ( $0.195 \pm 0.009$ ,  $0.171 \pm 0.011$  and  $0.150 \pm 0.007$ ) for collected results at 2, 4 and 6 min, respectively) and maintained similar ranges of temperature ( $18.61 \pm 0.59$  °C,  $27.53 \pm 0.41$  °C, and  $34.75 \pm 0.68$  °C for every 2 min step), when compared to the orderly and pre-determined strategies. For the mashed potato samples (Table III-3), similar declined *HUI* values with time were also observed.



However, the dynamic strategy did not show significant better heating uniformity results than the other two frequency shifting strategies for the top surface temperature results.

#### 3.4.2.2 Performance comparison after heating

To further compare the final heating performance of the whole product among the three frequency shifting strategies, both top and middle layer thermal images were collected by a more precise handheld thermal imaging camera.

The average temperature and *HUI* values of the three replications at the top and middle layers are summarized in Figure III-13 for gellan gel and in Figure III-14 for mashed potato. Note that the top surface results were slightly different from the results collected by the top camera owing to the time to remove the foods from the oven after heating, and the camera differences. The combined top and middle layer results (average temperature, *HUI* values, and estimated power efficiency of the three replications) are shown in Table III-4 for gellan gel and Table III-5 for mashed potato.

For the gellan gel samples, the average temperatures at the top layer (Figure III-13A) for the three algorithms (orderly, pre-determined complementary, and dynamic complementary) were  $34.97 \pm 0.26$  °C,  $35.50 \pm 0.87$  °C, and  $35.46 \pm 0.36$  °C, respectively, with little differences. The average temperature at the middle layer also did not show significant difference with values of  $37.60 \pm 0.62$  °C,  $38.44 \pm 1.76$  °C, and  $37.74 \pm 0.72$  °C, for the three algorithms, respectively. While in terms of the heating uniformity (Figure III-13B), the *HUI* value at the top layer of the dynamic complementary strategy was  $0.141 \pm 0.008$ , which was significantly smaller than that of the orderly shifting strategy ( $0.170 \pm 0.013$ ) and the pre-determined complementary strategy ( $0.172 \pm 0.008$ ), indicating better heating uniformity for the dynamic strategy. This was because the dynamic complementary-frequency shifting strategy evaluated the top layer *HUI* values at each frequency shifting step and determined the next complementary frequency that had the best potential to result in good heating uniformity.

Similarly, the *HUI* of the dynamic strategy ( $0.177 \pm 0.011$ ) at the middle layer was significantly lower than the pre-determined strategy ( $0.210 \pm 0.004$ ), and considerably lower than the orderly shifting strategy ( $0.201 \pm 0.014$ ).

When combining the top and middle layers together for analysis, as summarized in Table III-4, the average temperatures of the three replications for all three algorithms were similar, while the *HUI* value of the dynamic complementary shifting algorithm was significantly lower than those of the other two algorithms, indicating a significantly improved heating uniformity by the dynamic algorithm. The estimated power efficiencies of the three algorithms were similar to each other, which aligned with the average temperature results.

Similar results were observed for the mashed potato samples, as shown in Figure III-14, where the average temperatures and *HUI* values of three replications at the top and middle layers did not show significant differences among the three shifting strategies, except that the *HUI* value at the top layer of the dynamic strategy was significantly lower than that of the orderly frequency shifting strategy. While for the combined top and middle layers, as shown in Table III-5, a significant increase of average temperature, a decrease of *HUI* value (better heating uniformity), and an increase of power efficiency were observed for the dynamic shifting strategy when compared to the orderly shifting strategy.

Overall, for both the gellan gel (low loss material) and mashed potato (high loss material) samples, the dynamic complementary-frequency shifting algorithm was better than the other two strategies in terms of the resulting microwave performance.

### **3.4.3 Usefulness and future work**

Compared to the previous research that used modeling results (Tang et al., 2018) and/or pre-experimental results (Yang et al., 2022) to develop frequency shifting sequences, the online closed-loop strategies developed in this study realized the

unification of data collection, data analysis, decision making (determining frequency sequences), and execution control (using determined frequencies for heating) within one heating process. The online closed-loop strategies also could accommodate different food products and/or sample variations, making them more robust to be applied in a real microwave heating process. The dynamic complementary-frequency shifting strategy developed in this work was the key contribution from the three online strategies. Microwave heating process is complicated and varies with the oven cavity, food product geometry, size, material, and temperature, etc., making it difficult to develop a universal heating strategy. The dynamic control of the microwave parameters based on their complementary heating performance enables the flexibility and ensures good heating performance.

This online closed-looped microwave heating process was achieved by combining the solid-state generator, thermal imaging camera, and control algorithms, which contributes to the ongoing smart kitchen development (Ding et al., 2011; Trieu Minh and Khanna, 2018). With the rapid development of smart household appliances, the smart microwave oven market revenue is also increasing, with an expected rise of up to 22% during 2020-2025 (The Express Wire, 2021). More novel techniques are now being embedded in the commercial microwave ovens, such as thermal sensors, humidity sensors, or Wi-fi techniques, aiming to realize the automatic cooking process. Besides, several studies reported the development of smart microwave ovens that could sense and modify the Electromagnetic field inside the oven cavity (Jin et al., 2019) and recognize food types for heating recommendations (Khan, 2020). Both ovens have closed-loop control systems to dynamically adjust heating processes in magnetron-based ovens, while the frequency shifting approaches in this study were conducted in a solid-state microwave system with more flexibilities for further development.

Although with significant potential to heat food products more uniformly, there are still limitations in this work that require further improvement for the development of a future solid-state microwave oven. First, the microwave power used in this study was 200

W, which is much lower than that of the current domestic microwave ovens (1000 ~ 1200 W). After 6 min heating, the average temperature of the gellan gel sample reached about 36 °C, and that of the mashed potato sample reached about 40 °C. Both of the final temperatures were lower than the expected temperature (~ 74 °C) (Diplock et al., 2019) after a typical microwave heating process. A higher power solid-state microwave source can be included for future research and would not affect the implementation of the online strategies. With a higher heating rate using higher microwave power, each frequency during sweeping and shifting can be used for less time to deliver similar heating results.

Another approach to increasing the power of the solid-state microwave system is to use multiple sources. In this study, only one port was used, allowing limited control over the operational parameters. For further improved heating performance, the use of multiple ports with more parameters (power level, relative phase) may provide more potential to deliver the desired heating results. But the complicated interactions among different sources and food products need to be comprehensively evaluated to develop robust control strategies.

Moreover, the spatial thermal contributions of the selected frequencies were determined only from the frequency sweeping stage, where the temperature was still low. However, as the temperature increase, the temperature-dependent dielectric properties may affect the spatial thermal contributions, especially at high temperatures. The spatial thermal contribution change was not severe in this study because of the relatively small temperature change. For future research with higher power input, the spatial thermal contributions may be determined periodically to determine appropriate complementary frequencies.

Another significant limitation of current solid-state microwave system is its much higher price of the solid-state power generator than the magnetron. Although the integration of a thermal camera and the dynamic control of complicated microwave parameter potentially increase the smartness of the solid-state system, it also further increases the price of the system. However, with the development of the semi-conductor

technology that is used for the solid-state microwave generator, the price is expected to decrease in the future. At current stage, the smart microwave ovens may be firstly used in the food service industry and institutions (e.g., hospitals) to cook commercial meals where there is a critical need for high-quality and safe products.

### **3.5 Conclusions**

This study developed three online frequency shifting strategies (orderly, pre-determined complementary, and dynamic complementary) and embedded algorithms into microwave heating processes which formed a closed-loop control system for food heating. The solid-state microwave generator and a radiometric-capable thermal camera were used to monitor the microwave power reflection and thermal images, respectively, during the microwave heating process. Three frequency shifting algorithms were developed to analyze the collected power and thermal image information and provided feedback to control the solid-state microwave system through two stages, including frequency sweeping and frequency shifting. The frequency sweeping processes in the proposed online strategies were to determine the high-power efficiency frequencies and/or characterize the spatial thermal profile contributions. The frequency shifting processes in three strategies were able to determine the frequency shifting sequences based on the corresponding algorithms. Among the three shifting strategies, the dynamic complementary-frequency shifting one based on dynamic heating performance evaluation and frequency shifting yielded significantly better heating uniformity than the orderly shifting and pre-determined complementary shifting strategies. The online closed-loop strategy could accommodate different food products and/or sample variations, making it more robust to be applied in future smart microwave heating processes.

### **3.6 Acknowledgements**

This project (or patent) is based on research that was supported by the Tennessee Agricultural Experiment Station with funding from the USDA National Institute of Food and Agriculture Hatch Multistate Research capacity funding program (Accession Number 1023982) and the USDA National Institute of Food and Agriculture, AFRI project (Grant No: 2021-67017-33444).

## List of References

- Alfaifi, B., Tang, J., Jiao, Y., Wang, S., Rasco, B., Jiao, S., & Sablani, S. (2014). Radio frequency disinfestation treatments for dried fruit: Model development and validation. *Journal of Food Engineering*, 120(1), 268–276.  
<https://doi.org/10.1016/j.jfoodeng.2013.07.015>
- Birla, S. L., Wang, S., & Tang, J. (2008). Computer simulation of radio frequency heating of model fruit immersed in water. *Journal of Food Engineering*, 84(2), 270–280.  
<https://doi.org/10.1016/j.jfoodeng.2007.05.020>
- Birla, S. L., Wang, S., Tang, J., & Tiwari, G. (2008). Characterization of radio frequency heating of fresh fruits influenced by dielectric properties. *Journal of Food Engineering*, 89(4), 390–398. <https://doi.org/10.1016/j.jfoodeng.2008.05.021>
- Chen, J., Pitchai, K., Birla, S., Gonzalez, R., Jones, D., & Subbiah, J. (2013). Temperature-dependent dielectric and thermal properties of whey protein gel and mashed potato. *Transactions of the ASABE*, 56(6), 1457–1467.  
<https://doi.org/10.13031/trans.56.10314>
- Datta, A. K., & Anantheswaran, R. C. (2001). *Handbook of Microwave Technology for Food Application*. [https://books.google.com/books?hl=zh-CN&lr=&id=-URZDwAAQBAJ&oi=fnd&pg=PP1&ots=NJXfuzk2we&sig=HxT\\_b20fGiHZoJfjaX61IbzuECI#v=onepage&q&f=false](https://books.google.com/books?hl=zh-CN&lr=&id=-URZDwAAQBAJ&oi=fnd&pg=PP1&ots=NJXfuzk2we&sig=HxT_b20fGiHZoJfjaX61IbzuECI#v=onepage&q&f=false)
- Dinani, S. T., Feldmann, E., & Kulozik, U. (2021). Effect of Heating by Solid-State Microwave Technology at Fixed Frequencies or by Frequency Sweep Loops on Heating Profiles in Model Food Samples. *Food and Bioproducts Processing*, 105084.  
<https://doi.org/10.1016/j.fbp.2021.03.018>
- Ding, D., Cooper, R. A., Pasquina, P. F., & Fici-Pasquina, L. (2011). Sensor technology for smart homes. *Maturitas*, 69(2), 131–136.  
<https://doi.org/10.1016/j.maturitas.2011.03.016>

Diplock, K. J., Jones-Bitton, A., Leatherdale, S. T., Rebellato, S., Hammond, D., & Majowicz, S. E. (2019). Food Safety Education Needs of High-School Students: Leftovers, Lunches, and Microwaves. *Journal of School Health*, 89(7), 578–586. <https://doi.org/10.1111/josh.12782>

Du, Z., Wu, Z., Gan, W., Liu, G., Zhang, X., Liu, J., & Zeng, B. (2019). Multi-physics modeling and process simulation for a frequency-shifted solid-state source microwave oven. *IEEE Access*, 7, 184726–184733. <https://doi.org/10.1109/ACCESS.2019.2960317>

Hunter, J. D. (2007). Matplotlib: A 2D Graphics Environment. In *Computing in Science & Engineering* (Vol. 9, Issue 3, pp. 90–95). <https://doi.org/10.1109/MCSE.2007.55>

Jin, H., Wang, J., Kumar, S., & Hong, J. (2019). Software-Defined Cooking using a Microwave Oven. *The 25th Annual International Conference on Mobile Computing and Networking*, 1–16. <https://doi.org/10.1145/3300061.3345441>

Khan, T. (2020). An Intelligent Microwave Oven with Thermal Imaging and Temperature Recommendation Using Deep Learning. *Applied System Innovation*, 3(1), 13. <https://doi.org/10.3390/asi3010013>

Lee, H., Fisher, S., Kallos, M. S., & Hunter, C. J. (2011). Optimizing gelling parameters of gellan gum for fibrocartilage tissue engineering. *Journal of Biomedical Materials Research - Part B Applied Biomaterials*, 98 B(2), 238–245. <https://doi.org/10.1002/jbm.b.31845>

Luan, D., Wang, Y., Tang, J., & Jain, D. (2017). Frequency Distribution in Domestic Microwave Ovens and Its Influence on Heating Pattern. *Journal of Food Science*, 82(2), 429–436. <https://doi.org/10.1111/1750-3841.13587>

Mao, R., Tang, J., & Swanson, B. G. (2000). Texture properties of high and low acyl mixed gellan gels. *Carbohydrate Polymers*, 41(4), 331–338. [https://doi.org/10.1016/S0144-8617\(99\)00108-3](https://doi.org/10.1016/S0144-8617(99)00108-3)



Okiror, G. P., & Jones, C. L. (2012). Effect of temperature on the dielectric properties of low acyl gellan gel. *Journal of Food Engineering*, 113(1), 151–155. <https://doi.org/10.1016/j.jfoodeng.2012.04.011>

OpenCV. (2021). OpenCV. Open Source Computer Vision Library. <https://opencv.org/>

Pitchai, K., Birla, S. L., Subbiah, J., Jones, D., & Thippareddi, H. (2012). Coupled electromagnetic and heat transfer model for microwave heating in domestic ovens. *Journal of Food Engineering*, 112(1–2), 100–111. <https://doi.org/10.1016/j.jfoodeng.2012.03.013>

Tang, Z., Hong, T., Liao, Y., Chen, F., Ye, J., Zhu, H., & Huang, K. (2018). Frequency-selected method to improve microwave heating performance. *Applied Thermal Engineering*, 131, 642–648. <https://doi.org/10.1016/j.applthermaleng.2017.12.008>

The Express Wire. (2021). Smart Microwave Oven Market Size and Analysis by 2021: Global Business Share and Rapidly Growing Opportunities, Industry Trends, Top Key Players Analysis, Trending Developments and Forecast 2025. The Express Wire. [https://www.theexpresswire.com/pressrelease/Smart-Microwave-Oven-Market-Size-and-Analysis-by-2021-Global-Business-Share-and-Rapidly-Growing-Opportunities-Industry-Trends-Top-Key-Players-Analysis-Trending-Developments-and-Forecast-2025\\_13487426](https://www.theexpresswire.com/pressrelease/Smart-Microwave-Oven-Market-Size-and-Analysis-by-2021-Global-Business-Share-and-Rapidly-Growing-Opportunities-Industry-Trends-Top-Key-Players-Analysis-Trending-Developments-and-Forecast-2025_13487426)

Trieu Minh, V., & Khanna, R. (2018). Application of Artificial Intelligence in Smart Kitchen. *International Journal of Innovative Technology and Interdisciplinary Sciences Wwww. IJTIS.Org*, 1(1), 1–8. <https://doi.org/10.1515/IJTIS.2018.1.1.1-8>

Yakovlev, V. v. (2018). Effect of frequency alteration regimes on the heating patterns in a solid-state-fed microwave cavity. *Journal of Microwave Power and Electromagnetic Energy*, 52(1), 31–44. <https://doi.org/10.1080/08327823.2017.1417105>

Yang, R., Fathy, A. E., Morgan, M. T., & Chen, J. (2022). Development of a complementary-frequency strategy to improve microwave heating of gellan gel in a solid-state system. *Journal of Food Engineering*, 314(April 2021), 110763.

<https://doi.org/10.1016/j.jfoodeng.2021.110763>

Yang, Y., Fan, Z., Hong, T., Chen, M., Tang, X., He, J., Chen, X., Liu, C., Zhu, H., & Huang, K. (2020). Design of microwave directional heating system based on phased-array antenna. *IEEE Transactions on Microwave Theory and Techniques*, 68(11), 4896–4904.

<https://doi.org/10.1109/TMTT.2020.3002831>

Zhang, H., & Datta, A. K. (2000). Coupled electromagnetic and thermal modeling of microwave oven heating of foods. *Journal of Microwave Power and Electromagnetic Energy*, 35(2), 71–85.

<https://doi.org/10.1080/08327823.2000.11688421>

Zhang, W., Luan, D., Tang, J., Sablani, S. S., Rasco, B., Lin, H., & Liu, F. (2015). Dielectric properties and other physical properties of low-acyl gellan gel as relevant to microwave assisted pasteurization process. *Journal of Food Engineering*, 149, 195–203.

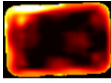
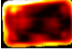
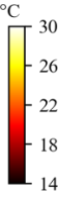
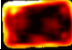
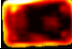
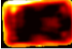
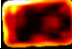
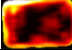
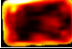
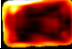
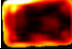
<https://doi.org/10.1016/j.jfoodeng.2014.10.014>

Zhu, X., Guo, W., & Wu, X. (2012). Frequency- and temperature-dependent dielectric properties of fruit juices associated with pasteurization by dielectric heating. *Journal of Food Engineering*, 109(2), 258–266.

<https://doi.org/10.1016/j.jfoodeng.2011.10.005>

## Appendix

**Table III-1. The calculated superimposed thermal results of microwave heating of gellan gum for the first dynamic frequency selection after frequency sweeping ( $t \approx 90$  s).**

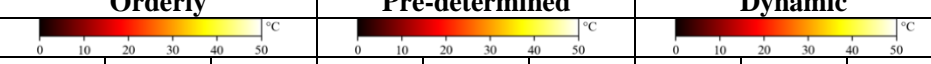



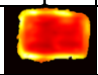

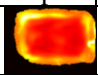
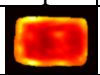
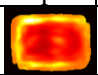
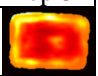
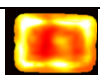


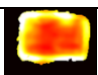

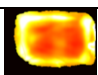
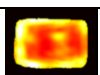
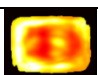

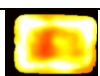





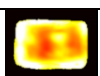


Thermal Image after Sweeping*	Superimposed Frequency, GHz	Superimposed Thermal Image*	Superimposed Average Temperature, °C	Superimposed HUI	Color Legend
 Temperature = 17.60 °C HUI = 0.238	2.40		18.80	0.252	
	2.41		18.57	0.247	
	2.42		18.29	0.246	
	2.43		17.79	0.250	
	2.44		18.59	0.249	
	2.45		<b>18.87</b>	0.243	
	<b>2.46</b>		<b>18.57</b>	<b>0.225</b>	
	2.47		18.68	0.246	
	2.48		18.44	0.246	

\* The images were obtained from the first replicate of gellan gum sample heated by the dynamic shifting algorithm.

**Table III-2. The thermal results collected by the top camera for gellan gum samples during 6 min microwave heating with different frequency shifting strategies.**

Algorithm	Orderly			Pre-determined			Dynamic		
Color Legend									
	Rep 1	Rep 2	Rep 3	Rep 1	Rep 2	Rep 3	Rep 1	Rep 2	Rep 3
<b>2 min</b>									
<b>Temperature, °C</b>	18.14	19.53	20.58	19.91	20.12	21.00	18.12	19.27	18.45
<b>HUI</b>	0.197	0.208	0.189	0.209	0.184	0.207	0.189	0.192	0.205
<b>4 min</b>									
<b>Temperature, °C</b>	27.21	28.26	29.93	28.21	29.18	30.57	27.07	27.83	27.70
<b>HUI</b>	0.192	0.205	0.189	0.205	0.191	0.207	0.162	0.183	0.167
<b>6 min</b>									
<b>Temperature, °C</b>	36.09	35.87	37.02	36.91	37.60	37.33	34.68	35.46	34.10
<b>HUI</b>	0.163	0.183	0.174	0.172	0.174	0.183	0.142	0.155	0.152

**Table III-3 The thermal results collected by the top camera for mashed potato samples during 6 min microwave heating with different frequency shifting strategies.**

Algorithm	Orderly			Pre-determined			Dynamic		
									
Color Legend	Rep 1	Rep 2	Rep 3	Rep 1	Rep 2	Rep 3	Rep 1	Rep 2	Rep 3
<b>2 min</b>									
Temperature, °C	24.04	23.43	25.46	24.23	24.14	25.37	21.95	25.09	25.07
HUI	0.296	0.337	0.301	0.338	0.294	0.280	0.310	0.282	0.294
<b>4 min</b>									
Temperature, °C	32.58	31.79	33.98	33.03	33.44	33.89	31.46	33.72	34.51
HUI	0.274	0.324	0.270	0.303	0.250	0.255	0.262	0.250	0.255
<b>6 min</b>									
Temperature, °C	40.20	39.97	41.12	42.16	42.00	41.10	38.50	40.25	40.75
HUI	0.236	0.270	0.229	0.245	0.206	0.205	0.228	0.215	0.220

**Table III-4 Microwave heating performances of combined top and middle layers with three different frequency shifting strategies on gellan gel samples.**

<b>Strategies</b>	<b>Average Temperature, °C</b>	<b>Heating Uniformity Index</b>	<b>Power Efficiency, %</b>
<b>Orderly</b>	36.22 ± 0.28 <sup>a</sup>	0.190 ± 0.013 <sup>a</sup>	62.77 ± 0.49 <sup>a</sup>
<b>Pre-determined</b>	36.92 ± 1.26 <sup>a</sup>	0.197 ± 0.008 <sup>a</sup>	63.99 ± 2.18 <sup>a</sup>
<b>Dynamic</b>	36.55 ± 0.37 <sup>a</sup>	0.164 ± 0.010 <sup>b</sup>	63.35 ± 0.65 <sup>a</sup>

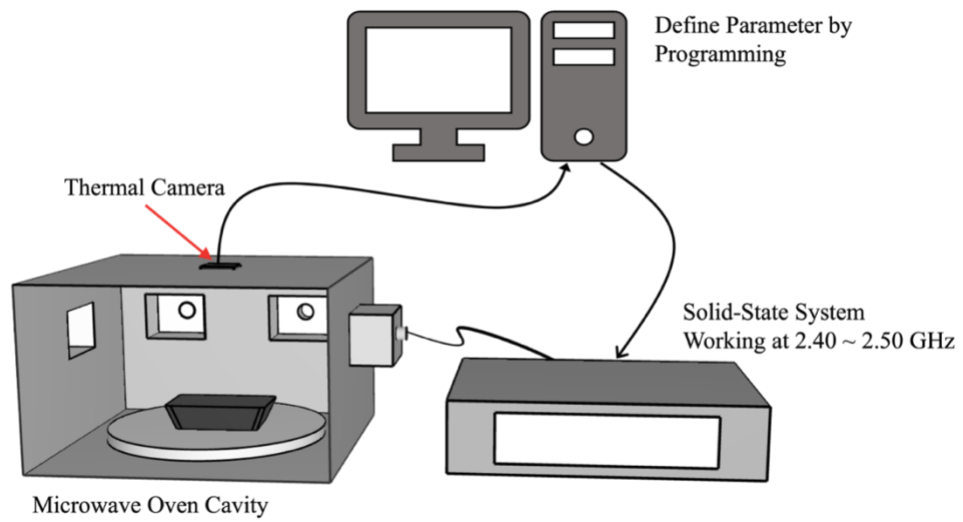
Results are shown as mean ± standard deviation. Different letters in the same column indicate statistically different results ( $p < 0.05$ ).

**Table III-5 Microwave heating performances of combined top and middle layers with three different frequency shifting strategies on mashed potato samples.**

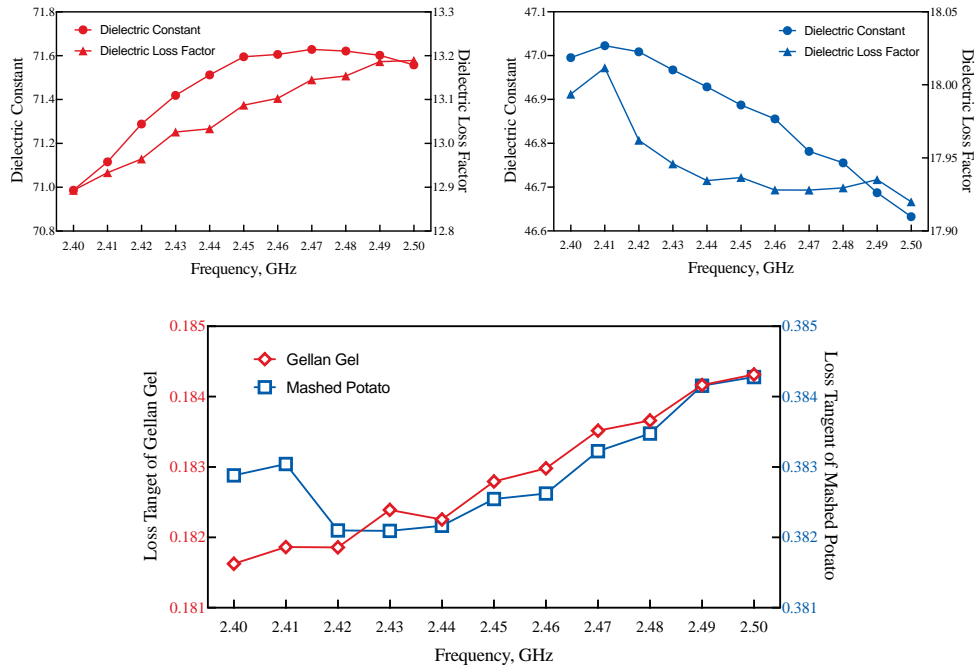
<b>Strategies</b>	<b>Average Temperature, °C</b>	<b>Heating Uniformity Index</b>	<b>Power Efficiency, %</b>
<b>Orderly</b>	38.94 ± 0.78 <sup>a</sup>	0.258 ± 0.012 <sup>a</sup>	61.33 ± 1.22 <sup>a</sup>
<b>Pre-determined</b>	39.54 ± 0.68 <sup>ab</sup>	0.235 ± 0.013 <sup>ab</sup>	62.27 ± 1.07 <sup>ab</sup>
<b>Dynamic</b>	40.52 ± 0.36 <sup>b</sup>	0.230 ± 0.002 <sup>b</sup>	63.82 ± 0.56 <sup>b</sup>

Results are shown as mean ± standard deviation. Different letters in the same column indicate statistically different results ( $p < 0.05$ ).

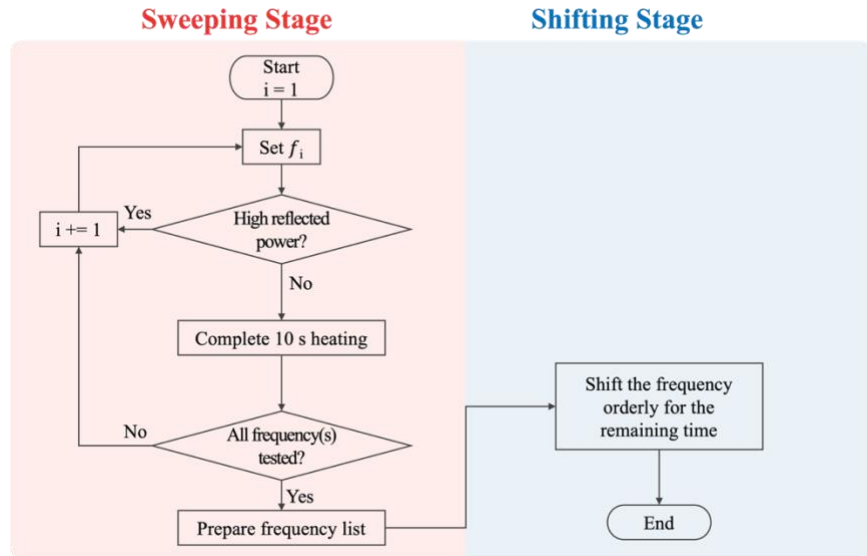




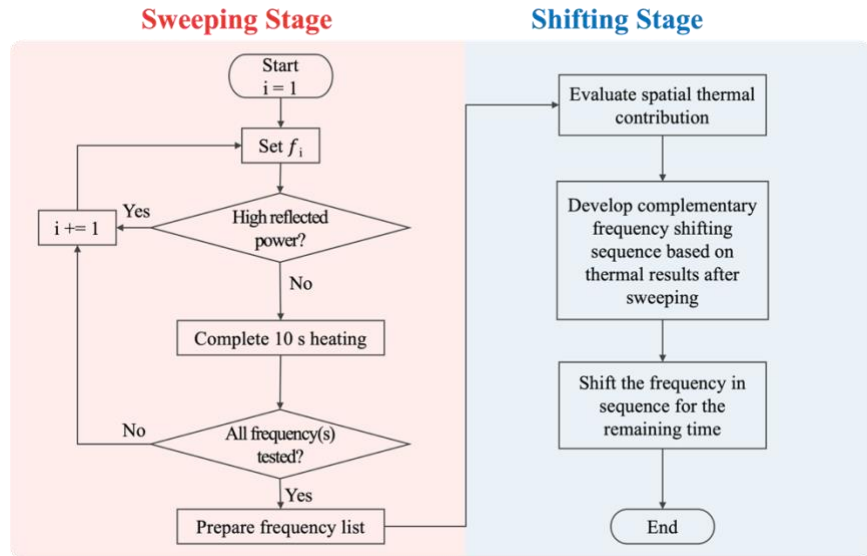
**Figure III-1 A schematic diagram for the solid-state microwave system setup.**



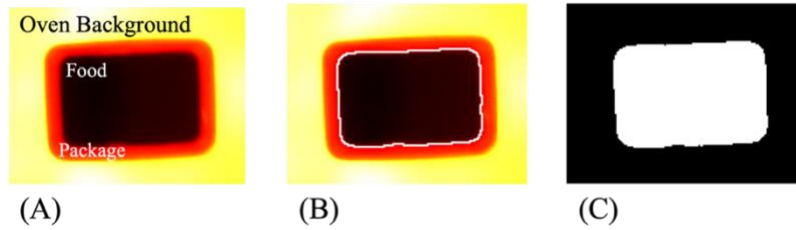
**Figure III-2 Frequency-dependent dielectric properties of gellan gel and mashed potatoes measured in triplicate at room temperature. (A) Dielectric constant (B) dielectric loss factor and (C) loss tangent (ratio of loss factor to dielectric constant).**



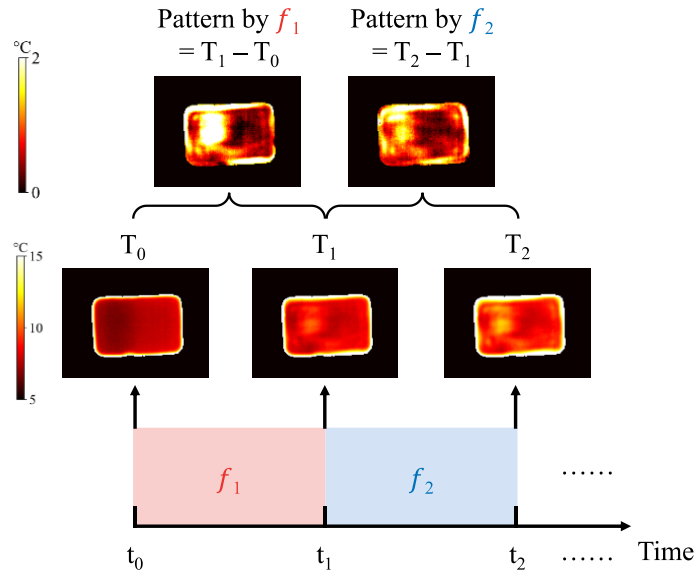
**Figure III-3 Orderly frequency shifting algorithm.**



**Figure III-4 Pre-determined complementary-frequency shifting algorithm.**



**Figure III-5 Illustration of the food boundary detection by the thermal imaging camera mounted at the top of the oven cavity. (A) thermal image captured by the top camera, (B) food boundary (white line) detected, (C) created mask used to determine the food domain for data analysis.**



**Figure III-6 Illustration of the superposition assumption to determine the spatial thermal contribution from each frequency.**

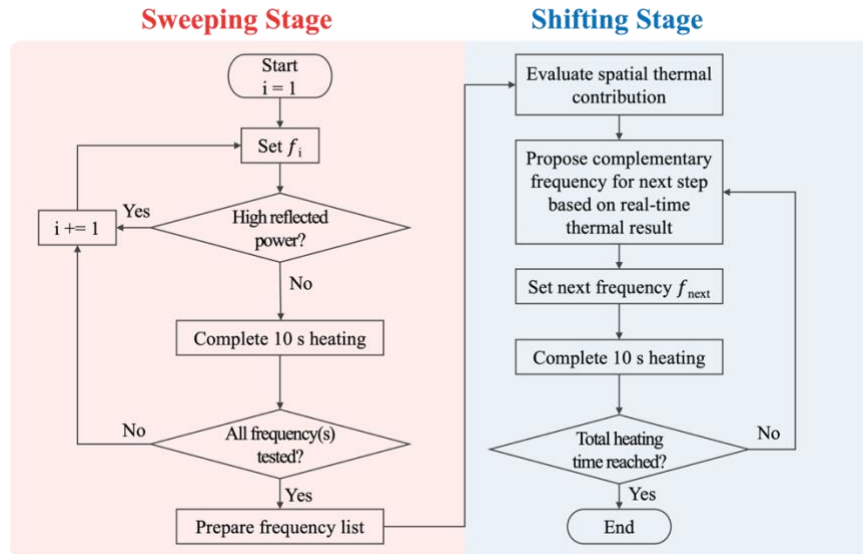
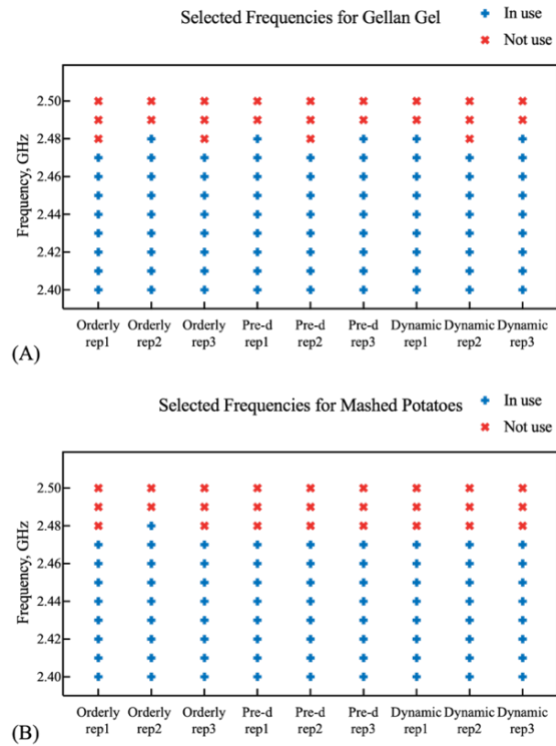
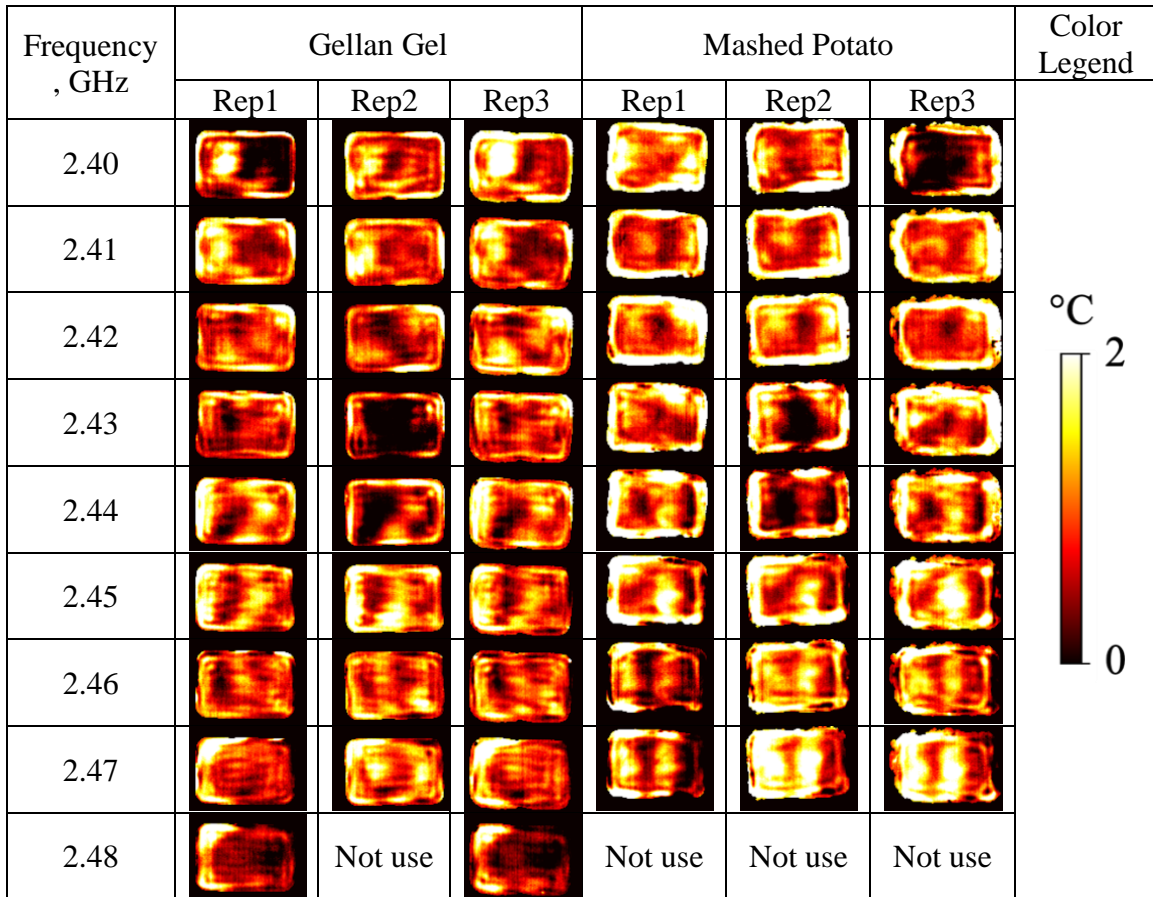


Figure III-7 Dynamic complementary-frequency shifting algorithm.

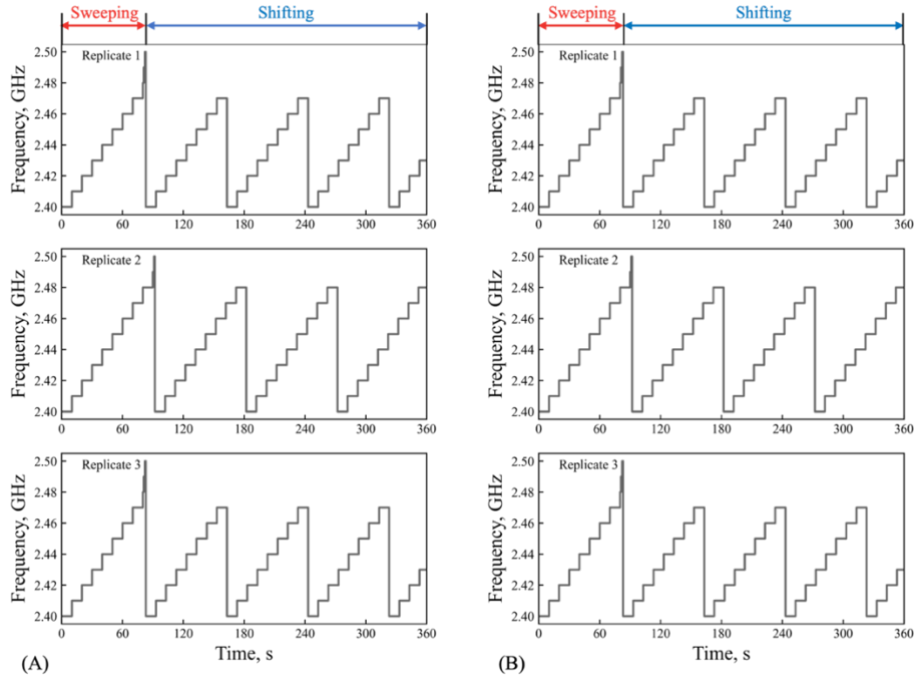


**Figure III-8 Selected frequencies by the frequency sweeping process for three replications of three algorithms (Orderly, Pre-determined, and Dynamic) for gellan gel (A) and mashed potato (B) samples.**

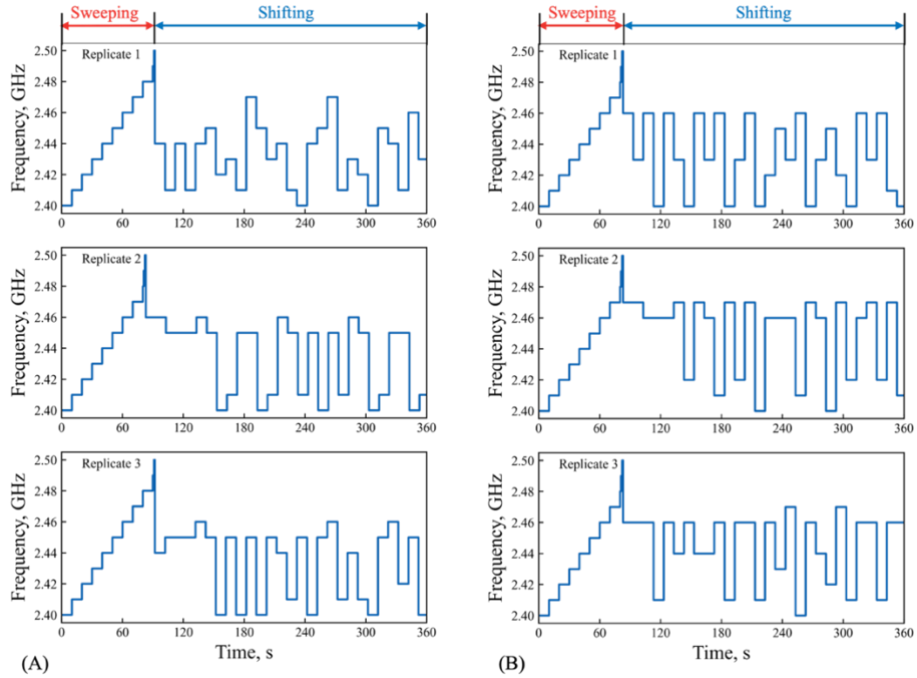




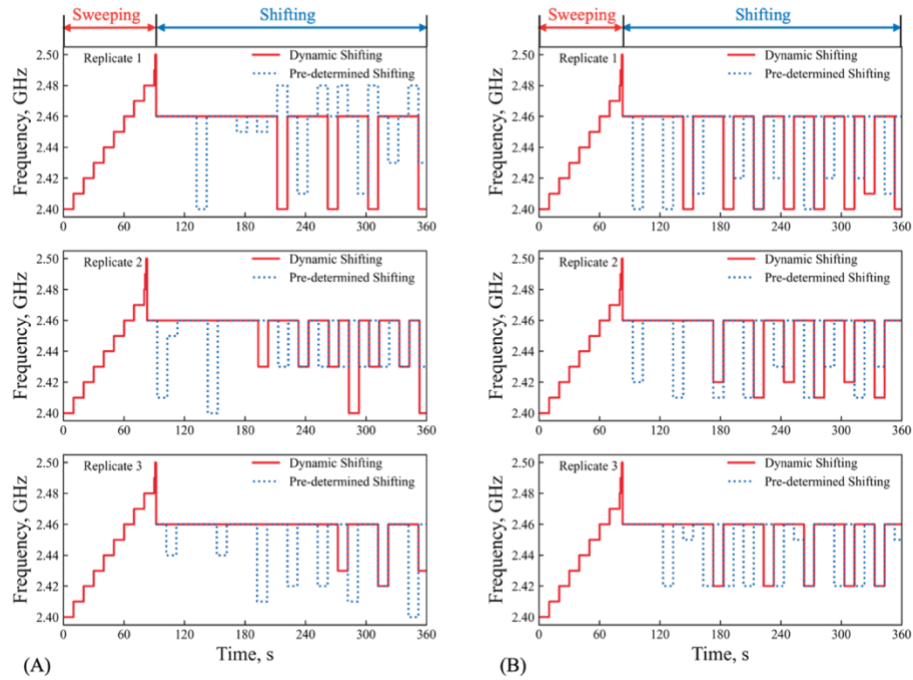
**Figure III-9 Determined spatial thermal contribution from the selected frequencies by pre-determined strategy, with only food domain shown in color.**



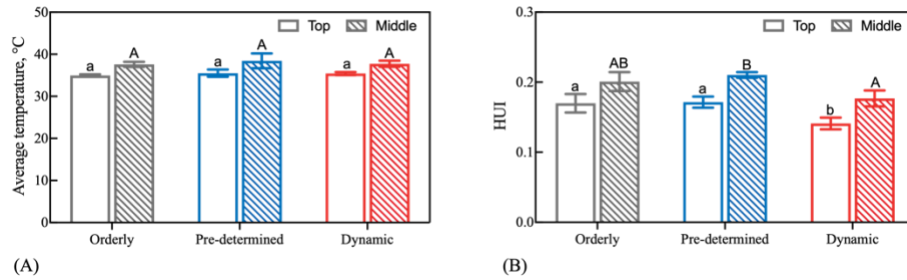
**Figure III-10** Developed orderly frequency shifting sequences for gellan gel (A) and mashed potato (B) samples.



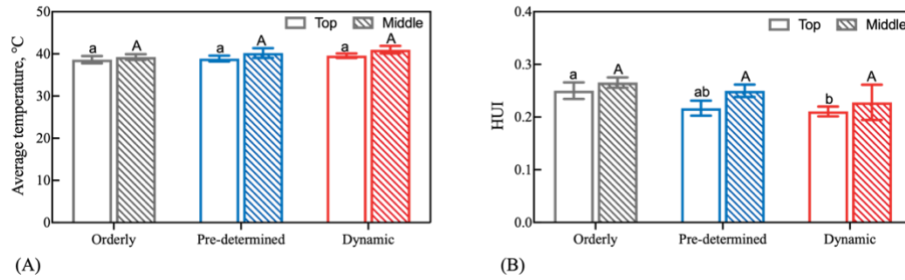
**Figure III-11 Developed pre-determined complementary-frequency shifting sequences for gellan gel (A) and mashed potato (B) samples.**



**Figure III-12** Developed frequency shifting sequences following the dynamic complementary algorithm (red lines) and pre-determined complementary algorithm (blue dash lines) for gellan gel (A) and mashed potato (B) samples.



**Figure III-13 Layered heating performance (A: Average temperature, B: *HUI* profiles) at top and middle layers for gellan gel samples after 6 min heating following the three different algorithms. The results and error bars were calculated as the average and standard deviation from triplicated experiments. Different letters (top layer with lower-case letters, middle layer with capital letters) indicate a significant difference ( $p < 0.05$ ).**



**Figure III-14 Layered heating performance (A: Average temperature, B: *HUI* profiles) at top and middle layers for mashed potato samples after 6 min heating following the three different algorithms. The results and error bars were calculated as the average and standard deviation from triplicated experiments. Different letters (top layer with lower-case letters, middle layer with capital letters) indicate a significant difference ( $p < 0.05$ ).**

**CHAPTER IV**  
**COMPREHENSIVE EVALUATION OF MICROWAVE HEATING**  
**PERFORMANCE USING DYNAMIC COMPLEMENTARY-**  
**FREQUENCY SHIFTING STRATEGY IN A SOLID-STATE**  
**SYSTEM**

A version of this chapter is currently under review for submission, by Yang, R., Morgan, M. T., Wang, Z., Fathy, A. E., Luckett, C., & Chen, J.

As the first author of this research article, I was the main contributor to Conceptualization, Methodology, Data curation, Investigation, Software, Visualization, Writing of the manuscript. Dr. Jiajia Chen, as the major professor and corresponding author, contributed to Conceptualization, Investigation, Supervision, Project administration, Funding acquisition, Writing - Reviewing and Editing of the manuscript. The co-authors, as the committed members of the Ph.D. program, offered suggestions in the experiment design, provided help in manuscript revising.

#### **4.1 Abstract**

Solid-state technique has the potential to address the nonuniform heating in magnetron-base microwave ovens. Previously developed dynamic complementary-frequency shifting strategy in solid-state systems showed better results than other orderly shifting strategies. However, the dynamic strategy has not been compared with magnetron-based microwave heating or tested on complicated commercial food products. To bridge this gap, this study comprehensively evaluated the microwave heating performance using the dynamic complementary-frequency shifting strategy on five commercial and/or prepared meals with different characteristics, including single-component Pulled Chicken, multicomponent Beef in Gravy, multilayer Lasagna, multicompartment Pulled Chicken & Lasagna, and multicompartment Mashed Potato & Beef in Gravy. Results showed that the dynamic complementary-frequency shifting strategy improved microwave performance on all food products, especially for multicompartment foods. The presence of liquid components or the use of steam-venting packages may negatively affect the thermal profile collection in the dynamic strategy, hindering the algorithm performance, although considerable improvement was still



observed. The complementary-frequency shifting strategy is highly promising to be incorporated in future solid-state microwave systems for improving microwave heating performance.

**Keywords:** Microwave heating, solid-state, magnetron, complementary-frequency, uniformity, commercial foods

## 4.2 Introduction

Microwave oven is a popular household kitchen appliance to reheat leftovers or to cook commercially prepared ready-to-eat meals for its fast heating and convenience. However, the inherent non-uniform heating issue has been the main drawback of current microwave ovens powered by magnetrons, which can be attributed to the fixed distribution of hot and cold spots due to standing wave patterns inside the oven cavity at a single frequency. In addition, the heterogeneous food compositions and their temperature-dependent properties also contribute to the heating nonuniformity, known as the ‘thermal-runaway’ phenomenon.

A promising technique, solid-state generator, has multiple advantages over the magnetron, making it possible to improve the microwave process with better heating performance. With a solid-state microwave generator, the microwave parameters, including frequency, relative phase (if multiple sources), and power level, can be precisely controlled in a wider range (Soltysiak et al., 2011; Taghian Dinani et al., 2021; Zhou et al., 2022). Moreover, the solid-state system provides feedback and enables adaptive process optimization according to the real-time retrieved feedback (Atuonwu and Tassou, 2018). Given all those benefits of the solid-state technique, it is vital to properly and efficiently utilize these functions.

Strategies on how to apply the solid-state generated microwaves have been proposed and proven effective to improve the heating performance. Du et al. (2019) compared the heating performance between heating scenarios using fixed frequency and those using orderly shifting frequencies. Results showed that, during the heating of refrigerated chicken blocks, orderly shifting frequencies could significantly improve the heating uniformity. Similar conclusions on refrigerated gellan gel samples were also reported by Dinani et al. (2021). Moreover, a complementary-frequency concept was proven to be applicable to improve the microwave performance further (Yang et al., 2022a). Rather than orderly shifting all frequencies, the complementary-frequency shifting strategy first collected heating patterns at different frequencies. The frequencies with complementary patterns were then selected and shifted in a specific sequence, which could further lower the nonuniformity when compared to the orderly shifting strategy.

The complementary-frequency strategy using pre-collected thermal profiles was further upgraded to be a dynamic strategy, making it applicable in real microwave heating process. This dynamic complementary-frequency shifting strategy used a thermal imaging camera mounted at the top of the microwave oven cavity to monitor the real-time heating performance and determine complementary microwave frequencies dynamically. Compared to the orderly frequency shifting strategy, the dynamic complementary-frequency shifting strategy improved the microwave heating uniformity of gellan gel by 14 % and mashed potato by 11 % (Yang et al., 2022b).

Even though significant improvement in heating uniformity has been reported by using various frequency-shifting strategies, there are considerable limitations in previous heating performance evaluations. First, most of the frequency shifting strategies, including the dynamic complementary-frequency shifting strategy, were only compared with the stationary heating either in the magnetron-based oven or in the solid-state oven using fixed frequency. However, most commercial magnetron-based microwave ovens are equipped with turntables to rotate the foods during heating, which has been proven to improve the heating performance considerably (Geedipalli et al., 2007). Thus, it is

necessary to conduct a direct comparison between the solid-state heating strategies and the rotatory magnetron heating to assess whether the proposed strategies could provide better microwave performance than the current commercial microwave ovens. Additionally, all the reported solid-state microwave heating results were only evaluated based on simple and homogenous model food products (e.g., gellan gel or potato slice). However, most commercial, or prepared microwaveable food products are in heterogeneous forms, such as multicomponent and multicompartments. The varied components/compartments in one food product would lower the heating uniformity caused by thermal runaway. Furthermore, some commercial food products also utilize their original packages, e.g., venting package, to improve the microwave heating uniformity (Biji et al., 2015). Considering so many affecting factors, either improve or worsen the heating results, it is necessary to evaluate the microwave heating performance of complex commercial or prepared foods, since the microwave performance is highly dependent on the sample types (Fakhouri and Ramaswamy, 1993).

Since the dynamic complementary-frequency shifting strategy has been reported to be better than the orderly frequency shifting strategy in heating uniformity, this study aims to comprehensively compare the microwave heating performance of complex commercial and/or prepared meals between only the dynamic strategy and the magnetron-based heating with rotatory turntable. The objectives of this study were to:

- 1) comprehensively compare the heating performance of the dynamic complementary-frequency strategy in a solid-state oven with the performance of currently used domestic ovens on various commercial and/or prepared foods;
- 2) quantitatively evaluate the performance improvement and identify the limitations of the dynamic strategy.

## **4.3 Materials and Methods**

### **4.3.1 Microwave systems**

A commercial magnetron-based domestic microwave oven (Panasonic Model NN-SN936W) equipped with a rotatory glass turntable (6 rpm) was used in this study.

To eliminate the potential performance variation due to the oven geometry difference, another oven cavity with the same mode number (Panasonic Model NN-SN936W) was used to assemble the solid-state microwave system. The glass turntable was kept in the oven to ensure the same position of the samples inside the cavity. The turntable coupler was removed to disable the rotation during heating. The magnetron was dismounted from the cavity and a solid-state microwave generator (PA-2400–2500 MHz-200 W-4, Junze Technology, China) was connected to the cavity through a waveguide (CWR340 CentricRF). A radiometric-capable thermal camera module (Lepton 3.5, 160 ×120) was attached over the top wall to support the heating scenarios using the dynamic complementary-frequency shifting strategy (Figure IV-1). The thermal profile collection, frequency selection, and microwave parameter control by the solid-state were realized by Python programming.

### **4.3.2 Food product preparation**

Food volume, shape, compositions, and layout are critical factors affecting the microwave performance (Bhattacharya and Basak, 2017; Chamchong and Datta, 1999; Gulati et al., 2015; He et al., 2020; Liu et al., 2013; Vilayannur et al., 1998). Another factor that affects the microwave process is the package over the food which helps keep the steam to improve the heating uniformity (Soares et al., 2002).

To comprehensively evaluate the performance of the dynamic complementary-frequency shifting strategy, different types of foods were selected based on their diverse dielectric properties, components, and food geometries (i.e., multilayer, multicompartment). Five commercial and prepared food products, including Pulled Chicken, Beef in Gravy, Lasagna, combination of Pulled Chicken & Lasagna, and combination of Mashed Potato & Beef in Gravy were used to represent simple

homogeneous, multicomponent, multilayer, and multicompartment products, as summarized in Table IV-1.

The commercial fully cooked Pulled Chicken (Kroger Company, Cincinnati, OH, USA) was used to represent the homogenous food, which included only pulled chicken meat and a few flavor seasonings (e.g., spices, salt, and citrus extract). The product was prepared following the cooking instruction before heating: a small opening was cut into the plastic pouch to release the excess steam.

Another commercial Beef in Gravy product (Slow Simmered Beef Tips & Gravy, Hormel Foods Corporation, Austin, MN, USA) was selected as a representative of multicomponent product, which consisted of solid beef chunks and thick liquid gravy. Following the cooking instructions, the product was directly placed in the microwave oven for heating.

Lasagna has been widely used as a representative heterogeneous food in microwave heating research (Fakhouri and Ramaswamy, 1993; Pitchai et al., 2015; Schiffmann, 2017; Wang et al., 2012). A refrigerated commercial Lasagna product (Giovanni Rana, Oak Brook, IL, USA) with six layers (cheese, pasta, meat sauce, pasta, cheese, and pasta) was selected on behalf of multilayer foods. The original packaged Lasagna had several servings and was too big for the microwave heating. To prepare the sample as a single-serving meal, the Lasagna product was cut into four portions and one portion ( $285 \pm 10$  g) was individually stored in a plastic microwavable container and then used for the heating experiments.

Two different multicompartment samples were used in this study. The first multicompartment meal consisted of Pulled Chicken (100 g) and single-serving Lasagna (285 g). The other multicompartment meal consisted of prepared Mashed Potato (150 g) and Beef in Gravy (150 g) from the previously mentioned commercial products (Slow Simmered Beef Tips & Gravy, Hormel Foods Corporation, Austin, MN, USA). The mashed potatoes (23.8% mashed potato flakes, 18.6% whole milk, 53.5% deionized

water, and 4.1% unsalted butter) were prepared in advance following a previous study (Yang et al., 2021).

All the meals were prepared in advance and stored at 4 °C overnight before experiments.

### **4.3.3 Heating strategies**

For comparison purposes, the same power inputs were used in both the magnetron-based oven and the solid-state microwave system to heat the products; and for the same foods, same heating time was used in the two system. Since the solid-state microwave generator used in this study only allows a power output up to 200 W, a suitable power level in the magnetron-based microwave oven was first determined to generate similar power outputs to those by the solid-state system. A smart energy monitor (Emporia Smart Plug, Emporia Corp., Littleton, CO, USA) was used to continuously record the total power consumption during a 10-min microwave heating process. The recorded power consumption by the magnetron-based microwave oven working under power level 1 (Figure IV-2) was in the range of 32 to 738 W, with an average of 239 W, which included the energy required to generate microwave power, operate the turntable motor, light and user panel. So, the total power applied as microwave output is about 200 W, which is similar to the highest power output by the solid-state generator. Thus, for the magnetron-based domestic oven, power level-1 was selected for use. For the solid-state oven, 200 W was used for heating all food products. During the experiments, the turntable in the solid-state system was disabled while that in the magnetron-based oven was enabled.

The solid-state oven was operated at full power (200 W) following the previously developed dynamic complementary-frequency shifting strategy as shown in Figure IV-1 (Yang et al., 2022b). In brief, the dynamic complementary-frequency shifting strategy continuously monitors the thermal profiles of the products in real-time and dynamically

updates microwave frequency that has complementary heating patterns. The whole dynamic microwave process includes two stages: frequency sweeping stage and frequency shifting stage. In the frequency sweeping stage, microwave frequency was orderly swept from 2.40 to 2.50 GHz at a step of 0.01 GHz/10 s to heat the food product. The thermal profiles were recorded by the top thermal camera after each 10-s heating, then the thermal contribution by each frequency was determined from the collected thermal profiles. Then, in the frequency shifting stage, one optimal frequency that could best complement the most current heating pattern is to be selected based on the thermal contribution and used for the upcoming shifting step (10 s). Such complementary frequency selection and updating process are repeated until the end of the whole heating process.

The refrigerated foods were placed at the center of the turntable, with rotation enabled in the domestic microwave oven and disabled in the solid-state system. The total heating time (as shown in Table IV-1 ) for each sample was determined by heating the foods in the domestic microwave oven until the surface average temperature went up to about 40 °C, which is a close number to those from previous studies (Yang et al., 2022b, 2022a). For comparison purpose, the heating duration for the same sample in the solid-state oven was the same as the one in the domestic oven. Either in the domestic oven or the solid-state oven, each sample was tested in triplicate.

#### **4.3.4 Heating performance evaluation**

A handheld thermal camera (FLIR C3, Boston, MA) was used to capture the final thermal images after heating (Figure IV-3A); since the foods used in this study were in irregular shapes, spatial temperature profiles from those images were then exported to be numerical temperature data (320 × 240) through FLIR Tools (2020 © FLIR® Systems, Inc.). The food boundary for each image was manually drawn using Image Segmenter App (MATLAB R2022a, The MathWorks, Inc., Natick, MA, USA) based on the thermal

result collected after heating, as illustrated in Figure IV-3B. A mask was then created based on the boundary (Figure IV-3C). Only temperature profiles within the food boundary would be used to evaluate the heating performance. For the Pulled Chicken, Beef in Gravy, combination of Pulled Chicken & Lasagna, and combination of Mashed Potato & Beef in Gravy, the thermal images were taken for the top surface only; for the Lasagna sample, the thermal images were captured for both the top (cheese) and middle (meat sauces) layers (Figure IV-4).

To quantitatively describe the heating results, the spatial average temperature, heating uniformity index (*HUI*), and cold spot temperature were evaluated and compared between the magnetron heating with rotation and the solid-state heating using dynamic complementary-frequency shifting without rotation.

The average temperature value was calculated as the mean value of pixel temperature data within the food boundary from each thermal image. The cold spot temperatures were the minimum temperature point from each thermal image.

The heating uniformity results were calculated as Heating Uniformity Index (*HUI*) following (Alfaifi et al., 2014):

$$HUI = \frac{\Delta STD}{\Delta \bar{T}} \quad (\text{IV-1})$$

where  $\Delta STD$  is the change in the standard deviation of the temperature profiles calculated below in Eq. (IV-2), and  $\Delta \bar{T}$  is the average temperature increase over the layer after heating. A smaller *HUI* value denotes a better heating uniformity.

$$\Delta STD = \frac{1}{S_{food}} \int_{S_{food}} \sqrt{(T - \bar{T})^2} dS_{food} \quad (\text{IV-2})$$

Where  $S_{food}$  is the area for a single layer of a food domain.



Besides, the temperature improvement (%) and uniformity improvement (%) by using the solid-state oven, compared with the magnetron oven with turntable, were calculated as:

$$T_{improvement} = \frac{\bar{T}_{solidstate} - \bar{T}_{magnetron}}{\bar{T}_{magnetron}} \times 100\% \quad (\text{IV-3})$$

$$HUI_{improvement} = \frac{\overline{HUI}_{magnetron} - \overline{HUI}_{solidstate}}{\overline{HUI}_{magnetron}} \times 100\% \quad (\text{IV-4})$$

where  $\bar{T}_{solidstate}$  and  $\overline{HUI}_{solidstate}$  are the average final temperature and average *HUI* of samples for the three replications by the solid-state oven, respectively.

$\bar{T}_{magnetron}$  and  $\overline{HUI}_{magnetron}$  are the average final temperature and average *HUI* for the three replications by the magnetron-based domestic oven, respectively.

#### 4.3.5 Data analysis

All data are expressed as the mean  $\pm$  standard deviation of the results from replicated experiments. For the comparison of the heating performance between the magnetron-based domestic oven and the solid-state oven using dynamic complementary-frequency shifting, statistical significance was determined using two-tailed t-test. Pairwise Pearson correlation analysis were conducted for the sample characteristics (surface area, sample weight, number of compartments, and heating time) and improvement indexes ( $T_{improvement}$  and  $HUI_{improvement}$ ) by applying the dynamic solid-state heating strategy.

The statistical analysis was performed using GraphPad Prism Version 9.0 (GraphPad Software, La Jolla California, USA), and *p* values smaller than 0.05 were considered statistically significant.

## 4.4 Results and Discussion

### 4.4.1 Microwave heating performance

This section discusses the complementary frequency recorded during the heating processes and the microwave heating performance (thermal image profiles, average temperature, and *HUI*) after the heating of five representative food products. The performance of the magnetron-based domestic microwave heating with the rotatory turntable is also discussed for comparison. For the Lasagna samples, the thermal image profiles at both the top and middle layers were evaluated for this multilayer product.

#### 4.4.2.1 Single-component commercial Pulled Chicken in original package

Figure IV-5 shows the microwave heating results of single-component Pulled Chicken in its original package with a small opening to release the steam. As shown in Figure IV-5A, after the frequency sweeping stage, several frequencies were selected for use during the shifting stages for their complementary pattern characteristics. Six to seven frequencies were used for shifting in different replications. The different frequency selections among replications were mainly attributed to the sample variation in geometrical factors, which was observed in the previous study of using dynamic complementary-frequency shifting (Yang et al., 2022b).

After 10-min heating, the heating patterns of the solid-state complementary heating were more uniform than those of the magnetron-based heating, as shown in Figure IV-5B. In magnetron-based heating, severe cold spots (dark blue color) were observed at the center of the Pulled Chicken products, although the steam trapped by the package could help improve the heating uniformity. The average temperature of products heated in the magnetron-based oven is similar to that in the solid-state oven, as shown in Figure IV-5C, while the heating uniformity of the solid-state heating ( $0.16 \pm 0.01$ ) is significantly better than that of the magnetron-based heating ( $0.23 \pm 0.03$ ), as shown in Figure IV-5D. Such improved heating uniformity and maintained average temperature by

the solid-state complementary-frequency shifting strategy was aligned with the previously reported work of gellan gel and mashed potato (Yang et al., 2022b).

#### 4.4.2.2 Multicomponent commercial Beef in Gravy in original package

The commercial Beef in Gravy product was heated in its original package (with film unpierced and no steam venting open) for 8 minutes, and the heating performances are shown in Figure IV-5. As can be seen from Figure IV-5A, three replications of complementary-frequency shifting strategy showed different selected frequencies. In replication 1 and 3, only 2.45 GHz was used in the frequency shifting stages, which was different from the second replication and the frequency shifting in Pulled Chicken products. The different frequency shifting behavior in the Beef in Gravy product might be due to the sample variations in different replications because the beef chunks presented differently in the gravy. Since the package is covered with film without steam venting holes, the generated steam and presence of the liquid component (gravy) may also influence the frequency shifting and heating performance, where the fluid movement and convective heat transfer obscured the heating patterns at different frequencies.

Figure IV-5B shows the thermal images for the commercial Beef in Gravy products heated in the magnetron oven and the solid-state system. After 8-min heating in the magnetron-based oven with rotation, about two-thirds of the top area showed low temperatures in the center region. For samples heated in solid-state microwave heating using the complementary-frequency shifting strategy, the area of cold spots was reduced, and the hot areas were enlarged, while no obvious changes in the temperature magnitudes of cold and hot spots were seen. The heating performance improvement by the solid-state heating compared to the magnetron-based heating can be observed from the higher average temperature (from  $46.08 \pm 1.55$  °C to  $42.51 \pm 1.51$  °C) and lower *HUI* values (from  $0.23 \pm 0.03$  to  $0.16 \pm 0.01$ ), as shown in Figure 5 C&D.

#### 4.4.2.3 Multilayer commercial Lasagna

The heating performance results for the multilayer commercial Lasagna are shown in Figure IV-6. Similar to the previous results on Pulled Chicken samples, different frequencies were used in the dynamic shifting process for the Lasagna (Figure IV-6A). For the three replications, three (2.42, 2.44, and 2.48 GHz), three (2.41, 2.45, and 2.47 GHz), and five (2.40, 2.42, 2.43, 2.44, and 2.47 GHz) different frequencies were used for the shifting stages, respectively. Not only the frequency shifting paths, but also the selected frequencies for the Lasagna samples differed much, which was because of the great variations among the multilayer heterogeneous Lasagna samples. While the varied frequency shifting scenarios for each individual sample further highlight the advantage of the dynamic frequency shifting strategy that could accommodate the product variations properly.

The thermal temperature profiles for the top and middle layers after 8-min heating are shown in Figure IV-6B. Severe cold spots were clearly seen at both top and middle layers in the magnetron-based heating. While for samples heated in the solid-state oven using complementary-frequency shifting strategy, hot spots were observed at both edge and center regions, implying more uniform heating patterns. The diminished cold regions and enlarged hot areas by the solid-state heating led to significantly higher average temperatures at both top (from  $41.65 \pm 3.11$  °C to  $50.05 \pm 1.69$  °C), middle (from  $40.12 \pm 1.96$  °C to  $47.71 \pm 1.10$  °C), and the combined (from  $40.85 \pm 2.47$  °C to  $48.77 \pm 1.44$  °C) layer results (Figure IV-6C), when compared to the magnetron-based heating. Different from the single-component Pulled Chicken and multicomponent Beef in Gravy products whose final temperatures were similar by using magnetron-based heating and solid-state based heating, the Lasagna samples were heated to higher temperatures using the solid-state complementary-frequency shifting strategy. This might be due to the enhanced microwave-food interactions between different food materials at different layers and varied frequencies. Meanwhile, the heating uniformity for top (from  $0.27 \pm 0.02$  to  $0.24 \pm 0.02$ ), middle (from  $0.29 \pm 0.03$  to  $0.22 \pm 0.02$ ) and combined (from  $0.28 \pm 0.02$  to  $0.23 \pm$

0.02) layers were also considerably improved, respectively, when compared to the magnetron-based heating (Figure IV-6D).

The overall results for such a multilayer food indicated that using the dynamic frequency shifting method in the solid-state oven could comprehensively improve the microwave heating performance. Even though the frequency shifting algorithm was only based on the real-time heating patterns over the top surface, the improved performance could be observed along both horizontal and vertical directions, regardless of the spatial variation in the materials.

#### 4.4.2.4 Multicompartment meal of Pulled Chicken & Lasagna

The microwave heating performance of the prepared multicompartment meal of Pulled Chicken & Lasagna samples is shown in Figure IV-7. The frequency shifting paths, similar to previous results on other samples, differed much among replicates, where 2.42, 2.44, and 2.46 GHz were used in the first replicate; 2.42, 2.44, 2.46, and 2.48 GHz were used in the second replicate; and 2.41, 2.42, 2.44, 2.45, and 2.46 GHz were selected for use in the third replicate (Figure IV-7A). Based on the after-heating thermal profiles of the top surface (Figure IV-7B), it can be seen that the temperature of extreme hot areas of the Pulled Chicken (left compartment) was reduced by the dynamic complementary-frequency shifting approach in the solid-state oven; and also, the cold areas of the Lasagna portion (right compartment) were diminished by the dynamic heating. This observation is consistent with the quantitative comparison results of the average temperature (Figure IV-7C) and the heating uniformity (Figure IV-7D). In magnetron-based heating, the average temperature of the Pulled Chicken was  $56.12 \pm 0.85$  °C and much higher than that of the Lasagna ( $33.07 \pm 0.49$  °C). Even with the turntable enabled, the heat distribution was quite nonuniform, which may be attributed to different dielectric and thermal properties of the two compartments. For example, the Lasagna components have a higher specific heat capacity than the chicken meat

(MURPHY et al., 1998; Pitchai et al., 2015). By using the solid-state dynamic heating strategy, the average temperature of Pulled Chicken was decreased to  $51.44 \pm 1.21$  °C, and Lasagna was increased to  $42.83 \pm 0.62$  °C, indicating a significantly narrowed temperature difference between the Pulled Chicken and Lasagna ( $23.05 \pm 1.33$  °C to  $8.61 \pm 1.06$  °C). The average temperature of the whole samples, which considered both compartments, was also increased by the solid-state heating, from  $43.44 \pm 0.58$  °C to  $46.76 \pm 0.70$  °C (Figure IV-7C), indicating an improved overall power efficiency.

The narrowed temperature difference between Pulled Chicken and Lasagna compartments, by using the dynamic complementary-frequency shifting strategy, resulted in significantly decreased *HUI* values, from  $0.33 \pm 0.01$  to  $0.18 \pm 0.02$  (Figure IV-7D). In addition, the heating uniformity of the Lasagna compartment was significantly improved, where the *HUI* was reduced from  $0.20 \pm 0.03$  to  $0.17 \pm 0.01$ .

#### 4.4.2.5 Multicompartment meal of Mashed Potato & Beef in Gravy

The results for the other multicompartment meal consisting of Mashed Potato & Beef in Gravy samples are summarized in Figure IV-8. The frequency shifting path, consistent with the previous conclusion, differed among each replicate (Figure IV-8A). In the thermal images (Figure IV-8B), the severe hot boundary for the Mashed Potato compartment on the left side was alleviated by the solid-state heating using the dynamic frequency strategy; also, the cold regions were heated more by the solid-state heating. In the Beef in Gravy compartment, the high-temperature area was enlarged with the solid-state heating, and the hot boundary was disturbed. The enhanced heating performance by using the dynamic frequency heating in the solid-state oven was further proven by the quantification comparison, where the final temperature (Figure IV-8C) of Beef in Gravy was significantly raised (from  $40.48 \pm 0.51$  °C to  $43.72 \pm 0.61$  °C). In addition, the uniformity (Figure IV-8D) of the Mashed Potato compartment was significantly improved (from  $0.25 \pm 0.00$  to  $0.15 \pm 0.01$ ), making the overall heating uniformity of the

whole product significantly improved as well. Similar to the multicomponent Beef in Gravy product, Beef in Gravy compartment in this multicompartiment meal also did not have significantly improved heating uniformity, which might be due to the convective heat transfer in the Beef in Gravy sample that helps improve microwave heating uniformity.

#### **4.4.2 Overall comparison of the microwave heating performance**

##### 4.4.2.1 Cold spot temperature

Asides from the typical indexes to score the microwave performance, namely averaged temperature that represents power absorption and *HUI* that represents heating nonuniformity level, cold spot temperature is an important factor that influences consumers' perception on the quality and safety of the microwave-heated food products. Figure IV-9 summarizes the cold spot temperatures of five representative products obtained from the thermal imaging profiles. Four of the five products had significantly increased cold spot temperature, from about 23 °C by using the magnetron-based oven to about 30 °C by using the dynamic complementary-frequency shifting strategy. The cold spot temperature of the multicomponent Beef in Gravy sample was raised significantly. This might be attributed to the improved convective heat transfer in the liquid gravy components, which contributed a lot to the enhanced microwave performance in the magnetron-based oven. The convective heat transfer in liquid also influenced the thermal contribution collected by the top thermal camera, which affected the operation of the complementary-frequency shifting strategy that relies on the thermal pattern information.

##### 4.4.2.2 Overall improvement

The temperature improvement and uniformity improvement by the dynamic solid-state heating for each type of sample are shown in Table IV-2. The temperature

improvement values were in the range of -1.68 % and +19.39 % and the *HUI* improvement values were between +12.54 % and +44.88 %. Except for the temperature improvement of the Pulled Chicken samples, which was -1.68 %, all other numerical values of temperature and *HUI* were positive, indicating the remarkable improvement in the microwave heating results by the dynamic solid-state heating. As for the mild decrease in the temperature of the chicken samples, if considering the three replicates conducted (Figure IV-5C), the difference was not significant enough to claim a reduction in a statistical sense.

The overall comparison of the heating performance between the magnetron-equipped oven with the rotatory turntable and the solid-state oven using the dynamic frequency strategy without rotatory turntable is shown in Figure IV-10, with all the five samples considered. Note that evaluation for the multilayer Lasagna was only based on the combined-layer results; and for the two-compartment samples (i.e., Chicken & Lasagna, Mashed Potato & Beef in Gravy), the combined-compartment results were included. The results showed that by using the dynamic solid-state heating, the average temperature was significantly raised from  $42.56 \pm 1.81$  °C to  $45.53 \pm 2.65$  °C, indicating a 7 % increase on average; and the *HUI* value was significantly reduced from  $0.30 \pm 0.08$  to  $0.22 \pm 0.09$ , representing a 26 % improvement. Based on the two indexes (i.e., average temperature and *HUI*), the improvement was more notable in the heating uniformity, which was owing to the complementary-frequency concept applied to the dynamic strategy. Thus, the performance of the dynamic solid-state heating that utilized the complementary-frequency shifting strategy successfully competed with the commercial magnetron-based rotatory microwave heating.

#### 4.4.2.3 Correlation between food product factors and the improvement

Figure IV-11A shows the correlation matrix that maps the relationships between microwave heating performance (average temperature and *HUI*) and sample factors



(weight, number of compartments, package types, and heating time shown in Table IV-1). The correlation structure illustrated that, regarding the performance variables (i.e., temperature improvement and uniformity improvement), the correlation between the uniformity improvement and the compartment number has the highest correlation coefficient ( $R = 0.79$ ), indicating that the number of compartments is highly correlated with the heating performance improvement. Figure IV-11B shows the *HUI* by the two heating methods, for single-compartment foods (Pulled Chicken, Beef in Gravy and Lasagna) and for two-compartment foods (Pulled Chicken & Lasagna, Mashed Potato & Beef in Gravy). Results showed that the single-compartment foods, if heated by the dynamic solid-state method, the *HUI* values could be decreased from  $0.31 \pm 0.09$  to  $0.26 \pm 0.10$  on average, implying an improvement of 18.25 %; while for the two-compartment foods, the *HUI* was cut down from  $0.27 \pm 0.06$  to  $0.17 \pm 0.02$ , denoting a 39.03 % improvement in heating uniformity. Given that the commercially prepared meals suffer from more severe nonuniformity heating, compared with single-compartment foods, because of the thermal runaway phenomenon due to the dielectric property variation between compartments, it is promising to use the dynamic solid-state heating to heat such prepared meals and to alleviate the nonuniformity problems in such commercial meals.

In addition, the negative correlation between temperature improvement and heating time ( $R = -0.60$ ) implied that the longer the heating duration was, the less improvement could be achieved by the dynamic solid-state heating. Therefore, the high power and fast microwave processes could benefit more from dynamic heating. Besides, the negative correlation between temperature improvement and sample weight ( $R = -0.56$ ) indicated that for larger size food, the dynamic solid-state heating yielded less improvement in power efficiency; thereby the proposed solid-state heating is more suitable for meals in smaller volumes, e.g., single-serving foods. Furthermore, the correlation between the uniformity improvement and the package ( $R = -0.52$ ) denotes that the use of steam-venting packages might hinder the performance of the dynamic solid-state heating, as the dynamic processes rely on the fixed thermal patterns under different

frequencies while the package disturbed the steam, and thereby, the thermal patterns inside. In this manner, the dynamic heating method is more suitable for foods that could provide clear patterns over the surface.

#### **4.4.3 Usefulness and future work**

Regarding the performance of various dynamic microwave heating processes based on the use of a solid-state system, compared with all previously reported results, this study conducted a direct comparison between the dynamic solid-state heating and the typical magnetron oven heating with a rotatory turntable, providing solid evidence that the solid-state dynamic complementary-frequency shifting strategy without rotation could yield better microwave heating performance. This conclusion could provide critical direction to the future design of microwave ovens if the solid-state will be used as the power source, including the dynamic strategies that are promising to improve the microwave heating performance, and the possibility of eliminating the turntable to enable the dynamic strategies.

The comparison results have comprehensively demonstrated the practicability of the dynamic complementary-frequency shifting heating method. Nevertheless, there is still room for further improvement in this solid-state system. First, the available power (200 W) was much lower than that of a typical domestic microwave oven (~ 1000 W). To regulate the after-heating temperature with such low power input, in our experiments we used a relatively long heating time, which would even out the heat nonuniformity by the microwaves, and thereby, made the improvement by the dynamic heating less significant. As demonstrated above in the correlation matrix, the dynamic solid-state strategy is more promising to enhance heating performance for shorter microwave processes.

Second, the current dynamic strategies, including all previously mentioned strategies reported by other groups, were all tested only for heating processes, where the samples were all refrigerated before experiments. There are still challenges to applying

this dynamic complementary strategy to defrosting processes where the dielectric properties change significantly. One challenge is that the thermal imaging camera mounted at the top of the oven cavity was not suitable for monitoring thermal profiles of frozen food products. The thermal pattern of each frequency also changes significantly during the defrosting process and differs from that during heating process. A more complicated frequency shifting strategy will be necessary for heating frozen food products to high temperatures. For example, one potential solution could be incorporating the dynamic adaptive power & frequency shifting strategy (Yang and Chen, 2022) into this dynamic complementary-frequency shifting strategy to realize the combined defrosting and heating scenario. To combine the defrosting and heating microwave functions, a criterion may be needed to determine when to switch from defrosting mode to heating mode to achieve optimal heating performance.

Third, from the correlation analysis, it could be seen that for some specific types of products, e.g., products in steam-venting packages and products with liquid components, the performance of the dynamic solid-state heating may be hindered. Even though compared with the magnetron oven, there is still raised performance by the dynamic solid-state heating, the significant convective heat transfer in liquid food products might limit the application of this dynamic complementary-frequency shifting strategy.

Moreover, the market price of the solid-state system is still high, especially compared with the magnetron microwave sources. While on one hand, the lifetime for the solid-state microwave source is much longer than that of the magnetron, making the unit time price for solid-state more reasonable (Atuonwu and Tassou, 2018). On the other hand, with the further development of the solid-state techniques, the price is expected to be reduced (Werner, 2015). Regarding immediate application, the solid-state equipped microwave devices could be suitable for heavy-duty ovens in food service industry.

## **4.5 Conclusions**

Experiments have been conducted with various types of realistic commercial and prepared food products in the forms of single component, multicomponent, multilayer, and multicompartiment to comprehensively compare the heating performance between the magnetron-equipped domestic microwave oven with food rotation and the dynamic solid-state oven using complementary-frequency shifting without food rotation. The quantification results showed that by using the dynamic solid-state heating without the rotatory turntable, the overall average temperature (power efficiency) of the five products was raised by 7 % and the heating uniformity was improved by 26 %. The microwave heating performance improvement by the dynamic solid-state heating is more prominent in multicompartiment meals, but less significant in food products with liquid components or with steam venting packages. Work can be extended in the future to strategy development for heating frozen products to high temperatures. High-power solid-state microwave generators at a lower price will promote the application of solid-state technology in domestic microwave ovens.

## **4.6 Acknowledgements**

This project (or patent) is based on research that was supported by the Tennessee Agricultural Experiment Station with funding from the USDA National Institute of Food and Agriculture Hatch Multistate Research capacity funding program (Accession Number 1023982) and the USDA National Institute of Food and Agriculture, AFRI project (Grant No: 2021-67017-33444).

## List of References

- Alfaifi, B., Tang, J., Jiao, Y., Wang, S., Rasco, B., Jiao, S., Sablani, S., 2014. Radio frequency disinfestation treatments for dried fruit: Model development and validation. *J Food Eng* 120, 268–276. <https://doi.org/10.1016/j.jfoodeng.2013.07.015>
- Atuonwu, J.C., Tassou, S.A., 2018. Quality assurance in microwave food processing and the enabling potentials of solid-state power generators: A review. *J Food Eng* 234, 1–15. <https://doi.org/10.1016/j.jfoodeng.2018.04.009>
- Bhattacharya, M., Basak, T., 2017. A comprehensive analysis on the effect of shape on the microwave heating dynamics of food materials. *Innovative Food Science and Emerging Technologies* 39, 247–266. <https://doi.org/10.1016/j.ifset.2016.12.002>
- Biji, K.B., Ravishankar, C.N., Mohan, C.O., Srinivasa Gopal, T.K., 2015. Smart packaging systems for food applications: a review. *J Food Sci Technol* 52, 6125–6135. <https://doi.org/10.1007/s13197-015-1766-7>
- Chamchong, M., Datta, A.K., 1999. Thawing of foods in a microwave oven: II. Effect of load geometry and dielectric properties. *Journal of Microwave Power and Electromagnetic Energy* 34, 22–32. <https://doi.org/10.1080/08327823.1999.11688385>
- Du, Z., Wu, Z., Gan, W., Liu, G., Zhang, X., Liu, J., Zeng, B., 2019. Multi-physics modeling and process simulation for a frequency-shifted solid-state source microwave oven. *IEEE Access* 7, 184726–184733. <https://doi.org/10.1109/ACCESS.2019.2960317>
- Fakhouri, M.O., Ramaswamy, H.S., 1993. Temperature uniformity of microwave heated foods as influenced by product type and composition. *Food Research International* 26, 89–95. [https://doi.org/10.1016/0963-9969\(93\)90062-N](https://doi.org/10.1016/0963-9969(93)90062-N)
- Geedipalli, S.S.R., Rakesh, V., Datta, A.K., 2007. Modeling the heating uniformity contributed by a rotating turntable in microwave ovens. *J Food Eng* 82, 359–368. <https://doi.org/10.1016/j.jfoodeng.2007.02.050>

Gulati, T., Zhu, H., Datta, A.K., Huang, K., 2015. Microwave drying of spheres: Coupled electromagnetics-multiphase transport modeling with experimentation. Part II: Model validation and simulation results. *Food and Bioprocess Processing* 96, 326–337. <https://doi.org/10.1016/j.fbp.2015.08.001>

He, J., Yang, Y., Zhu, H., Li, K., Yao, W., Huang, K., 2020. Microwave heating based on two rotary waveguides to improve efficiency and uniformity by gradient descent method. *Appl Therm Eng* 178, 115594. <https://doi.org/10.1016/j.applthermaleng.2020.115594>

Liu, S., Fukuoka, M., Sakai, N., 2013. A finite element model for simulating temperature distributions in rotating food during microwave heating. *J Food Eng* 115, 49–62. <https://doi.org/10.1016/j.jfoodeng.2012.09.019>

MURPHY, R.Y., MARKS, B.P., MARCY, J.A., 1998. Apparent Specific Heat of Chicken Breast Patties and their Constituent Proteins by Differential Scanning Calorimetry. *J Food Sci* 63, 88–91. <https://doi.org/10.1111/j.1365-2621.1998.tb15682.x>

Pitchai, K., Chen, J., Birla, S., Jones, D., Gonzalez, R., Subbiah, J., 2015. Multiphysics Modeling of Microwave Heating of a Frozen Heterogeneous Meal Rotating on a Turntable. *J Food Sci* 80, E2803–E2814. <https://doi.org/10.1111/1750-3841.13136>

Schiffmann, R., 2017. 13 - Packaging for microwave foods, in: Regier, M., Knoerzer, K., Schubert, H.B.T.-T.M.P. of F. (Second E. (Eds.), *Woodhead Publishing Series in Food Science, Technology and Nutrition*. Woodhead Publishing, pp. 273–299. <https://doi.org/https://doi.org/10.1016/B978-0-08-100528-6.00013-9>

Soares, N.F.F., Rutishauser, D.M., Melo, N., Cruz, R.S., Andrade, N.J., 2002. Inhibition of microbial growth in bread through active packaging. *Packaging Technology and Science* 15, 129–132. <https://doi.org/10.1002/pts.576>

Soltysiak, M., Celuch, M., Erle, U., 2011. Measured and simulated frequency spectra of the household microwave oven. *IEEE MTT-S International Microwave Symposium Digest* 1–4. <https://doi.org/10.1109/MWSYM.2011.5972844>

Taghian Dinani, S., Feldmann, E., Kulozik, U., 2021. Effect of heating by solid-state microwave technology at fixed frequencies or by frequency sweep loops on heating profiles in model food samples. *Food and Bioproducts Processing* 127, 328–337. <https://doi.org/10.1016/j.fbp.2021.03.018>

Vilayannur, R.S., Puri, V.M., Anantheswaran, R.C., 1998. Size and shape effect on nonuniformity of temperature and moisture distributions in microwave heated food materials: Part II experimental validation. *J Food Process Eng* 21, 235–248. <https://doi.org/10.1111/j.1745-4530.1998.tb00449.x>

Wang, J., Luechapattaporn, K., Wang, Y., Tang, J., 2012. Radio-frequency heating of heterogeneous food – Meat lasagna. *J Food Eng* 108, 183–193. <https://doi.org/10.1016/j.jfoodeng.2011.05.031>

Werner, K., 2015. RF energy systems: realizing new applications. *Microw J (Int Ed)* 58, 22–34.

Yang, R., Chen, J., 2022. Dynamic solid-state microwave defrosting strategy with shifting frequency and adaptive power improves thawing performance. *Innovative Food Science & Emerging Technologies* 103157. <https://doi.org/10.1016/j.ifset.2022.103157>

Yang, R., Chen, Q., Chen, J., 2021. Comparison of heating performance between inverter and cycled microwave heating of foods using a coupled multiphysics-kinetic model. *Journal of Microwave Power and Electromagnetic Energy* 55, 45–65. <https://doi.org/10.1080/08327823.2021.1877244>

Yang, R., Fathy, A.E., Morgan, M.T., Chen, J., 2022a. Development of a complementary-frequency strategy to improve microwave heating of gellan gel in a solid-state system. *J Food Eng* 314, 110763. <https://doi.org/10.1016/j.jfoodeng.2021.110763>






Yang, R., Fathy, A.E., Morgan, M.T., Chen, J., 2022b. Development of online closed-loop frequency shifting strategies to improve heating performance of foods in a solid-state microwave system. *Food Research International* 154, 110985. <https://doi.org/10.1016/j.foodres.2022.110985>

Zhou, X., Zhang, S., Tang, Z., Tang, J., Takhar, P.S., 2022. Microwave frying and post-frying of French fries. *Food Research International* 159, 111663.  
<https://doi.org/10.1016/j.foodres.2022.111663>



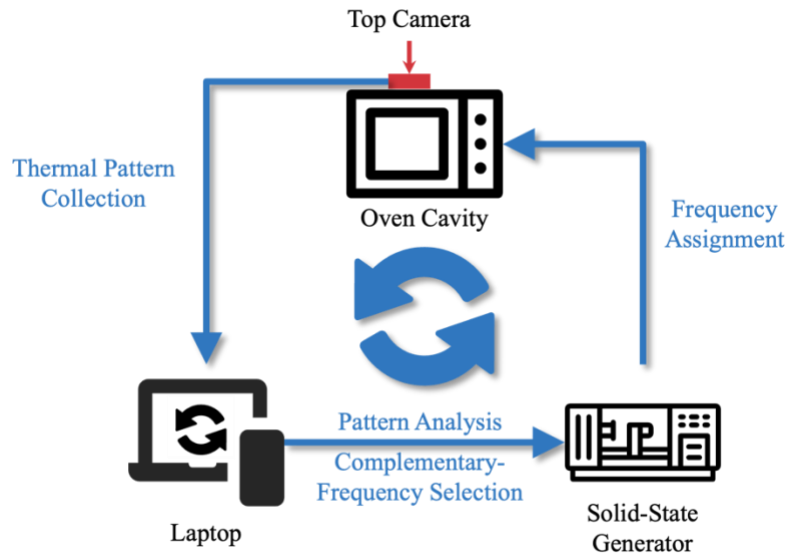
## Appendix

**Table IV-1 Sample information**

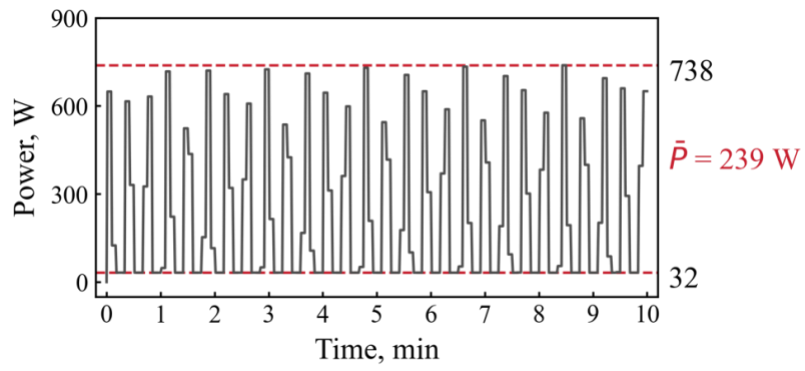
<b>Food</b>	<b>Weight, g</b>	<b>Compartment</b>	<b>Stem-venting Package</b>	<b>Heating Time, min</b>	<b>Image</b>
<b>Pulled Chicken</b>	453g	1	Yes	10	
<b>Beef in Gravy</b>	425g	1	Yes	8	
<b>Lasagna</b>	285 ± 10	1	No	8	
<b>Pulled Chicken &amp; Lasagna</b>	285 (± 10) &100 (± 1)	2	No	9	
<b>Mashed Potato &amp; Beef in Gravy</b>	150 (± 1) & 150 (±1)	2	No	8	

**Table IV-2 Overall improvement in Temperature and Uniformity by using solid-state microwave with dynamic frequency**

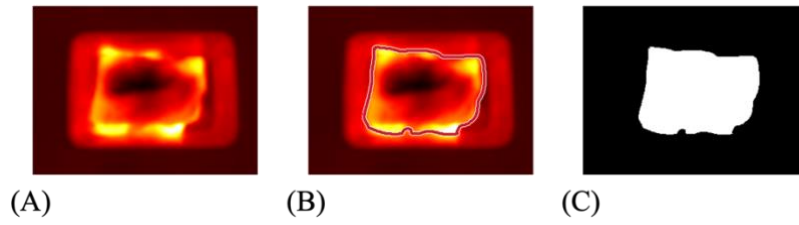
<b>Food</b>	<b>Temperature improvement, %</b>	<b>HUI improvement, %</b>
<b>Pulled Chicken</b>	-1.68	+27.41
<b>Beef in Gravy</b>	+8.33	+12.54
<b>Lasagna</b>	+19.39	+19.66
<b>Pulled Chicken &amp; Lasagna</b>	+7.62	+44.88
<b>Mashed Potato &amp; Beef in Gravy</b>	+2.00	+30.15



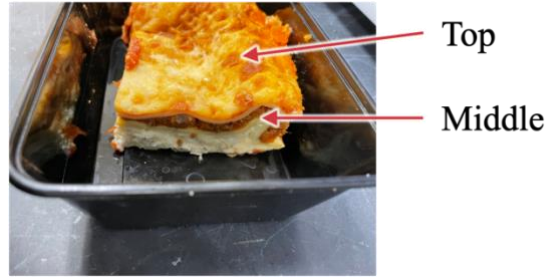
**Figure IV-1 Illustration for the solid-state microwave system and the dynamic complementary-frequency shifting.**



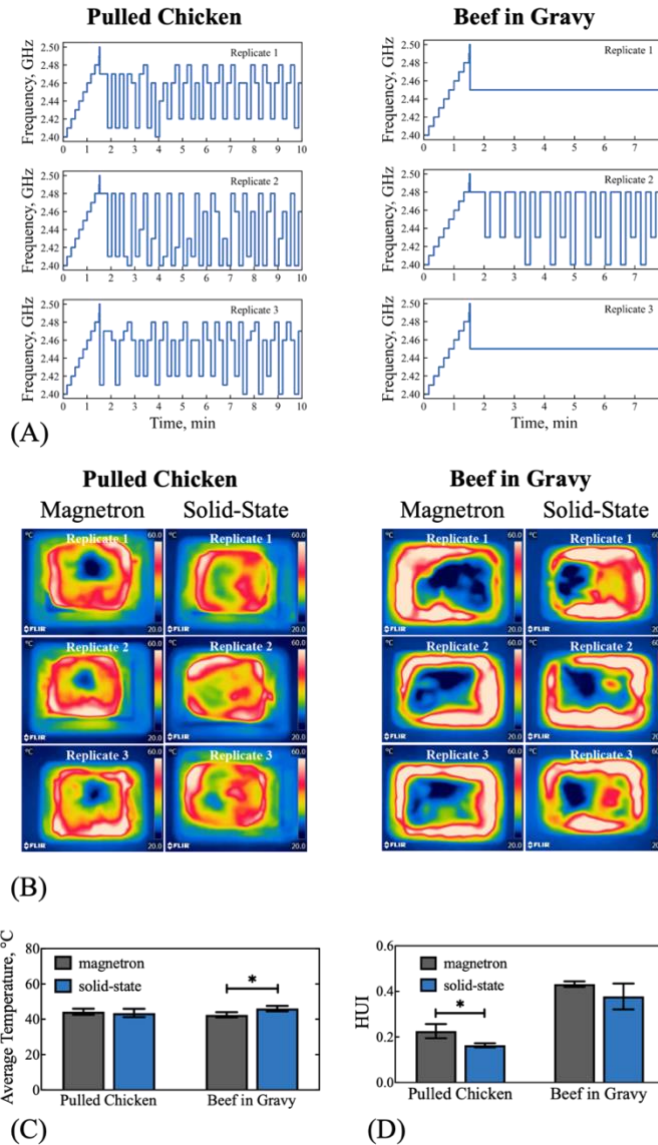
**Figure IV-2 Magnetron-based microwave power output records under power level 1 for calibration.**



**Figure IV-3 Image processing (A) raw thermal image, (B) manually drawn food boundary (red line), (C) mask created based on the boundary in (B).**

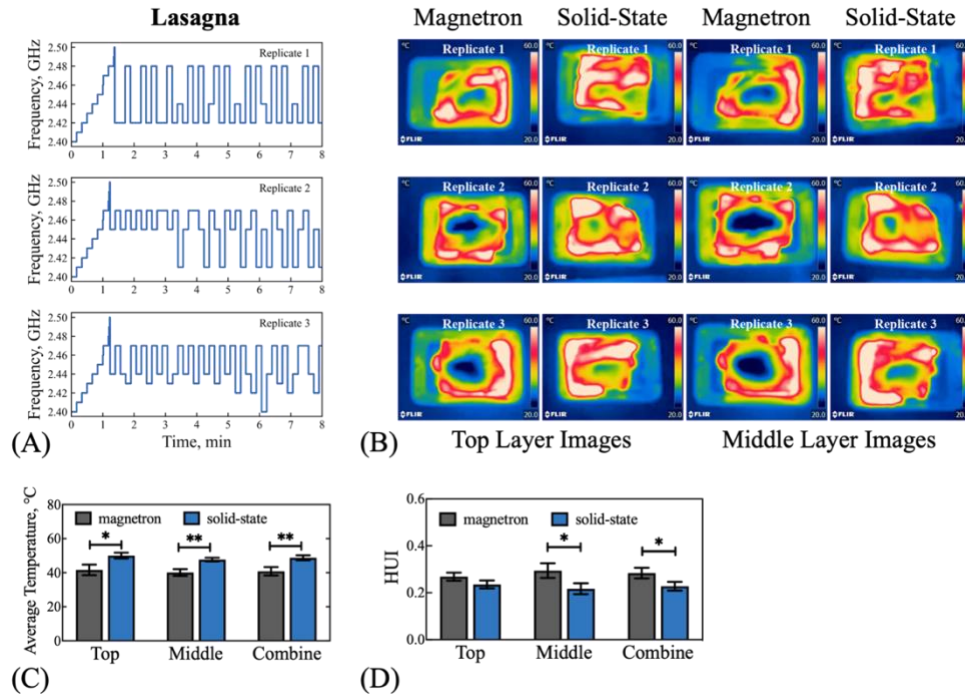


**Figure IV-4 Top and middle layers of Lasagna samples for heating performance evaluation.**

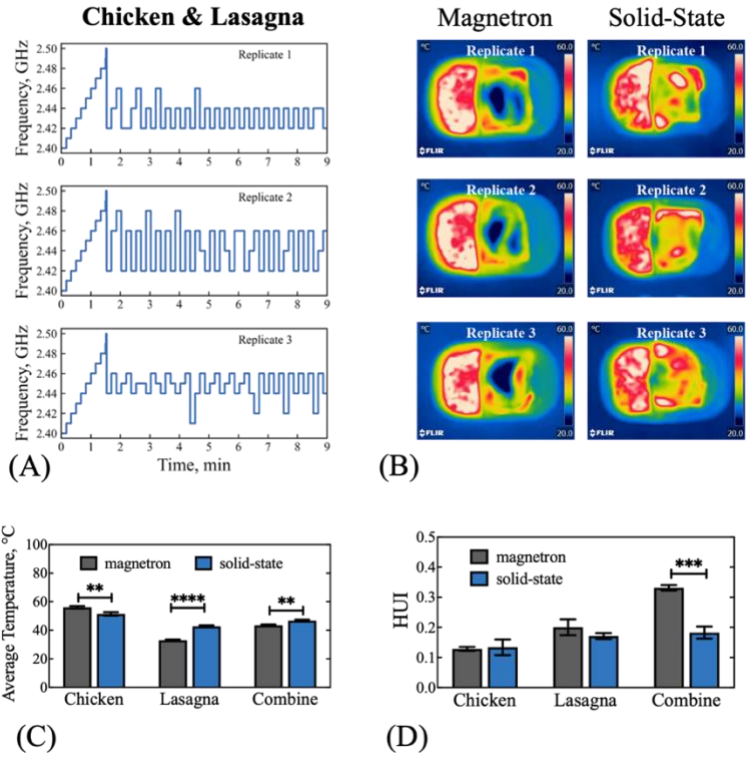


**Figure IV-5 Heating performance of Pulled Chicken and Beef in Gravy samples heated in original packages (A) solid-state frequency records; (B) final thermal images; (C) after-heating temperature, (D) after-heating *HUI*. The results and error bars were calculated as the average and standard deviation from triplicated experiments. (\*  $p < 0.05$ , \*\*  $p < 0.01$ , \*\*\*  $p < 0.001$ , \*\*\*\*  $p < 0.0001$ ).**

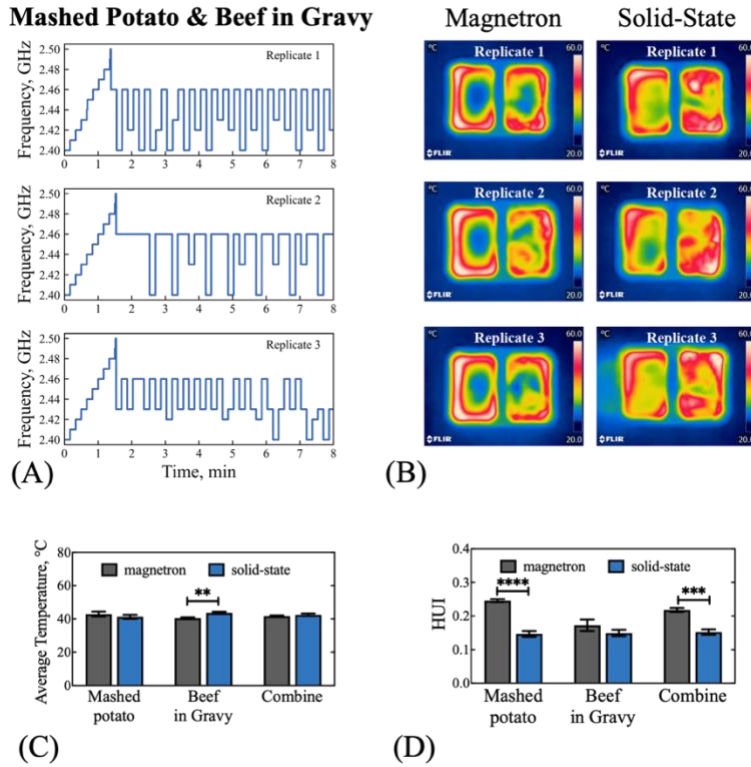




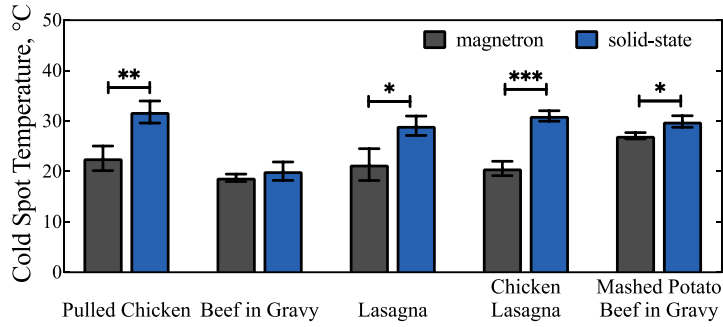
**Figure IV-6 Heating performance of sliced Lasagna heated in rectangular container (A) solid-state frequency records; (B) final thermal images for both top and middle layers; (C) after-heating temperature, and (D) after-heating *HUI* for top, middle and combined layers. The results and error bars were calculated as the average and standard deviation from triplicated experiments (\*  $p < 0.05$ , \*\*  $p < 0.01$ , \*\*\*  $p < 0.001$ , \*\*\*\*  $p < 0.0001$ ).**



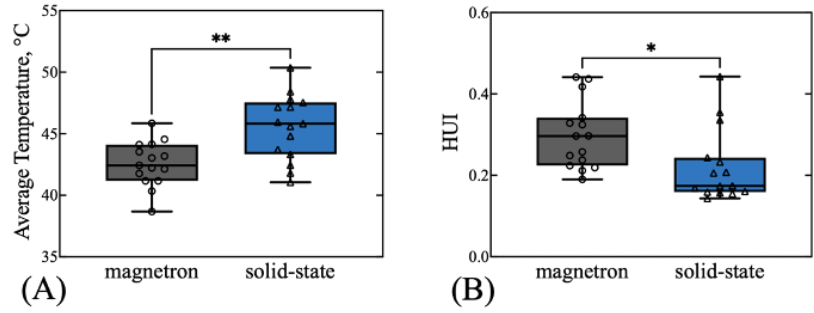
**Figure IV-7 Heating performance of Pulled Chicken & Lasagna heated in two-compartment containers. (A) solid-state frequency records; (B) final thermal images; (C) after-heating temperature, and (D) after-heating *HUI* for separate and combined portions. The results and error bars were calculated as the average and standard deviation from triplicated experiments (\*  $p < 0.05$ , \*\*  $p < 0.01$ , \*\*\*  $p < 0.001$ , \*\*\*\*  $p < 0.0001$ ).**



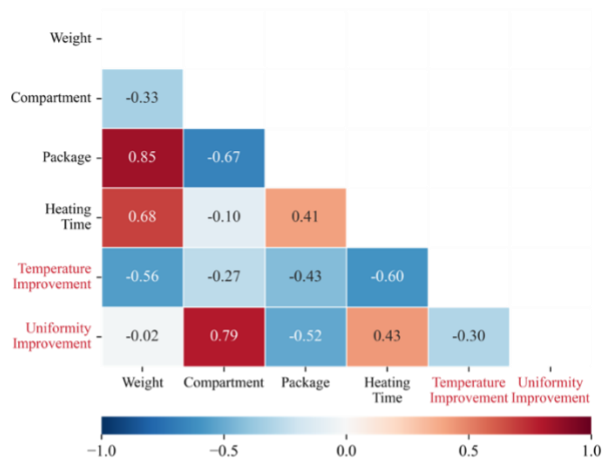
**Figure IV-8 Heating performance of Mashed Potato & Beef in Gravy heated in two-compartment container (A) solid-state frequency records; (B) final thermal images; (C) after-heating temperature, and (D) after-heating *HUI*. The results and error bars were calculated as the average and standard deviation from triplicated experiments (\*  $p < 0.05$ , \*\*  $p < 0.01$ , \*\*\*  $p < 0.001$ , \*\*\*\*  $p < 0.0001$ ).**



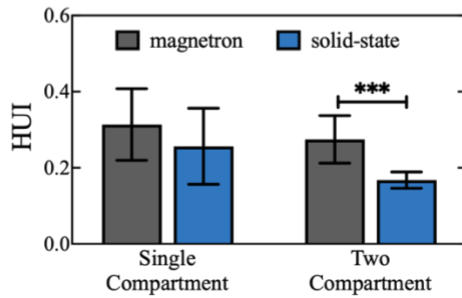
**Figure IV-9 Cold spot temperature of different food products after heating obtained from thermal imaging profiles. The results and error bars were calculated as the average and standard deviation from triplicated experiments (\*  $p < 0.05$ , \*\*  $p < 0.01$ , \*\*\*  $p < 0.001$ , \*\*\*\*  $p < 0.0001$ ).**



**Figure IV-10 Comparison of overall performance by different heating methods. The results and error bars were calculated as the average and standard deviation from triplicated experiments (\*  $p < 0.05$ , \*\*  $p < 0.01$ , \*\*\*  $p < 0.001$ , \*\*\*\*  $p < 0.0001$ ).**



(A)



(B)

**Figure IV-11 (A) Correlation heatmap with correlation coefficients between every two variables. Labels in black color denote sample properties, and in red color denote performance variables to be studied. (B) *HUI* comparison between dynamic solid-state heating and rotatory magnetron heating with the number of container compartment as an affecting factor.**

**CHAPTER V**  
**CONCLUSIONS AND FUTURE WORK**

## 5.1 Conclusions

Solid-state is an innovative technique and shows its promise in improving microwave performance compared with the current magnetron-equipped microwave ovens. The microwaves generated by a solid-state could vary in frequency and thereby, create various thermal patterns, which shall be utilized to address the standing wave patterns formed in the magnetron-based ovens. While yet limited work has been reported to implement realistic microwave frequency control algorithms for use by the solid-state system. The overall goal of this study was to develop a robust complementary-frequency control algorithm that could improve the microwave heating performance and automatically accommodate the sample variation.

In Chapter II, Objective 1 demonstrated that the complementary heating patterns generated by different microwave frequencies (in the range of 2.40 to 2.50 GHz) could be utilized to design the frequency shifting path. Compared with the more general orderly frequency shifting strategies, the proposed complementary-frequency shifting strategy, that determined the shifting path with pre-collected thermal pattern information, yielded significantly raised power efficiency while maintaining similar heating uniformity on model foods (i.e., gellan gel, mashed potato). In addition, with the complementary-frequency shifting strategy applied, the frequency shifting rate did not significantly affected the heating performance. And overall, the complementary-frequency concept was proven to be useful in designing the frequency shifting path.

In Chapter III, Objective 2 further utilized the demonstrated complementary-frequency concept, and developed online frequency shifting algorithms where the process of preliminary thermal pattern collection was eliminated. The online process was divided into two stages, including a sweeping stage that collected thermal patterns and shifting stages that adjusted frequency following three different algorithms. The shifting algorithms included orderly frequency shifting, pre-determined complementary-frequency shifting, and dynamic complementary-frequency shifting. Experimental results showed that among the three shifting algorithms, the dynamic frequency shifting method,



which shifted the frequencies based on real-time collected thermal images, yielded the optimal heating performance on model foods, where the heating uniformity was significantly better while the power efficiency was maintained, compared with other two algorithms.

In Chapter IV, Objective 3 directly compared the heating performance by the proposed dynamic complementary-frequency shifting method in a solid-state oven and the typical rotatory microwave heating in a magnetron-equipped domestic oven. Comparison was comprehensively conducted with various types of refrigerated foods, where the sample weight, number of compartments of the container, use of package during heating, and heating time were considered as potential affecting factors. Results showed that, in sum, the dynamic solid-state heating without rotation could provide better microwave performance than the rotatory magnetron heating. The presence of liquid components or the use of steam-venting packages may negatively affect the thermal profile collection in the dynamic strategy, hindering the algorithm performance, although considerable improvement was still observed. The complementary-frequency shifting strategy is highly promising to be incorporated in future solid-state microwave systems for improving microwave heating performance.

By completing this study, a dynamic frequency shifting algorithm for use by the novel solid-state system that utilizes real-time collected thermal data and the complementary-frequency concept has been successfully developed, implemented, and comprehensively tested. And the experimental results indicated that the proposed algorithm could compete with the currently applied rotatory microwave heating using a magnetron, where the enhanced heating performance was achieved in various realistic foods, denoting the robustness of the dynamic algorithm and the promise of applying the solid-state technique to serve the food industry.

## 5.2 Future work

Results in this project have proposed and implemented a dynamic complementary-frequency shifting algorithm for use by the solid-state microwave system, and this algorithm has been demonstrated to yield better heating performance than the current magnetron-equipped domestic microwave ovens. This algorithm showed its promise for direct use by the microwave system for food cooking. However, there is still much room for further improvement.

For research purpose, in this project, the power level of the solid-state was limited to under 200 W, which was much lower than the regular value for a domestic microwave oven (~ 1000 W). Hence, for more robust experimental results, a high-power system will be needed to raise the sample temperatures. Besides, the microwave parameters control algorithm proposed here only focused on the frequency. But in addition to frequency, the solid-state system also provides control for the power level and relative phase of multiple sources, which shall be helpful for further improving the microwave heating performance. More research will be needed to explore more advanced algorithms with more parameters considered.

For commercialization purpose, on the one hand, by now, all solid-state algorithms, including the current one, are only developed and tested on refrigerated foods. While for the microwave defrosting processes, the strategy for performance optimization shall be different. Given that the solid-state could also control the microwave power level and relative phase of multiple sources, more advanced algorithm will be needed to implement more comprehensive strategies that could handle both the defrosting and the heating processes at the same time. More specific microwave heating modes, e.g., defrosting, heating, or cooking from frozen, shall be separately embedded into the system for users' choice. On the other hand, another concern about the future popularization of the solid state-equipped microwave ovens is the high price. This asks for continuous collaboration with the manufacturer to depress the price; and for now, such solid-state generators could be first used for heavy-duty ovens in the food service

industry, where the food safety and quality, rather than the equipment price, are more concerned.

## VITA

Original from China, Ran grew up and had been studying in China. After high school, she entered Jiangnan University for a bachelor program in Food Science and Technology department. Three years later, she went to the University of California, Davis as an exchange student in 2016. After finishing the exchange undergraduate program, she went to the University of Massachusetts for her master's degree since 2017. With two-year training as a graduate student, she then chose the University of Tennessee, Knoxville for her Ph.D. degree, with a research focus on food engineering field since 2019. After graduation in 2022, she will continue her research in UTK as a postdoctoral researcher.